(12) INTERNATIONAL APPLICATION PUBLISHED UNDER THE PATENT COOPERATION TREATY (PCT)

(19) World Intellectual Property Organization
International Bureau

(43) International Publication Date
10 May 2013 (10.05.2013)

WIPO | PCT

(10) International Publication Number
WO 2013/066269 A1

(51) International Patent Classification:
*C01B 31/04* (2006.01) *B82Y 10/00* (2011.01)

(21) International Application Number:
PCT/SG2012/000412

(22) International Filing Date:
1 November 2012 (01.11.2012)

(25) Filing Language: English

(26) Publication Language: English

(30) Priority Data:
61/554,620 2 November 2011 (02.11.2011) US

(71) Applicant: **NANYANG TECHNOLOGICAL UNIVERSITY** [SG/SG]; 50 Nanyang Avenue, Singapore 639798 (SG).

(72) Inventors: **DU, Zehui**; 50 Nanyang Avenue, Singapore 639798 (SG). **YIN, Zongyou**; 50 Nanyang Avenue, Singapore 639798 (SG). **ZHANG, Hua**; 50 Nanyang Avenue, Singapore 639798 (SG).

(74) Agent: **VIERING, JENTSCHURA & PARTNER LLP**; P.O. Box 1088, Rochor Post Office, Rochor Road, Singapore 911833 (SG).

(81) Designated States *(unless otherwise indicated, for every kind of national protection available)*: AE, AG, AL, AM, AO, AT, AU, AZ, BA, BB, BG, BH, BN, BR, BW, BY, BZ, CA, CH, CL, CN, CO, CR, CU, CZ, DE, DK, DM, DO, DZ, EC, EE, EG, ES, FI, GB, GD, GE, GH, GM, GT, HN, HR, HU, ID, IL, IN, IS, JP, KE, KG, KM, KN, KP, KR, KZ, LA, LC, LK, LR, LS, LT, LU, LY, MA, MD, ME, MG, MK, MN, MW, MX, MY, MZ, NA, NG, NI, NO, NZ, OM, PA, PE, PG, PH, PL, PT, QA, RO, RS, RU, RW, SC, SD, SE, SG, SK, SL, SM, ST, SV, SY, TH, TJ, TM, TN, TR, TT, TZ, UA, UG, US, UZ, VC, VN, ZA, ZM, ZW.

(84) Designated States *(unless otherwise indicated, for every kind of regional protection available)*: ARIPO (BW, GH, GM, KE, LR, LS, MW, MZ, NA, RW, SD, SL, SZ, TZ, UG, ZM, ZW), Eurasian (AM, AZ, BY, KG, KZ, RU, TJ, TM), European (AL, AT, BE, BG, CH, CY, CZ, DE, DK, EE, ES, FI, FR, GB, GR, HR, HU, IE, IS, IT, LT, LU, LV, MC, MK, MT, NL, NO, PL, PT, RO, RS, SE, SI, SK, SM, TR), OAPI (BF, BJ, CF, CG, CI, CM, GA, GN, GQ, GW, ML, MR, NE, SN, TD, TG).

**Published**:

— *with international search report (Art. 21(3))*

(54) **Title**: METHOD OF FORMING OD, ID, OR 3D GRAPHENE AND USE THEREOF

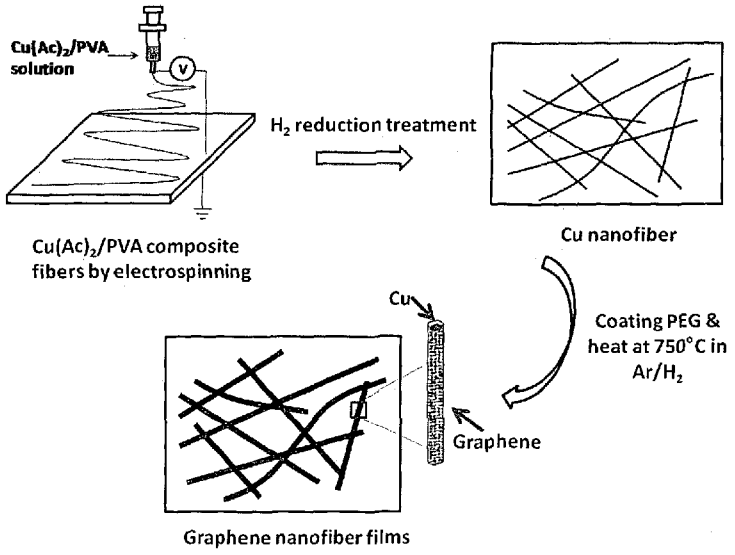


(57) **Abstract**: The present invention relates to a method of forming graphene on a OD (dimensional), ID or 3D metallic nanostructure, comprising coating the metallic nanostructure with a layer of liquid carbon precursor, carbonizing the layer of liquid carbon precursor coated on the metallic nanostructure at a carbonizing temperature to convert the layer of liquid carbon precursor to a layer of amorphous carbon, crystallizing the layer of amorphous carbon at a crystallizing temperature to convert the layer of amorphous carbon to a layer of crystallized graphene, and quenching the layer of crystallized graphene. The so-formed OD, I D or 3D graphene can be processed further to produce high-performance electrical conductors for electronics, batteries, supercapacitors and hydrogen storage, and nanocomposites for heat spreading.

WO 2013/066269 A1

# METHOD OF FORMING 0D, 1D, OR 3D GRAPHENE AND USE THEREOF

## Cross-Reference to Related Application

[001] This application claims the benefit of priority of United States of America Provisional Patent Application No. 61/554,620, filed 02 November 2011, the contents of which being hereby incorporated by reference in its entirety for all purposes.

## Technical Field

[002] The invention relates to methods of forming graphene, and in particular, to forming graphene in zero dimension (0D), one dimension (1D), and three dimensions (3D). The invention further relates to the use of 0D, 1D, or 3D graphene in high performance electrical conductors for electronics, batteries, supercapacitors and hydrogen storage, and in nanocomposites for heat spreading.

## Background

[003] Graphene is a one-atom-thick planar sheet of $sp^2$-bonded carbon atoms that are densely packed in a honeycomb crystal lattice. Graphene initially is a two-dimensional (2D) carbon material. From the 2D configuration, graphene can be formed into other dimensions. For example, graphene can be wrapped up into a 0D buckyball, rolled into a 1D nanofiber or crosslinked to form a 3D foam or aerogel. Compared to the 2D graphene which only exhibits attractive *in-plane* electrical, thermal, mechanical and structural properties, the remaining multidimensional graphene materials (i.e. configurations other than 2D) can extend the respective properties to many different directions and hence demonstrate greater potential in applications such as electronics, batteries, supercapacitors, hydrogen storage and heat spreading, for example.

**[004]** While there exist technologies to prepare graphene as such, most of the approaches focus on forming 2D graphene sheets.

**[005]** Therefore, there is a need to provide for methods of forming graphene directly in dimensions in addition to 2D, such as in 0D, 1D, or 3D.

## Summary

**[006]** The present invention is based on the inventors' surprising discovery that graphene in dimensions other than 2D, such as in 0D, 1D, or 3D, can be directly formed without being converted or processed from 2D graphene. The inventors have further found a general and common method to form graphene in these alternative or additional dimensions.

**[007]** Accordingly, in a first aspect of the invention, there is provided a method of forming graphene on a metallic nanostructure, comprising:

(i) coating the metallic nanostructure with a layer of liquid carbon precursor;

(ii) carbonizing the layer of liquid carbon precursor coated on the metallic nanostructure at a carbonizing temperature to convert the layer of liquid carbon precursor to a layer of amorphous carbon;

(iii) crystallizing the layer of amorphous carbon at a crystallizing temperature to convert the layer of amorphous carbon to a layer of crystallized graphene; and

(iv) quenching the layer of crystallized graphene.

**[008]** The metallic nanostructure can be a 0D nanoparticle such that 0D graphene can be formed by the method of the first aspect.

**[009]** Alternatively, the metallic nanostructure can be a 1D nanofiber such that 1D graphene can be formed by the method of the first aspect.

**[010]** Yet alternatively, the metallic nanostructure can be a 3D foam or aerogel such that 3D graphene can be formed by the method of the first aspect.

**[011]** In another aspect of the invention, there is provided a method of forming an electrode comprising graphene, the method comprising:

(a) forming at least one layer of metallic nanostructures on a substrate;

(b) coating the metallic nanostructures with a layer of liquid carbon precursor;

(c) carbonizing the layer of liquid carbon precursor coated on the metallic nanostructure at a carbonizing temperature to convert the layer of liquid carbon precursor to a layer of amorphous carbon;

(d) crystallizing the layer of amorphous carbon at a crystallizing temperature to convert the layer of amorphous carbon to a layer of crystallized graphene; and

(e) quenching the layer of crystallized graphene.

**[012]** The substrate can be rigid or flexible such that rigid or flexible electrodes comprising graphene can be formed.

**[013]** Accordingly, in yet another aspect, there is provided a method of forming a flexible electrode comprising graphene, the method comprising:

(i) coating metallic nanostructures with a layer of liquid carbon precursor;

(ii) carbonizing the layer of liquid carbon precursor coated on the metallic nanostructures at a carbonizing temperature to convert the layer of liquid carbon precursor to a layer of amorphous carbon;

(iii) crystallizing the layer of amorphous carbon at a crystallizing temperature to convert the layer of amorphous carbon to a layer of crystallized graphene;

(iv) quenching the layer of crystallized graphene to obtain metallic nanostructures coated with graphene;

(v) coating a polymer solution on the metallic nanostructures coated with graphene, wherein the polymer solution comprises the polymer of a flexible substrate; and

(vi) curing the polymer solution to form a polymer film having the metallic nanostructures coated with graphene.

**[014]** Further, transparency of the electrodes can be tuned from being transparent to non-transparent by tuning the thickness and/or number of layers of graphene formed on the electrodes.

**[015]** Thus, in a further aspect of the invention, there is provided a method of forming a transparent electrode comprising graphene, the method comprising:

(i) coating metallic nanostructures with a layer of liquid carbon precursor;

(ii) carbonizing the layer of liquid carbon precursor coated on the metallic nanostructure at a carbonizing temperature to convert the layer of liquid carbon precursor to a layer of amorphous carbon;

(iii) crystallizing the layer of amorphous carbon at a crystallizing temperature to convert the layer of amorphous carbon to a layer of crystallized graphene;

(iv) quenching the layer of crystallized graphene to obtain metallic nanostructures coated with graphene;

(v) dispersing the metallic nanostructures coated with graphene in a solution;

(vi) coating the solution of (v) onto a substrate; and

(vii) drying the coating of (vi).

**[016]** In yet another aspect of the invention, there is provided a method of forming a heat spreader comprising graphene nanocomposite, the method comprising:

(i) coating metallic nanostructures with a layer of liquid carbon precursor;

(ii) carbonizing the layer of liquid carbon precursor coated on the metallic nanostructure at a carbonizing temperature to convert the layer of liquid carbon precursor to a layer of amorphous carbon;

(iii) crystallizing the layer of amorphous carbon at a crystallizing temperature to convert the layer of amorphous carbon to a layer of crystallized graphene;

(iv) quenching the layer of crystallized graphene to obtain metallic nanostructures coated with graphene;

(v) mixing the metallic nanostructures coated with graphene with a metal powder;

(vi) processing the mixture of (v) to form the graphene nanocomposite.

[017] The mixture of metal nanostructures coated with graphene and the metal powder may be processed by hot pressing, moulding, or sintering.

**Brief Description of the Drawings**

[018] In the drawings, like reference characters generally refer to the same parts throughout the different views. The drawings are not necessarily drawn to scale, emphasis instead generally being placed upon illustrating the principles of various embodiments. In the following description, various embodiments of the invention are described with reference to the following drawings.

[019] **Fig. 1** shows the field emission scanning electronic microscope (FESEM) image of Cu nanofibers prepared by an electrospinning technique, followed by pyrolysis and $H_2$ reduction.

[020] **Fig. 2A** and **Fig. 2B** show the FESEM and transmission electronic microscope (TEM) images, respectively, of core-shell Cu nanofibers with C in the core. The carbon core can improve the resistance of the Cu nanofibers to thermal impact during the growth of graphene.

[021] **Fig. 3** shows a schematic illustration of the formation of graphene nanofiber films for rigid transparent conductor.

[022] **Fig. 4A** and **Fig. 4B** show FESEM image and Raman spectra, respectively, of the 0D graphene with Cu nanoparticle as the template. The G and 2D peaks are the characteristic peaks for graphene.

[023] **Fig. 5A** and **Fig. 5B** show FESEM image and Raman spectra, respectively, of graphene nanofibers with Ni in core. The G and 2D peaks are the characteristic peaks for

graphene. The D peak with extremely low intensity indicates the obtained graphene has few defects.

[024] **Fig. 6A** and **Fig. 6B** shows FESEM image and Raman spectra, respectively, of 3D graphene with Ni foam as the template. The G and 2D peaks are the characteristic peaks for graphene. The D peak with extremely low intensity indicates the obtained graphene has few defects.

[025] **Fig. 7** shows transmission spectra of the graphene nanofiber films with Ni in core.

[026] **Fig. 8** shows field emission scanning electronic microscope (FESEM) image of parallel graphene nanofibers with Ni in the core.

[027] **Fig. 9** shows FESEM image of crossed graphene nanofibers with Ni in the core.

**Description**

[028] The following detailed description refers to the accompanying drawings that show, by way of illustration, specific details and embodiments in which the invention may be practised. These embodiments are described in sufficient detail to enable those skilled in the art to practise the invention. Other embodiments may be utilized and structural, logical, and electrical changes may be made without departing from the scope of the invention. The various embodiments are not necessarily mutually exclusive, as some embodiments can be combined with one or more other embodiments to form new embodiments.

[029] The present invention is based on the inventors' surprising discovery that graphene in dimensions other than 2D, such as in 0D, 1D, or 3D, can be directly formed without being converted or processed from 2D graphene. The inventors have further found a general and common method to form graphene in these alternative or additional dimensions.

**[030]** Accordingly, a method of forming graphene on a metallic nanostructure is disclosed. The method comprises coating the metallic nanostructure with a layer of liquid carbon precursor and carbonizing the layer of liquid carbon precursor coated on the metallic nanostructures at a carbonizing temperature to convert the layer of liquid carbon precursor to a layer of amorphous carbon. The layer of amorphous carbon is next crystallized at a crystallizing temperature to convert the layer of amorphous carbon to a layer of crystallized graphene, followed by quenching the layer of crystallized graphene. The quenched crystallized graphene results in graphene being formed on the metallic nanostructure.

**[031]** Graphene is a substance made of pure carbon, with atoms arranged in a regular hexagonal pattern similar to graphite, but in a one-atom thick sheet. It is an allotrope of carbon whose structure is a single planar sheet of $sp^2$-bonded carbon atoms that are densely packed in a honeycomb crystal lattice.

**[032]** A nanostructure is a structure or object that can have any form and has dimensions typically ranging from 1 to 100 nm (nanometre). More specifically, a nanostructure has at least one dimension being less than 100 nm. Nanostructures can be classified, for example, into the following dimensional types: zero dimensional (0D) including, but not limited to, nanospherical particles (also called nanoparticles or nanospheres); one dimensional (1D) including, but not limited to, nanorods, nanowires (also called nanofibers) and nanotubes; two dimensional (2D) including, but not limited to, nanoflakes, nanodiscs, nanocubes and nanofilms; three dimensional (3D) including, but not limited to, porous foam or aerogel having nanosized pores therein. "0D graphene" refers to the graphene growing on the surface of the nanoparticles. "1D graphene" refers to the graphene nanofibers with

graphene deposited on the surface of the nanofibers. "3D graphene" refers to the micro/nanoporous graphene foams or graphene aerogels. In such 3D graphere structures, the graphene grows on the metallic walls interconnected with nanopores in the 3D metallic foam or aerogel. The metallic portions can be etched off to form pure graphene nanoparticles (0D), nanofibers (1D), foams and aerogels (3D). The thickness of the graphene can be one to a few atomic layers. In the present context, while the following description and Examples describe in detail nanostructures in 0D, 1D, or 3D form, it is to be understood and appreciated that the form of the nanostructures is not limited to such only and accordingly, forms such as 2D nanostructures are also included. Further, a mixture of different dimensional nanostructures can be used for the formation of graphene, such as but not limited to, a mixture of 0D and 1D nanostructures, a mixture of 0D and 3D nanostructures, a mixture of 1D and 3D nanostructures, or a mixture of 0D, 1D, and 3D nanostructures.

**[033]** In the present context, the nanostructures are metallic. The metallic nanostructures advantageously and simultaneously act as substrates for the growth of graphene thereon and as catalysts for the formation and growth of graphene. The nanostructures can be formed of pure metals, mixtures of metals, alloys, or metal-carbon mixtures. Examples of metallic nanostructures formed of pure metals include, but are not limited to, Ni, Co, Fe, Cu, Zn, Mn, Ga, Ge, As, Se, In, Sn, Sb, Te, Al, Pd, Pt, Au, Ag, Nb, Mo, Ta, W, Rh, Re, Ti, V, Cr, Zr, Hf, Ru, Os, Ir, or a mixture thereof. Examples of metallic nanostructures formed of alloys include, but are not limited to, at least one metal selected from the group consisting of Ni, Co, Fe, Cu, Zn, Mn, Ga, Ge, As, Se, In, Sn, Sb, Te, Al, Pd, Pt, Au, Ag, and/or at least one refractory metal selected from the group consisting of Nb, Mo, Ta, W, Rh, Re, Ti, V,

Cr, Zr, Hf, Ru, Os, and Ir. The molar percentage of the refractory metals in the alloy based on total content of the allow can vary from 0 to 40%. In addition, the metallic nanostructures can also be made of steels containing different types of alloying elements such as carbon steels, nickel steels, nickel-chromium steels, molybdenum steels, chromium steels, chromium-vanadium steels, tungsten steels, nickel-chromium-vanadium steels, or silicon-manganese steels. For example, the metallic nanostructures can be made of nickel-containing steels such as the steels with the SAE (Society of Automotive Engineers) grade 200 series, 300 series, and 800 series, such as, grade-310 and grade-316 stainless steels.

**[034]** In the present context, 0D graphene refers to graphene wrapped up into buckyball-shape particles continuously or discontinuously. The nanoparticles are substantially spherical, though not necessarily always the case. The "buckyball" is not limited to a spherical shape. 0D graphene can also be cylindrical, discoidal, tabular, ellipsoidal, equant or irregular in shape. The nanoparticles can be prepared by chemical reduction of metal precursors with surfactant and/or nano templates. The reduction can be carried out under hydrothermal conditions. Further, commercially available metallic nanoparticles are also suitable for use in the present methods. The nanoparticles can be used as such with or without further surface treatment.

**[035]** In the present context, 1D graphene refers to graphene rolled into nanofiber shape continuously or discontinuously. The nanofibers can be less than 1μm in diameter and above 5μm in length, with an aspect ratio of length/diameter of 5 or more. The cross-section of the nanofibers can be spherical, cylindrical, discoidal, tabular, ellipsoidal, equant or irregular shape. The core of the nanofibers can be hollow (i.e. nanotubes) or filled (i.e. nanorods). In various embodiments, the nanofibers are parallelly aligned, gridded (i.e. cross

aligned), or randomly grown with or without a substrate support. The nanofibers can be prepared by chemical reduction of metal precursors with surfactant and nano templates under hydrothermal conditions. The nanofibers can also be prepared by electrospinning, pyrolysis followed by $H_2$ reduction. In an exemplary embodiment, **Fig. 1** shows one example of Cu nanofibers prepared by electrospinning. The nanofibers can also be commercially available metallic nanofibers. The nanofibers can be used as such with or without further surface treatment.

**[036]** In various embodiments, the nanofibers are formed of core-shell structure. The core-shell structure can be formed by a metal comprised in the shell and a refractory metal, oxide or carbon based material comprised in the core. Examples of suitable metals, refractory metals, oxide or carbon based materials for forming the core-shell structure are described in above paragraphs. In certain embodiments, the core-shell nanofibers with a refractory metal in the core are prepared by a coaxial electrospinning method. Two solutions containing different metal precursors are electrospun at the same time through a coaxial needle. A first solution passes through an inner needle while a second solution passes through an outer needle. The thus-obtained wet nanofibers are then dried and annealed at 300 to 600°C in atmosphere for 0.5 to 4 hours to obtain the metal oxide nanofibers. The metal oxide nanofibers are further reduced in a $H_2$ atmosphere for 0.5 to 3 hours to obtain metallic nanofibers.

**[037]** In further embodiments, core-shell nanofibers with oxide in the core are prepared by the electrospinning of a solution containing the metal precursor and at least one polymer selected from poly(vinyl alcohol) (PVA), polyaniline (PANI), poly(vinyl pyrrolidone) (PVP), polyethylene oxide (PEO), polycarbonate (PC), polymethylmethacrylate (PMMA),

nylon, polyurethane, polylactic acid, polystylene (PS), polyimide (PI), polyvinyl chloride (PVC), polyvinyl phenol, polypropylene (PP), polyethylene (PE), polyethylene naphthalate (PEN), polyethylene terephthalate (PET), cellulose acetate, collagen, proteins, sugar, natural polymers, modified natural polymers, synthetic polymers, or their copolymers. The wet composite nanofibers are heated at 150 to 550°C for about 1 hour in atmosphere to obtain the oxide nanofibers. The nanofibers are then heated at 300 to 750°C in argon and $H_2$ mixed gases environment for a short period ranging from 0.5 to 60 min to reduce the surface layer of the nanofibers to metal while the core is kept to be oxide.

**[038]** In yet further embodiments, the core-shell nanofibers with metal in the shell and carbon in the core are prepared by the electrospinning of a solution containing the metal precursor and at least one polymer selected from PVA, PANI, PVP, PEO, PC, PMMA, PS, PI, PVC, PP, PE, PEN, PET, nylon, polyurethane, polylactic acid, polyvinyl phenol, cellulose acetate, collagen, proteins, sugar, natural polymers, modified natural polymers, synthetic polymers, or their copolymers. The wet composite nanofibers are heated to 100 to 350°C at the ramping rate of 0.1 to 10°C/min and dwelled for 1 to 2 hour in atmosphere. The samples are then ramped up to 300 to 600°C in argon and dwelled for another 0.5 to 3 hours. Finally the nanofibers are reduced in $H_2$-containing atmosphere for 0.5 to 30 min. **Fig. 2A** and **Fig. 2B** show examples of the core-shell nanofibers with copper in the shell and the carbon in the core.

**[039]** Porous foams are 3D metallic material containing large volume fraction of pores that are connected to each other to form an interconnected network. The porosity of the foams is defined to be more than 30 vol%. The pore size is in the range of several nanometers to hundreds of micrometers. The foams can be prepared by directly foaming the

metal melts with gas injection, or adding blowing agents such as metal hydride and $CaCO_3$ followed by solidification. The foams can also be commercially available foams. For example, commercially available foams include Ni or Cu based foams supplied by Lyrun Metal Foam (China), Mitshubshi Materials corporation (Japan), Reade Advanced Materials (USA) or RECEMAT Internationals (Netherlands).

**[040]** In the present context, 3D graphene refers to graphene crosslinked into porous foams or aerogels. The pores inside the foams or aerogels are varied in a few nanometers to tens of micrometers in size. Porous aerogels are similar to the porous foams except that the pores and the walls between the pores are less than 100 nm. The porosity of the aerogels is defined to be more than 80 vol%. The aerogels can be prepared by a sol-gel processing method in which, the metal alkoxides or metal inorganic salt are first mixed in a solvent with chelating agents, surfactant and/ or polymers, followed by crosslinking them into M-O-M or M-OH-M networks (where M: metal; O: oxygen; H: hydrogen) by hydrolysis and condensation reactions. When the crosslinking is stopped, the solution turns into a gel. After driving off the solvent by supercritical drying, freeze drying or vacuum drying, the gel is annealed and then reduced to aerogel. The aerogels can also be commercially available aerogels.

**[041]** The method includes coating the metallic nanostructure with a layer of liquid carbon precursor. By "coating" is meant that a layer of the liquid carbon precursor is applied onto the metallic nanostructure surface. The metallic nanostructure surface may be coated entirely or partially with the layer of the liquid carbon precursor. The coating step may be carried out once, twice, thrice, or more. The thickness of the coating layer may be less than 100 nm, such as 90 nm, 80 nm, 70 nm, 60 nm, 50 nm, 40 nm, 30 nm, 20 nm, 10 nm, or less.

**[042]** In certain embodiments, the coating step comprises dip coating. For example, in the dip coating step, the metallic nanostructure is dipped into a liquid carbon precursor coating solution and then is withdrawn from the solution at a controlled speed. Coating thickness generally increases with faster withdrawal speed. A faster withdrawal speed pulls more fluid up onto the surface of the metallic nanostructure before it has time to flow back down into the solution. The coating thickness is primarily affected by fluid viscosity, fluid density, and surface tension. The applied coating may remain wet for several minutes until the solvent evaporates. Once the layer is formed, another layer may be applied on top of it with another dip coating step.

**[043]** In alternative embodiments, the coating step comprises spin coating. For example, in the spin coating step, an excess amount of the liquid carbon precursor solution is placed on a substrate including the metallic nanostructures, which is then rotated at high speed in order to spread the fluid by centrifugal force. Rotation is continued while the fluid spins off the edges of the substrate, until the desired thickness of the coating is achieved. The higher the angular speed of spinning, the thinner the coating.

**[044]** In yet further embodiments, the coating step comprises spray coating. For example, in the spray coating step, a spraying equipment is used to apply the liquid carbon precursor solution by pressurizing the solution and atomizing the solution into small droplets depositing onto the surface of the metallic nanostructures.

**[045]** In various embodiments, the liquid carbon precursor comprises a hydrocarbon compound in liquid phase at room temperature (i.e. 25°C) and atmospheric pressure (i.e. 101.325 kPa). The liquid carbon precursor wets the surface of the metallic nanostructure with a contact angle of less than 90°. Examples of the liquid carbon precursors include, but

are not limited to, $C_5$-$C_{12}$ alkanes (e.g. pentane, octane, dodecane), $C_{18}$-$C_{60}$ alkenes and their polymers and copolymers, alkyne and their polymers and copolymers, polyol compounds and their polymers and copolymers (e.g. ethylene glycol, propylene glycol, dipropylene glycol, glycerol, poly(ethylene glycol), polypropylene glycol, ethers, polyethers, esters, carboxylic acids, aromatic compounds, mineral oils (e.g. paraffinic oils, naphthenic oils, aromatic oils), vegetation oils (e.g. olive oil, palm oil, soybean oil, canola oil, pumpkin seed oil, corn oil, sunflower oil, safflower oil, peanut oil, grape seed oil, sesame oil, argan oil), animal oil (e.g. fish oil), synthetic oil and their mixtures. Further exemplary liquid carbon precursors can also be polymer containing solutions. The weight percentage of the polymers in the solutions should be less than 40%. The polymers can have -C(-C)$_n$-C- as the main chains. Examples include, but are not limited to, PVA, PANI, PVP, PEO, PMMA, PE, PP, PS, PEN, nylon, polyvinyl phenol, natural polymers, modified natural polymers, synthetic polymers and their copolymers.

**[046]** The method further includes carbonizing the layer of liquid carbon precursor coated on the metallic nanostructure at a carbonizing temperature to convert the layer of liquid carbon precursor to a layer of amorphous carbon. By "carbonizing" is meant converting the liquid carbon precursor into carbon residue through pyrolysis, and in the present context, the carbon residue is amorphous carbon, which is a carbon material without long-range crystalline order.

**[047]** In various embodiments, the carbonizing step includes heating the layer of liquid carbon precursor coated on the metallic nanostructure at a carbonizing temperature of 180 to 600 °C, such as 200 to 550 °C, 200 to 500 °C, 200 to 450 °C, 200 to 400 °C, 200 to 350 °C, or 200 to 300 °C. The carbonizing temperature can be appropriately determined by a

person skilled in the art once the composition/nature of the liquid carbon precursor used in the coating step is known. In one exemplified embodiment, liquid carbon precursor used in the coating step is polyethylene glycol (PEG200) and the carbonizing temperature selected for the carbonizing step can be from 200 to 300 °C, such as about 250 °C.

**[048]** In further embodiments, the carbonizing step includes heating the layer of liquid carbon precursor coated on the metallic nanostructure for a period of 1 to 120 min, such as 10 to 110 min, 10 to 100 min, 10 to 90 min, 10 to 80 min, 10 to 70 min, 10 to 60 min, 10 to 50 min, or 10 to 40 min. The period for the carbonizing step can be appropriately determined by a person skilled in the art once the composition/nature of the liquid carbon precursor used in the coating step and therefore the carbonizing temperature are known. In one exemplified embodiment, liquid carbon precursor used in the coating step is polyethylene glycol (PEG200), the carbonizing temperature selected for the carbonizing step is about 250 °C, and the period for carbonizing at this temperature can be from 20 to 40 min, such as 30 min.

**[049]** The carbonizing step may be carried out in an enclosed environment or heating chamber, such as a furnace. The furnace can be pre-heated to the carbonizing temperature of between 180 and 600 °C such that the dwelling time is kept to a minimum. The coated metallic nanostructure may be loaded into the furnace immediately after the coating step so that the maximum thickness of the layer of the liquid carbon precursor is maintained at the surface and therefore converted to the layer of amorphous carbon. Alternatively, if a thinner layer of graphene is desired to be formed (for example, when the graphene is used to form transparent electrodes to be described in later paragraphs), the coated metallic nanostructure

may be allowed to dry off or otherwise reduce the thickness of the coating of the liquid carbon precursor before loading into the furnace for carbonization.

**[050]** In various embodiments, the carbonizing step is carried out in a non-oxidising environment, such as an inert or a reductive environment. For example, the carbonizing step is carried out in an inert environment filled with argon (Ar). In another example, the carbonizing step is carried out in a reductive environment filled with a gas mixture of Ar and hydrogen ($H_2$).

**[051]** In further embodiments, the carbonizing step is carried out in an inert or a reductive environment with a total gas flow rate of 200 to 500 sccm, such as 200 to 450 sccm, 200 to 400 sccm, 200 to 350 sccm, 200 to 300 sccm, or 200 to 250 sccm. In one embodiment, the carbonizing step is carried out in a reductive environment with a total gas flow rate of about 200 sccm, and the gas mixture comprises a molar ratio of 1:5 ($H_2$:Ar).

**[052]** After forming the layer of amorphous carbon on the metallic nanostructures, the method next includes crystallizing the layer of amorphous carbon at a crystallizing temperature to convert the layer of amorphous carbon to a layer of crystallized graphene. In this crystallizing step, the non-crystalline ordered amorphous carbon is heated to a point where the carbon atoms are re-arranged to form a one-atom-thick planar sheet of $sp^2$-bonded carbon atoms that are densely packed in a honeycomb crystal lattice, i.e. graphene.

**[053]** The crystallizing step is carried out in an enclosed environment. In various embodiments, the crystallizing step includes increasing the temperature to a crystallizing temperature of 450 to 1,000 °C, such as 450 to 650 °C, 450 to 750 °C, 450 to 850 °C, 450 to 950 °C, 450 to 1000 °C. In illustrative embodiments, the crystallizing step includes increasing the temperature to a crystallizing temperature of about 750 or 800 °C.

**[054]** In certain embodiments, the crystallizing step is carried out in the same furnace where the carbonizing step is carried out. In alternative embodiments, the crystallizing step is carried out in another enclosed environment or heating chamber. In the embodiments where both the carbonizing and crystallizing steps are carried out in the same furnace, after carbonizing the metallic nanostructures at the carbonizing temperature for a dwelling period, the furnace is quickly brought to the crystalling temperature without removing the carbonized metallic nanostructures from the furnace. In various embodiments, the temperature of the furnace is quickly brought up to the crystallizing temperature at a ramping rate of 0.5 to 200 °C/min, such as 5 to 180 °C/min, 5 to 160 °C/min, 5 to 140 °C/min, 5 to 120 °C/min, 5 to 100 °C/min, or 10 to 100 °C/min. After ramping up the temperature to the crystallizing temperature, the crystallizing temperature is maintained for a period of time. For example, the furnace is maintained at the crystallizing temperature for 1 sec to 30 min, such as 5 sec to 25 min, 1 to 20 min, 5 to 20 min, or 5 to 15 min. In exemplified embodiments, the crystallizing temperature is maintained for about 5 min, or 8 min, or 15 min.

**[055]** In various embodiments, the crystallizing step is carried out in a non-oxidising environment, such as an inert or a reductive environment. For example, the crystallizing step is carried out in an inert environment filled with argon (Ar). In another example, the crystallizing step is carried out in a reductive environment filled with a gas mixture of Ar and hydrogen ($H_2$).

**[056]** In further embodiments, the crystallizing step is carried out in an inert or a reductive environment with a total gas flow rate of 200 to 500 sccm, such as 200 to 450 sccm, 200 to 400 sccm, 200 to 350 sccm, 200 to 300 sccm, or 200 to 250 sccm. In one embodiment, the

crystallizing step is carried out in a reductive environment with a total gas flow rate of about 200 sccm, and the gas mixture comprises a molar ratio of 1:5 ($H_2$:Ar).

**[057]** In either one of the carbonizing step or crystallizing step, or both, the heating environment may be provided by, for example, induction heating, radiant heating, infrared, ultraviolet, microwave, laser, or plasma. Other heating sources or means may likewise be used.

**[058]** The method further includes quenching the layer of crystallized graphene to form the graphene. During the crystallizing step, the carbon atoms rearrange their order and arrangement. Once the crystal lattice of graphene is formed, the crystallized graphene is quenched to fix the orderly arrangement permanently. By "quenching" is meant rapid cooling of the heated and crystallized graphene layer on the metallic nanostructure.

**[059]** In various embodiments, the quenching step includes reducing the temperature of the layer of crystallized graphene to room temperature in less than a few minutes, such as less than 10 min, 9 min, 8 min, 7 min, 6 min, 5 min, 4 min, 3 min, 2 min, 1 min, or less. For example, the quenching step can be carried out in an inert environment with a total gas flow rate of 50 to 200 sccm to rapidly cool the layer of crystallized graphene. The inert environment may be provided by Ar or a mixture of Ar and $H_2$. Alternatively, the quenching step may be carried out by immersing the heated and crystallized graphene layer on the metallic nanostructure in a bath of quenching medium. The bath of quenching medium may be provided by ice water, for example.

**[060]** In certain embodiments, the metallic nanostructures may be etched away to obtain pure 0D, 1D, or 3D graphene. For example, the metallic nanostructures may be etched with

an etching solution such as, but is not limited to, hydrochloride acid, nitric acid, hydrofluoric acid, sulfate acid, or a mixture thereof.

**[061]** The so-formed graphene, with or without the metallic nanostructures, may be used to further form electrodes or nanocomposite heat spreader.

**[062]** Thus, in another aspect, a method of forming an electrode comprising graphene is provided. The method comprises:

(a) forming at least one layer of metallic nanostructures on a substrate;

(b) coating the metallic nanostructures with a layer of liquid carbon precursor;

(c) carbonizing the layer of liquid carbon precursor coated on the metallic nanostructures at a carbonizing temperature to convert the layer of liquid carbon precursor to a layer of amorphous carbon;

(d) crystallizing the layer of amorphous carbon at a crystallizing temperature to convert the layer of amorphous carbon to a layer of crystallized graphene; and

(e) quenching the layer of crystallized graphene.

**[063]** The coating, carbonizing, crystallizing, and quenching steps in forming graphene have been described in detail in previous paragraphs corresponding to the respective step in the first aspect and are not repeated hereinafter. In addition, it is to be understood and appreciated that the forming of at least one layer of metallic nanostructures on a substrate (i.e. step (a)) can be carried out before or after forming the graphene.

**[064]** The substrate can be rigid or flexible such that rigid or flexible electrodes comprising graphene can be formed. Further, transparency of the electrodes can be tuned

from being transparent to non-transparent by tuning the thickness and/or number of layers of graphene formed on the electrodes.

**[065]** Transparent conductive electrodes comprising graphene formed herein possess the following characteristics: (1) large surface area, (2) high electronic conductivity and thermal conductivity, (3) excellent chemical stability, (4) high flexibility, and (5) work function at about 4.6 eV, close to that of tin indium oxide (ITO, 4.7 eV). Further, the transparency of the transparent conductive electrodes can be in the range of 50 to 99.9% and the sheet resistance in the range of 1 to 1000 Ω/sq. The transparent electrodes may be employed for touch screens, thin-film solar cell, flexible displays, or solid-state lighting especially organic light emitting diodes.

**[066]** While the graphene described herein relates mostly to 0D or 1D graphene, 3D graphene are equally suitable depending on the intended use or applications. The 1D nanofibers can be processed to form parallel, crossed, or random patterns. The transparency of the graphene films can be adjusted by controlling the graphene nanofiber or nanoparticle density and coating thickness. Nanofiber or nanoparticle density here refers to the number of the nanofibers or nanoparticle per $cm^2$. The substrates used may be rigid transparent substrates, such as but are not limited to, glass, BK7 (a kind of borosilicate crown optical glass), fused silica, crystal quartz, $CaF_2$, ZnSe, sapphire, $MgF_2$, MgO, Germanium (Ge), and calcite ($CaCO_3$). The substrates used may also be flexible transparent substrates such as, but are not limited to, polydimethylsiloxane (PDMS), PET, PEN, PC, PVA, polyethersulfone (PES), PVC, PI, PMMA, or various commercial available acrylic glass.

**[067]** In various embodiments where rigid electrodes are desired, the forming step comprises electrospinning the metallic nanostructures onto a rigid substrate and annealing

the rigid substrate to form the at least one layer of metallic nanostructures thereon. For example, to prepare transparent conductive electrodes on a rigid substrate, graphene nanofibers may be grown on the rigid transparent substrates such as quartz, fused silica, or sapphire.

**[068]** In an illustrative embodiment, the growth process is schematically illustrated in **Fig. 3**. Firstly, the nanofibers are formed by electrospinning, followed by pyrolysis and $H_2$ reduction. The electrospinning solution consists of at least one metal precursor and one polymer. The metal precursors may be, but are not limited to, metal acetate, ethoxide, propoxide, butoxide, acetylacetonate, nitrate, chloride, fluoride, suphate, or phosphate. At least 10% of the metal precursors are easily ionisable, such as metal nitrate, chloride, fluoride, suphate, or phosphate. The polymers may be PVA, PANI, PVP, PEO, or PC. After electrospinning, the obtained electrospun composite nanofibers are then dried and annealed at 300 to 600 °C in atmosphere for 0.5 to 4 hours to form the pure metal oxide nanofibers. The metal oxide nanofibers are next reduced to metal nanofibers in $H_2$ atmosphere for 0.5 to 3 hours. The prepared metal nanofibers are then coated with a liquid carbon precursor and loaded into a tube furnace which was pre-filled with a 1:5 mixture of $H_2$ and Ar at a total gas flow rate of 200 to 500 sccm. The liquid carbon precursor is first carbonized to amorphous carbon at a carbonizing temperature of 300 to 600 °C for 1 to 40 minutes, followed by crystallizing into graphene at a crystallizing temperature of 450 to 900 °C. During the carbonizing and/or crystallizing step, the nanofibers simultaneously are annealed and attached to the rigid substrate. The carbonizing time and/or crystallizing time for graphene formation is typically in the range of tens of seconds to a few minutes, which determines the number of layers of graphene finally grown on the nanofiber and also serves

to avoid the deformation of the metallic nanofibers. The crystallized graphene is then quenched to room temperature within a few minutes in a flow of 200 sccm Ar to form graphene nanofibers with a metal in the core, and thus the transparent conductive electrodes on a rigid substrate.

**[069]** In various embodiments where flexible electrodes are desired, such as transparent conductive electrodes on flexible substrates, the forming step comprises coating metallic nanostructures with a layer of liquid carbon precursor, carbonizing the layer of liquid carbon precursor coated on the metallic nanostructures at a carbonizing temperature to convert the layer of liquid carbon precursor to a layer of amorphous carbon, crystallizing the layer of amorphous carbon at a crystallizing temperature to convert the layer of amorphous carbon to a layer of crystallized graphene, quenching the layer of crystallized graphene to obtain metallic nanostructures coated with graphene, coating a polymer solution on the metallic nanostructures coated with graphene, wherein the polymer solution comprises the polymer of a flexible substrate, and curing the polymer solution to form a polymer film having the metallic nanostructures coated with graphene. The cured polymer film may then be peeled off to form free-standing flexible electrode. In one illustrative embodiment, metallic nanofibers are first prepared. For example, parallel or cross aligned (i.e. gridded) Ni nanofibers are prepared by electrospinning using a rotating, electrically-grounded wheel as the receptor. The above described graphene formation steps are then carried out on the Ni nanofibers. After growing graphene, the graphene nanofibers are transferred onto flexible substrates such as PDMS, PES, PET, PEN, PC, PVA, PVC, PI, PMMA. In this step, the polymer solution of the substrate is spin coated or slowly poured onto the graphene nanofibers and cured at 50 to 100 °C. Next, the polymer layers buried

with the parallel or cross patterned graphene nanofibers are peeled off to form a self-stand electrode.

**[070]** Non-transparent conductive electrodes are the electrodes with transparency less than 50%, such as less than 40%, 30%, 20%, 10%, or less, and sheet resistance in the range of 1 to 500 Ω/sq, such as 1 to 400 Ω/sq, 1 to 300 Ω/sq, 1 to 200 Ω/sq, or 1 to 100 Ω/sq. The non-transparent conductive electrodes referred herein can be used as electrodes for various electronics, batteries, supercapacitors and hydrogen storage, RFID (radio frequency identification) antennas, flexible circuits, LED strings/arrays and for EMI (electromagnetic) shielding.

**[071]** In various embodiments, more than one layer of metallic nanostructures is formed on the substrate. The substrate can be rigid or flexible. By forming more than one layer of metallic nanostructures, such as two layers, three layers, or more, transparency of the thus-formed conductive electrode is gradually reduced. In certain embodiments, the transparency of the conductive electrode may tuned from being transparent to non-transparent state. For example, the non-transparent electrode is a graphene paper consisting of 1D graphene with or without the metallic nanostructure template. The 1D graphene may be grown on nanofibers formed by electrospinning followed by pyrolysis and $H_2$ reduction described above. The nanofibers may be interlaced with each other to form a layer with a total thickness of more than 1 μm, for example. After coating with the liquid carbon precursor, the nanofiber layers are then carbonized, crystallized, and quenched to form the graphene paper. The graphene paper may be etched to remove the metallic nanostructure template. The advantage of the graphene paper produced by this procedure is that there is no polymer binder or surfactant contained in the papers. Further, by controlling the number of

nanostructure layers and therefore the total thickness of the resultant graphene paper, transparency of the electrode can be tuned.

**[072]** In alternative embodiments, 3D graphene are used to form non-transparent electrodes. For example, free-standing 3D graphene porous foams or aerogels with or without the metallic nanostructure template may be used. The pore size in the electrodes may be less than 1 μm and porosity may be higher than 50%. The 3D graphene porous foam or aerogel electrodes have the following features: (1) ultralarge surface area; (2) flexible; (3) highly conductive; (4) excellent chemical stability; and (5) with a work function at about 4.6 eV, close to that of tin indium oxide (ITO, 4.7 eV).

**[073]** In another aspect, a method of forming an electrode comprising graphene is provided. The method comprises:

(i) coating metallic nanostructures with a layer of liquid carbon precursor;

(ii) carbonizing the layer of liquid carbon precursor coated on the metallic nanostructures at a carbonizing temperature to convert the layer of liquid carbon precursor to a layer of amorphous carbon;

(iii) crystallizing the layer of amorphous carbon at a crystallizing temperature to convert the layer of amorphous carbon to a layer of crystallized graphene;

(iv) quenching the layer of crystallized graphene to obtain metallic nanostructures coated with graphene;

(v) dispersing the metallic nanostructures coated with graphene in a solution;

(vi) coating the solution of (v) onto a substrate; and

(vii) drying the coating of (vi).

[074] The coating, carbonizing, crystallizing, and quenching steps in forming graphene have been described in detail in previous paragraphs corresponding to the respective step in the first aspect and are not repeated hereinafter.

[075] The electrodes formed can be transparent or non-transparent.

[076] In various embodiments, the transparent conductive electrodes are prepared by coating a graphene-containing solution on either rigid or flexible transparent substrates. The graphene used herein can be nanoparticles or nanofibers. The graphene nanoparticles or nanofibers may be ultrasonically dispersed to form a graphene solution. The graphene solution may contain 0.1 to 60 wt% of the graphene nanoparticles and/or nanofibers, 0 to 10 wt% of surfactants and 0 to 30 wt% polymeric binders. The surfactant used may include, but is not limited to, sodium dodecylbenzene sulfonate (SDBS), alkylazides, 11-azidoundecanol (AUO), 11-azidoundecanoic acid,sodium cholate, cetyltrimethylammonium bromide, hexadecyl trimethyl ammonium bromide, triton X-100, or PVP. The polymer binder may include, but is not limited to, polyurethane resin, polyester resin, alkyd resin, butyral resin, acetal resin, polyamide resin, acrylic resin, styrene-acrylic resin, styrene resin, nitrocellulose, benzyl cellulose, styrene-maleic anhydride resin, polybutadiene resin, poly(vinyl chloride) resin, poly(vinyl acetate) resin, fluororesin, silicone resin, epoxy resin, phenol resin, maleic acid resin, urea resin, melamine resin, benzoguanamine resin, ketone resin, rosin, chlorinated polyolefin resin, or chlorinated polyurethane resin. The type of the polymer binder used can be determined by the criteria of the coating method and the types of substrates used. The solvent of the graphene solution may include, but is not limited to, de-ionized water, organic solvent such as methanol, ethanol, iso-propanol, n-butanol, i-butanol, neopentyl butanol, hexanol, octanol, ethylene glycol, benzyl alcohol, chloroform,

*N*-methyl-pyrrolidone, *N*-methyl-2-pyrrolidone (NMP), dimethylformamide (DMF), glycidyl ether such as n-butyl glycidyl ether (BGE), isopropyl glycidyl ether (IGE) and phenyl glycidyl ether (PGE), aromatic solvent such as benzene, toluene, xylene, ethyl benzene, diethyl benzene, $C_5$-$C_{20}$ alkyl benzene, chlorobenzene, or dichlorobenzene. The graphene solution may be coated onto the substrates by spray coating, dip coating, spin coating or mayer-rod coating methods. The obtained wet coatings are then hot pressed by a punch laminator to improve the adherence of the coatings. The temperature for the laminating may be set at 25 to 180 °C. The graphene solutions may also form patterned electrodes by screen printing or inkjet printing.

**[077]** In various embodiments, the graphene used for forming non-transparent electrodes is 0D and/or 1D graphene with or without metallic nanostructure template. The 0D and/or 1D graphene is firstly ultrasonically dispersed in a solution to form an ink and then coated onto a substrate. The substrates can be rigid or flexible materials such as, but are not limited to, non-transparent materials including ceramics (for example, $Al_2O_3$ and $ZrO_2$), metals, oxides, semiconductors (for example, Si, GaN, GaAs, InAs and InP) and polymers. The substrates may also be ceramic, metal, oxide, semiconductor, or polymer foams. Compared to the graphene solutions for forming transparent electrodes, the graphene solutions in such cases contain a higher content of graphene, for example, 30 to 80 wt% of graphene, 0 to 10 wt% of surfactants and 0 to 20 wt% polymeric binders. The surfactant may include, but is not limited to, SDBS, alkylazides, AUO, 11-azidoundecanoic acid, sodium cholate, cetyltrimethylammonium bromide, hexadecyl trimethyl ammonium bromide, triton X-100, or PVP. The polymer binder may include, but is not limited to, thermosetting polymer such as polyurethane resin, polyester resin, alkyd resin, butyral resin, acetal resin, polyamide

resin, acrylic resin, styrene-acrylic resin, styrene resin, nitrocellulose, benzyl cellulose, styrene-maleic anhydride resin, polybutadiene resin, poly(vinyl chloride) resin, poly(vinyl acetate) resin, fluororesin, silicone resin, epoxy resin, phenol resin, maleic acid resin, urea resin, melamine resin, benzoguanamine resin, ketone resin, rosin, chlorinated polyolefin resin, or chlorinated polyurethane resin. The solvent of the graphene solution may include, but is not limited to, de-ionized water, organic solvent such as methanol, ethanol, iso-propanol, n-butanol, i-butanol, neopentyl butanol, hexanol, octanol, ethylene glycol, propylene glycol, benzyl alcohol, chloroform, *N*-methyl-pyrrolidone, DMF, glycidyl ether such as BGE, IGE and PGE, and aromatic solvent such as benzene, toluene, xylene, ethyl benzene, diethyl benzene, $C_5$-$C_{20}$ alkyl benzene, chlorobenzene, or dichlorobenzene. The inks may be coated onto the substrates by mayer-rod coating, spray coating, dip coating, or spin coating. The coatings are then dried by a hot plate or oven with a temperature of 80 to 150 °C. The graphene inks may also form the patterned electrodes by screen printing or inkjet printing.

**[078]** In yet further aspect, a method of forming a heat spreader comprising graphene nanocomposite is disclosed. The method comprises:

(i) coating metallic nanostructures with a layer of liquid carbon precursor;

(ii) carbonizing the layer of liquid carbon precursor coated on the metallic nanostructures at a carbonizing temperature to convert the layer of liquid carbon precursor to a layer of amorphous carbon;

(iii) crystallizing the layer of amorphous carbon at a crystallizing temperature to convert the layer of amorphous carbon to a layer of crystallized graphene;

(iv) quenching the layer of crystallized graphene to obtain metallic nanostructures coated with graphene;

(v) mixing the metallic nanostructures coated with graphene with a metal powder;

(vi) processing the mixture of (v) to form the graphene nanocomposite .

**[079]** The coating, carbonizing, crystallizing, and quenching steps in forming graphene have been described in detail in previous paragraphs corresponding to the respective step in the first aspect and are not repeated hereinafter.

**[080]** In various embodiments, the processing step comprises hot pressing, moulding, or sintering the mixture of the metallic nanostructures coated with graphene and the metal powder.

**[081]** The step of processing the graphene nanocomposite may further include sawing, machining and polishing the nanocomposite article to the desired shape or size.

**[082]** In illustrative embodiments, a nanocomposite comprising 0.1 to 80 wt% of graphene prepared herein and 20 to 99.9 wt% of metal matrix is developed for heat spreading. The graphene used may be 0D, 1D and/or 3D graphene, such as 1D and 3D graphene with or without the metallic nanostructure template. The metal matrix may include metals with high thermal conductivity (more than 100 W/mK), such as but are not limited to, copper, aluminum, silver, gold, molybdenum, or alloy thereof. The nanocomposite containing the as-prepared graphene has an improved thermal conductivity compared to the pure metal matrix. Due to this improved and superior thermal conductivity, the nanocomposite containing graphene may be used to form thermal conducting components such as heat spreaders and heat sinks for high power electronic packaging,

integrated circuits (for example, CPUs or chipsets), display device (for example, plasma display panel or liquid crystal display) and other thermal management applications.

**[083]** In various embodiments, nanoparticles with copper as the nanostructure template are used to form nanocomposites. The nanoparticles may be used alone or mixed with other metal powders having high thermal conductivity to form the nanocomposite. The nanoparticles are firstly mixed and then placed in a graphite die to form a pellet. The pellet is then hot pressed at a temperature of 650 to 850 °C and a pressure of 30 to 120 MPa for 1 to 45 minutes to form a nanocomposite with relative density higher than 90% compared to pure copper density. Alternatively, the pellet may be sintered by spark plasma sintering to form the nanocomposite. The sintering may be performed at a temperature ranging from 500 to 700 °C and a working pressure of 50 to 100 Mpa for 1 to 15 minutes. Finally, processing steps such as sawing, machining and polishing may be performed to manufacture a plate having a desired shape and size. The plate may be used as a heat spreader or heat sink.

**[084]** In alternative embodiments, nanofibers with copper as the nanostructure template are used to form the nanocomposite. The nanofibers may be dispersed in a solvent with a low evaporation temperature such as alcohol, acetone or isopropanol. Then metal nanopowders are added into the solution with mechanically stirring. The average size of the metal nanopowders may be less than 1 μm. The mixture is then centrifuged, dried and hot pressed or spark plasma sintered at 500 to 1,100 °C to form the nanocomposite. Alternatively, the mixture may also be cold pressed at room temperature and sintered at 650 to 1,200 °C under vacuum or by microwave. Finally, processing steps such as sawing,

machining and polishing may be performed to manufacture a plate having a desired shape and size. The plate may be used as a heat spreader or heat sink.

**[085]** In yet further embodiments, 1D or 3D graphene in dry form is used. The 1D or 3D graphene is added into a hot melting metal liquid with mechanical stirring. The mixed solution may then be poured into a mold and gradually cooled down to form the nanocomposite with various desired shape and size.

**[086]** In order that the invention may be readily understood and put into practical effect, particular embodiments will now be described by way of the following non-limiting examples.

**[087]** **Examples**

**[088]** Example 1: Preparation of 0D graphene

**[089]** A sample of copper nanoparticles purchased from Alfa Aesar (MA, USA) were dip coated with a thin layer of polyethylene glycol (PEG) with molecular weight of 200 (PEG200) which were then dissolved in ethanol. The PEG coated copper nanoparticles were then transferred to a tube furnace pre-filled with Ar and heated at 250 °C for 30 min. The nanoparticles were then rapidly heated to 800 °C and dwelled for 5 min. After that, the nanoparticles were quenched to room temperature within a few minutes in a flow of 200 sccm Ar.

**[090]** **Fig. 4A** and **Fig. 4B** show FESEM image and Raman spectra, respectively, of the 0D graphene with Cu nanoparticle as the template.

**[091]** Example 2: Preparation of 1D graphene

**[092]** A sample of nickel nanofibers was prepared by electrospinning a solution containing 10 wt% nickel acetate, 4 wt% nickel chloride, 12 wt% polyacrylonitrile (PAN)

polymer and 74 wt% N, N dimethylformamide, followed by pyrolysis at 500 °C for 1 hour. The nanofibers were then reduced in $H_2$ at 500 °C for 30 min. The nickel nanofibers are then dip coated with a thin layer of PEG200 solution. The PEG200 coated Ni nanofibers were then transferred to a tube furnace pre-filled with Ar and heated at 250 °C for 30min. The nanofibers were then rapidly heated to 800 °C and dwelled for 5 minute. After that, the nanofibers were quenched to room temperature within a few minutes in a flow of 200 sccm Ar.

**[093]** **Fig. 5A** and **Fig. 5B** show FESEM image and Raman spectra, respectively, of 1D graphene with Ni nanofibers as the template. The G and 2D peaks are the characteristic peaks for graphene. The D peak with extremely low intensity indicates the obtained graphene has few defects.

**[094]** Example 3: Preparation of 3D graphene

**[095]** A sample of nickel foam with pore size of a few micrometers (purchased from Reade Advanced Materials, USA) was dip coated with a thin layer of PEG200 solution. The PEG200 coated nickel foam was then transferred to a tube furnace pre-filled with Ar and heated at 250 °C for 30 min. The foam was then rapidly heated to 800 °C and dwelled for 5 minute. After that, the foam was quenched to room temperature within a few minutes in a flow of 200 sccm Ar.

**[096]** **Fig. 6A** and **Fig. 6B** shows FESEM image and Raman spectra, respectively, of 3D graphene with Ni foam as the template. The G and 2D peaks are the characteristic peaks for graphene. The D peak with extremely low intensity indicates the obtained graphene has few defects.

**[097]** Example 4: Preparation of rigid transparent electrode

**[098]** A sample of a thin layer of nickel composite nanofiber was prepared by electrospinning a solution containing 10 wt% nickel acetate, 12 wt% PAN polymer, and 78 wt% N,N dimethylformamide on a PAN coated quartz substrate with a size of 2 cm × 7.5 cm. The sample was then pyrolyzed at 500 °C for 30 minutes and then reduced by $H_2$ for 10 min. The nickel nanofibers were then spin coated with a thin layer of PEG200. The PEG200 coated nanofibers were then transferred to a tube furnace pre-filled with Ar and heated at 250 °C for 30 min. The nanofibers were then rapidly heated to 750 °C and dwelled for 8 minute. After that, the nanofibers were quenched to room temperature within a few minutes in a flow of 50 sccm Ar.

**[099]** The rigid transparent electrodes formed thereof have a transparency of about 80-90% at a wavelength of 300-1100 nm and possess a sheet resistivity of about 50 Ω/sq.

**[0100]** **Fig. 7** shows the transmission spectra of the graphene nanofiber films with Ni in core.

**[0101]** Example 5: Preparation of flexible transparent electrode

**[0102]** Graphene nanofibers prepared in Example 2 were ultrasonically dispersed in a solution of 3 mg/ml polymer binder, polyvinyl pyrroridol (PVP). The solution was then mayer-rod coated on an A4-sized polyethylene terephthalate (PET) sheet.

**[0103]** The flexible transparent electrodes formed thereof have a transparency of about 85-90% at a wavelength of 300-1100nm and possess a sheet resistivity of about 70 Ω/sq.

**[0104]** Example 6: Preparation of patterned, flexible and transparent electrodes

**[0105]** Parallel Ni nanofibers and cross aligned Ni nanofibers were separately prepared by electrospinning using a rotating, electrically-grounded wheel as a receptor. In each case, after growing graphene on the Ni nanofibers, the nanofibers were transferred onto flexible

substrates, such as polydimethylsiloxane (PDMS). In this step, a Sylgard 184 silicone elastomer kit produced by Dow Corning Corporation was used to produce the PDMS substrate. The base and its curing agent was mixed in 10:1 mass ratio and the solution was then slowly poured on the graphene nanofibers and cured at 70 °C for 12 hours. Finally, the films were peeled off to form a self-standing substrate with the parallel or cross patterned graphene electrodes.

**[0106] Fig. 8** shows field emission scanning electronic microscope (FESEM) image of parallel graphene nanofibers with Ni in the core.

**[0107] Fig. 9** shows FESEM image of crossed graphene nanofibers with Ni in the core.

**[0108]** Example 7: Preparation of non-transparent electrode with graphene foam

**[0109]** 3D graphene foam prepared in the Example 3 was cut into a thin layer with a thickness of about 100 μm. It was then bound to a dense copper foil to form an electrode with a high surface area.

**[0110]** Example 8: Preparation of non-transparent electrode-graphene paper

**[0111]** A layer of nickel composite nanofibers with a thickness of about 100 μm was prepared by electrospinning a solution containing 14 wt% nickel acetate, 12 wt% PAN polymer, and 74 wt% N,N dimethylformamide on an Al foil. The layer of nanofibers was then dried at 60 °C for 24 hours in vacuum to remove the solvent. The composite nanofiber layer was then peeled off to form a free-standing membrane. It was pyrolyzed at 500 °C for 30 minutes and then reduced by $H_2$ for 10 min. The layer of nickel nanofibers was then dip coated with a thin layer of PEG200. The layer of PEG200 coated Ni nanofibers was then transferred to a tube furnace pre-filled with Ar and heated at 250 °C for 30 min. The layer of nanofibers was then rapidly heated to 750 °C and dwelled for 15 min. After that, the

layer of nanofibers was quenched to room temperature within a few minutes in a flow of 50 sccm Ar. The graphene paper obtained thereof possesses a sheet resistivity of about 20 Ω/sq.

**[0112]** Example 9: Preparation of nanocomposite for heat spreading

**[0113]** The 0D graphene nanoparticles prepared in Example 1 were put in a graphite die. The die was then put in a chamber of a high vacuum furnace and was hot pressed at 750 °C and 50 MPa for 15 min. The sample was then polished by 400 grit sand paper. The final dimension of the sample size was 13 mm (diameter) × 2 mm (height). Thermal conductivity of the sample was tested by LFA 447 NanoFlash (Netzsch, Germany) at room temperature. The measured thermal conductivity reached 392.6 W/mK, which was higher than that of pure copper prepared and tested under the same conditions (333.2 W/mK).

**[0114]** In summary, compared to conventional gaseous growth method, the present method of using liquid carbon source enables the growth of graphene on all external and internal surfaces for the 0D, 1D and 3D nanostructures. On the other hand, conventional gaseous growth method only enables the growth of graphene on portions of the nanostructure's surface which are in contact with the gaseous carbon source during chemical vapour deposition growth. Therefore, graphene obtained by the present method using liquid carbon source is more continuous and uniform. The present forming method is easily applicable and adopted in manufacturing industries to produce graphene in large scale, for example in mass production of electrodes or heat spreaders, by simply coating the large amount of the metallic nanostructure catalyst with the liquid carbon source and then crystallizing the coated nanostructures.

**[0115]** Further, compared to graphene obtained by conventional gaseous growth methods, the present graphene layer is more continuous and uniform. The better graphene quality leads to enhanced properties and thus makes presently obtained graphene-based electrodes more attractive over ITO-based electrodes, such as highly flexible, better chemical stability, lower cost and rich in resource. Compared with Cu or Ag nanofiber-based conductors, the present graphene films have better chemical stability since graphene can protect the metal cores from oxidation/corrosion. Furthermore, the present graphene films have a work function of 4.6eV, close to that of ITO (about 4.7eV), while for metal fibers, the work function is lower. As such, the present graphene-based electrodes can directly replace ITO-based electrodes for existing ITO-based devices. Further compared with pure graphene films, the present graphene films is expected to possess better conductivity since the metal cores can connect those area where the graphene lattice network might break or meet with defects.

**[0116]** By "comprising" it is meant including, but not limited to, whatever follows the word "comprising". Thus, use of the term "comprising" indicates that the listed elements are required or mandatory, but that other elements are optional and may or may not be present.

**[0117]** By "consisting of" is meant including, and limited to, whatever follows the phrase "consisting of". Thus, the phrase "consisting of" indicates that the listed elements are required or mandatory, and that no other elements may be present.

**[0118]** The inventions illustratively described herein may suitably be practiced in the absence of any element or elements, limitation or limitations, not specifically disclosed herein. Thus, for example, the terms "comprising", "including", "containing", etc. shall be read expansively and without limitation. Additionally, the terms and expressions employed

herein have been used as terms of description and not of limitation, and there is no intention in the use of such terms and expressions of excluding any equivalents of the features shown and described or portions thereof, but it is recognized that various modifications are possible within the scope of the invention claimed. Thus, it should be understood that although the present invention has been specifically disclosed by preferred embodiments and optional features, modification and variation of the inventions embodied therein herein disclosed may be resorted to by those skilled in the art, and that such modifications and variations are considered to be within the scope of this invention.

**[0119]** By "about" in relation to a given numberical value, such as for temperature and period of time, it is meant to include numerical values within 10% of the specified value.

**[0120]** The invention has been described broadly and generically herein. Each of the narrower species and sub-generic groupings falling within the generic disclosure also form part of the invention. This includes the generic description of the invention with a proviso or negative limitation removing any subject matter from the genus, regardless of whether or not the excised material is specifically recited herein.

**[0121]** Other embodiments are within the following claims and non- limiting examples. In addition, where features or aspects of the invention are described in terms of Markush groups, those skilled in the art will recognize that the invention is also thereby described in terms of any individual member or subgroup of members of the Markush group.

## Claims

1. A method of forming graphene on a metallic nanostructure, comprising:

   (i) coating the metallic nanostructure with a layer of liquid carbon precursor;

   (ii) carbonizing the layer of liquid carbon precursor coated on the metallic nanostructure at a carbonizing temperature to convert the layer of liquid carbon precursor to a layer of amorphous carbon;

   (iii) crystallizing the layer of amorphous carbon at a crystallizing temperature to convert the layer of amorphous carbon to a layer of crystallized graphene; and

   (iv) quenching the layer of crystallized graphene.

2. The method of claim 1, wherein the metallic nanostructure comprises a metal, an alloy, or a metal-carbon mixture.

3. The method of claim 2, wherein the alloy comprises at least one metal selected from the group consisting of Ni, Co, Fe, Cu, Zn, Mn, Ga, Ge, As, Se, In, Sn, Sb, Te, Al, Pd, Pt, Au, and Ag, and/or at least one refractory metal selected from the group consisting of Nb, Mo, Ta, W, Rh, Re, Ti, V, Cr, Zr, Hf, Ru, Os and Ir.

4. The method of claim 3, wherein the molar percentage of the at least one refractory metal in the alloy based on total content of the alloy is between 0 and 40%.

5. The method of claim 2, wherein the metal-carbon mixture is selected from the group consisting of carbon steel, nickel steel, nickel-chromium steel, molybdenum steel, chromium steel, chromium-vanadium steel, tungsten steel, nickel-chromium-vanadium steel, silicon-manganese steel, and a mixture thereof.

6. The method of any one of claims 1 to 5, wherein the liquid carbon precursor comprises a hydrocarbon compound in liquid phase at room temperature (i.e. 25°C) and atmospheric pressure (i.e. 101.325 kPa).

7. The method of any one of claims 1 to 6, wherein coating in step (i) comprises dip coating, spray coating or spin coating.

8. The method of any one of claims 1 to 7, wherein carbonizing in step (ii) comprises heating the layer of liquid carbon precursor coated on the metallic nanostructure at a carbonizing temperature of 180 to 600 °C.

9. The method of claim 8, wherein carbonizing in step (ii) comprises heating the layer of liquid carbon precursor coated on the metallic nanostructure at a carbonizing temperature of 200 to 300 °C.

10. The method of claim 8 or 9, wherein carbonizing in step (ii) further comprises heating the layer of liquid carbon precursor coated on the metallic nanostructure for a period of 1 to 120 min.

11. The method of claim 10, wherein carbonizing in step (ii) further comprises heating the layer of liquid carbon precursor coated on the metallic nanostructure for a period of 20 to 40 min.

12. The method of any one of claims 1 to 11, wherein crystallizing in step (iii) comprises increasing the temperature to a crystallizing temperature of 450 to 1,000 °C.

13. The method of claim 12, wherein crystallizing in step (iii) comprises increasing the temperature to a crystallizing temperature of 750 to 850 °C.

14. The method of claim 12 or 13, wherein crystallizing in step (iii) further comprises increasing the temperature to the crystallizing temperature at a ramping rate of 0.5 to 200 °C/min.

15. The method of claim 14, wherein crystallizing in step (iii) further comprises increasing the temperature to the crystallizing temperature at a ramping rate of 10 to 100 °C/min.

16. The method of any one of claim 12 to 15, wherein crystallizing in step (iii) further comprises maintaining the crystallizing temperature for a period of 1 sec to 30 min.

17. The method of claim 16, wherein crystallizing in step (iii) further comprises maintaining the crystallizing temperature for a period of 5 to 15 min.

18. The method of any one of claims 1 to 17, wherein the carbonizing step (ii) and/or the crystallizing step (iii) is carried out in an inert or reductive environment.

19. The method of claim 18, wherein the carbonizing step (ii) and/or the crystallizing step (iii) is carried out in an inert environment with a total gas flow rate of 200 to 500 sccm.

20. The method of claim 19, wherein the carbonizing step (ii) and/or the crystallizing step (iii) is carried out in an inert environment with a total gas flow rate of 200 to 300 sccm.

21. The method of any one of claims 18 to 20, wherein the inert environment comprises argon, or argon and hydrogen.

22. The method of any one of claims 1 to 21, wherein quenching in step (iv) comprises reducing the temperature of the layer of crystallized graphene to room temperature in less than 10 min.

23. The method of claim 22, wherein the quenching step (iv) is carried out in an inert environment with a total gas flow rate of 50 to 200 sccm.

24. The method of claim 23, wherein the inert environment comprises argon, or argon and hydrogen.

25. The method of any one of claims 1 to 24, wherein the metallic nanostructure is a zero-dimension nanoparticle, one-dimension nanofiber, or three-dimension foam or aerogel.

26. A method of forming an electrode comprising graphene, the method comprising:

(a) forming at least one layer of metallic nanostructures on a substrate;

(b) coating the metallic nanostructures with a layer of liquid carbon precursor;

(c) carbonizing the layer of liquid carbon precursor coated on the metallic nanostructures at a carbonizing temperature to convert the layer of liquid carbon precursor to a layer of amorphous carbon;

(d) crystallizing the layer of amorphous carbon at a crystallizing temperature to convert the layer of amorphous carbon to a layer of crystallized graphene; and

(e) quenching the layer of crystallized graphene.

27. The method of claim 26, wherein forming in step (a) comprises electrospinning, pyrolysis and $H_2$ reduction to form the at least one layer of metallic nanostructures on a rigid substrate.

28. The method of claim 26 or 27, wherein more than one layer of metallic nanostructures is formed on the substrate.

29. A method of forming a flexible electrode comprising graphene, the method comprising:

(i) coating metallic nanostructures with a layer of liquid carbon precursor;

(ii) carbonizing the layer of liquid carbon precursor coated on the metallic nanostructures at a carbonizing temperature to convert the layer of liquid carbon precursor to a layer of amorphous carbon;

(iii) crystallizing the layer of amorphous carbon at a crystallizing temperature to convert the layer of amorphous carbon to a layer of crystallized graphene;

(iv) quenching the layer of crystallized graphene to obtain metallic nanostructures coated with graphene;

(v) coating a polymer solution on the metallic nanostructures coated with graphene, wherein the polymer solution comprises the polymer of a flexible substrate; and

(vi) curing the polymer solution to form a polymer film having the metallic nanostructures coated with graphene.

30. A method of forming an electrode comprising graphene, the method comprising:

(i) coating metallic nanostructures with a layer of liquid carbon precursor;

(ii) carbonizing the layer of liquid carbon precursor coated on the metallic nanostructures at a carbonizing temperature to convert the layer of liquid carbon precursor to a layer of amorphous carbon;

(iii) crystallizing the layer of amorphous carbon at a crystallizing temperature to convert the layer of amorphous carbon to a layer of crystallized graphene;

(iv) quenching the layer of crystallized graphene to obtain metallic nanostructures coated with graphene;

(v) dispersing the metallic nanostructures coated with graphene in a solution;

(vi) coating the solution of (v) onto a substrate; and

(vii) drying the coating of (vi).

31. A method of forming a heat spreader comprising graphene nanocomposite, the method comprising:

(i) coating metallic nanostructures with a layer of liquid carbon precursor;

(ii) carbonizing the layer of liquid carbon precursor coated on the metallic nanostructures at a carbonizing temperature to convert the layer of liquid carbon precursor to a layer of amorphous carbon;

(iii) crystallizing the layer of amorphous carbon at a crystallizing temperature to convert the layer of amorphous carbon to a layer of crystallized graphene;

(iv) quenching the layer of crystallized graphene to obtain metallic nanostructures coated with graphene;

(v) mixing the metallic nanostructures coated with graphene with a metal powder;

(vi) processing the mixture of (v) to form the graphene nanocomposite.

32. The method of claim 31, wherein processing in step (vi) comprises hot pressing, moulding, or sintering the mixture of metal nanostructures coated with graphene and the metal powder.

33. Graphene formed on metallic nanostructures according to a method of any one of claims 1 to 25.

34. An electrode comprising graphene formed according to a method of any one of claims 26 to 30.

35. A heat spreader comprising graphene nanocomposites formed according to a method of claim 31 or 32.

FIG. 1

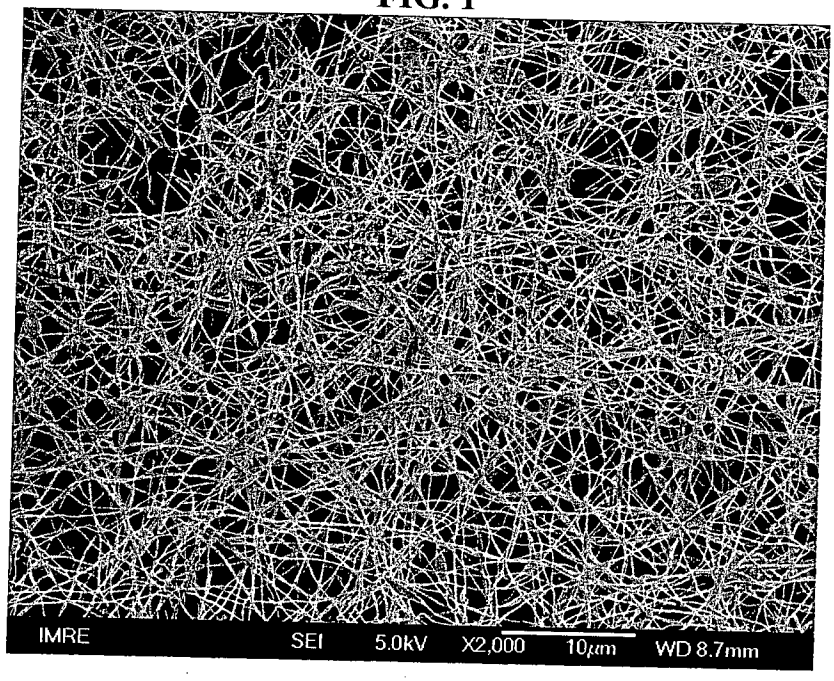
IMRE SEI 5.0kV X2,000 10μm WD 8.7mm

FIG. 2A

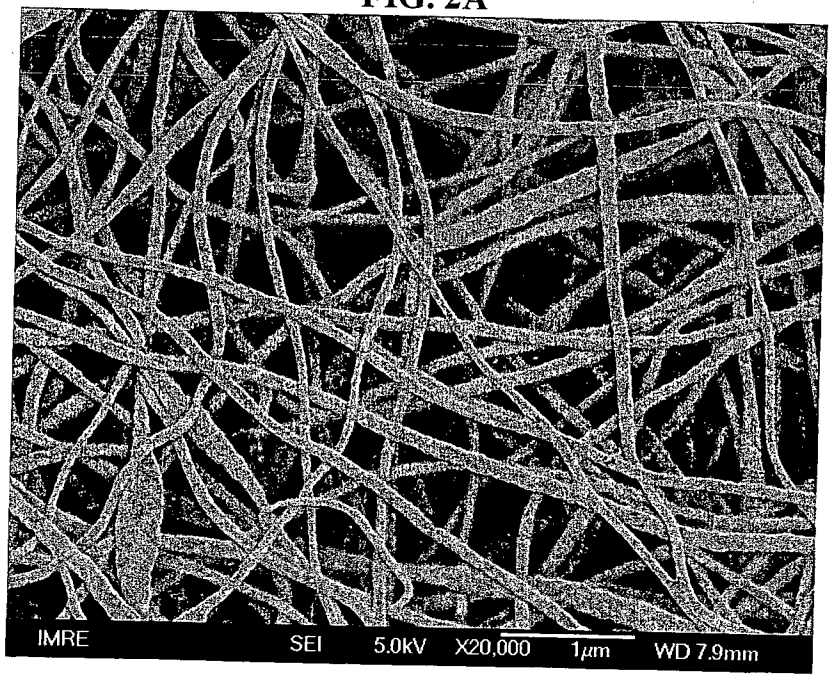
IMRE SEI 5.0kV X20,000 1μm WD 7.9mm

FIG. 2B

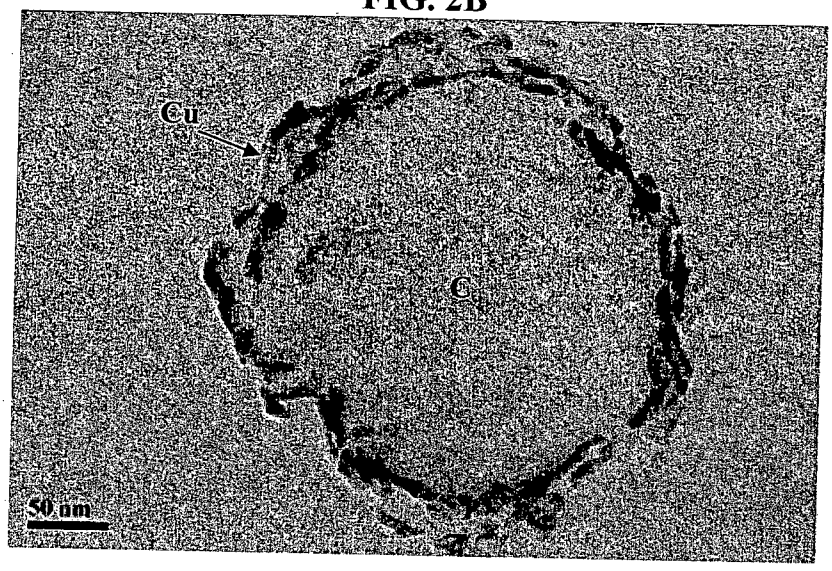
Cu
C
50 nm

FIG. 3

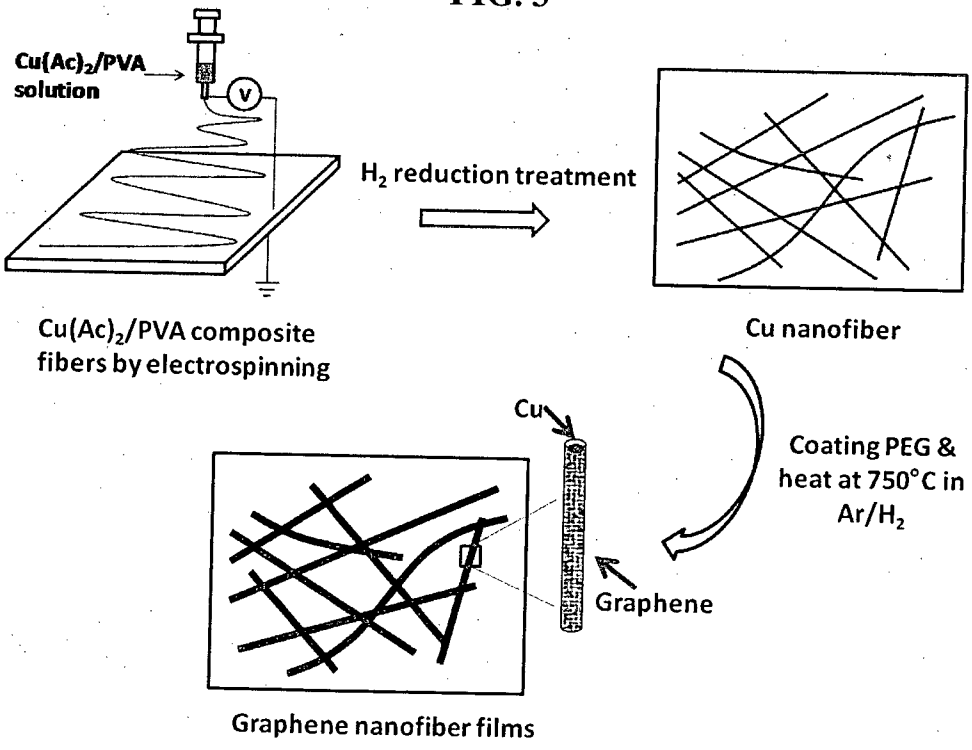
Cu(Ac)2/PVA solution
V
H2 reduction treatment
Cu(Ac)2/PVA composite fibers by electrospinning
Cu nanofiber
Coating PEG & heat at 750°C in Ar/H2
Cu
Graphene
Graphene nanofiber films

FIG. 4A

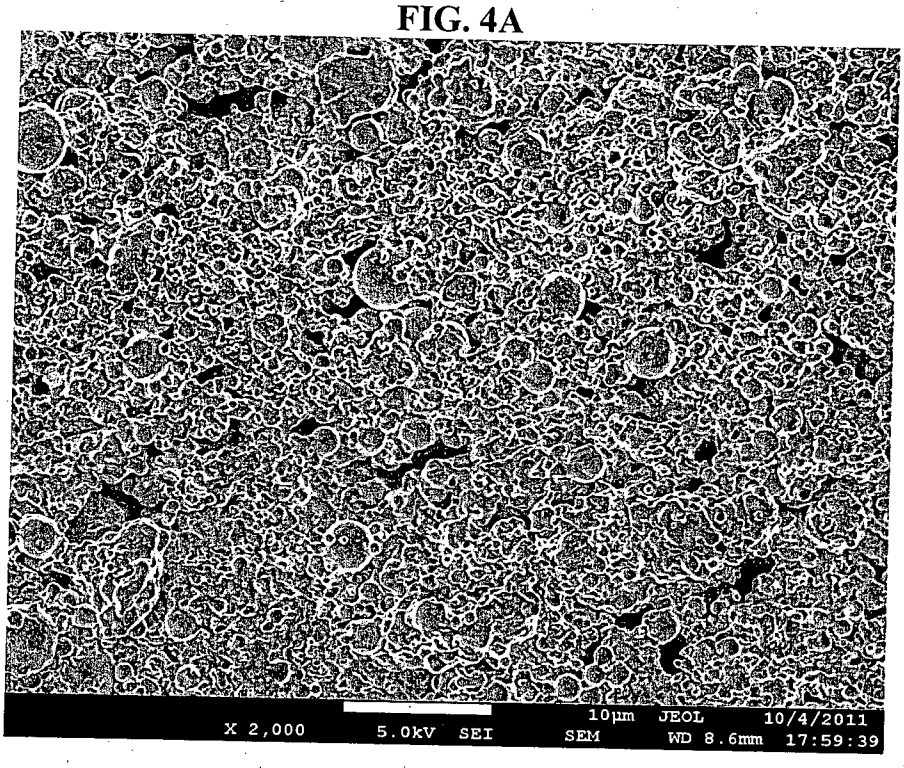
X 2,000
5.0kV SEI
10µm JEOL
SEM
10/4/2011
WD 8.6mm 17:59:39

FIG. 4B

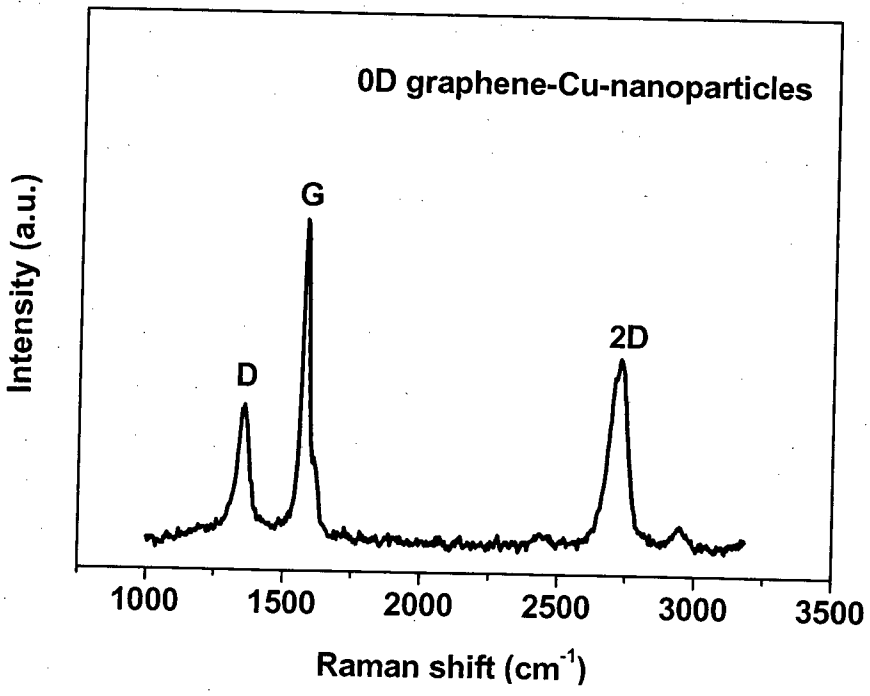
0D graphene-Cu-nanoparticles
G
D
2D
Intensity (a.u.)
1000
1500
2000
2500
3000
3500
Raman shift (cm-1)

FIG. 5A

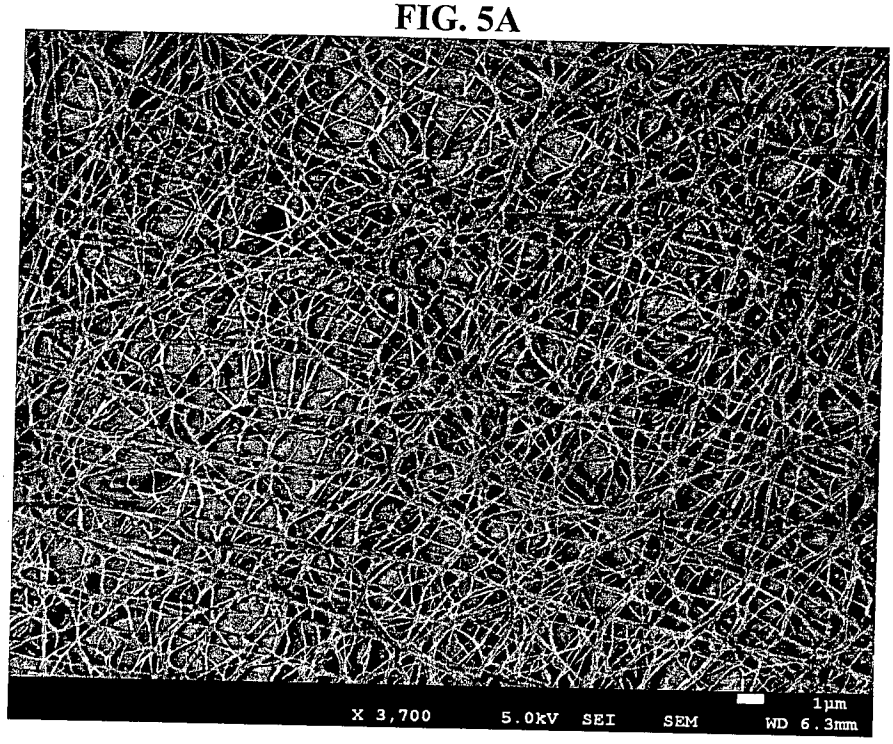
X 3,700
5.0kV SEI SEM
1µm
WD 6.3mm

FIG. 5B

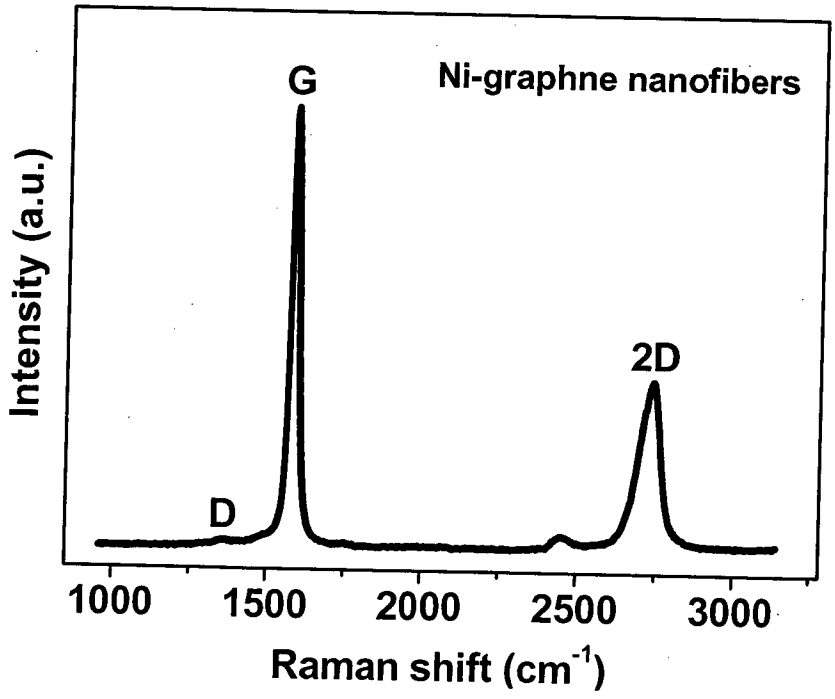
Ni-graphne nanofibers
G
2D
D
Intensity (a.u.)
1000
1500
2000
2500
3000
Raman shift (cm-1)

FIG. 6A

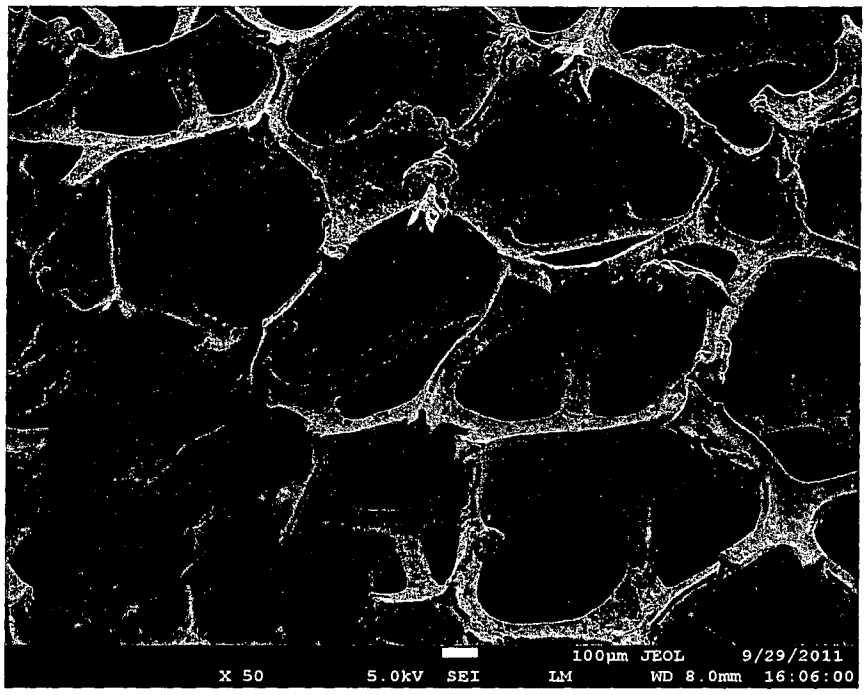
X 50
5.0kV SEI
100µm JEOL
LM
WD 8.0mm
9/29/2011
16:06:00

FIG. 6B

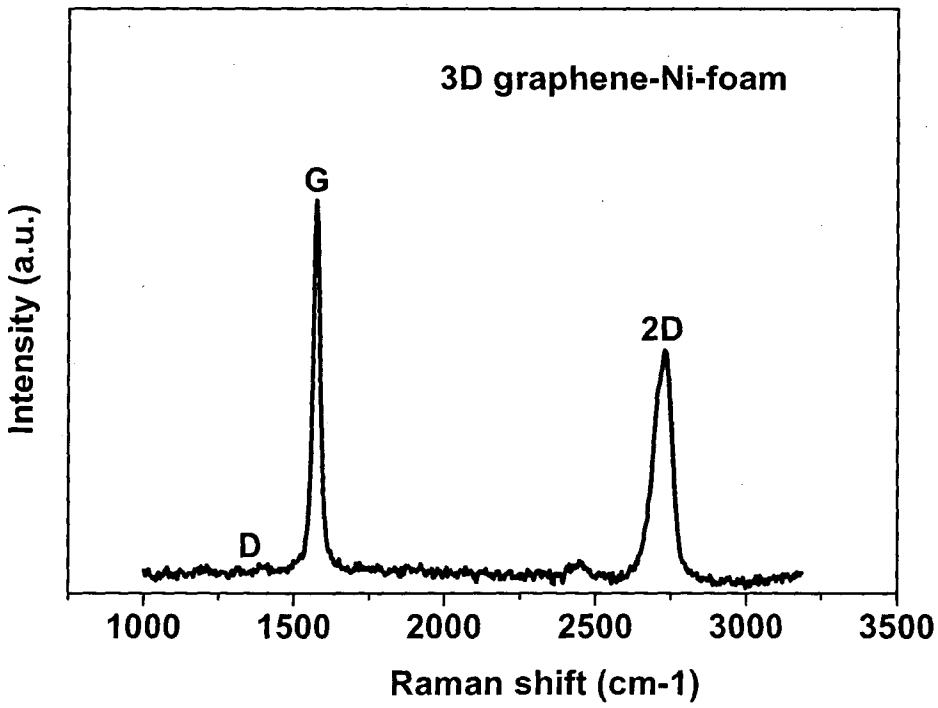
3D graphene-Ni-foam
G
2D
D
Intensity (a.u.)
1000
1500
2000
2500
3000
3500
Raman shift (cm-1)

FIG. 7

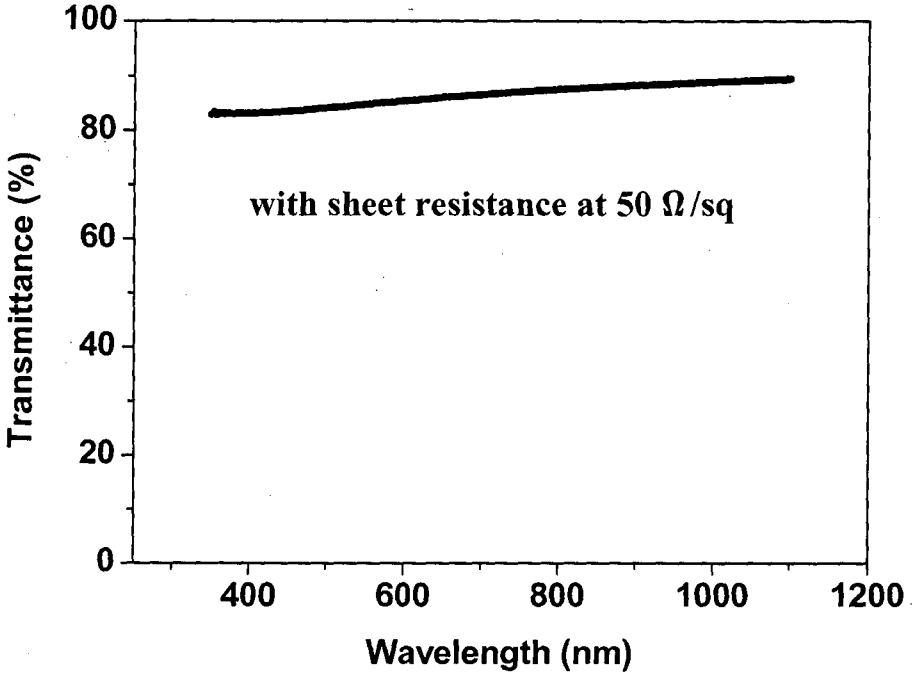
100
80
60
40
20
0
Transmittance (%)
with sheet resistance at 50 Ω/sq
400
600
800
1000
1200
Wavelength (nm)

FIG. 8

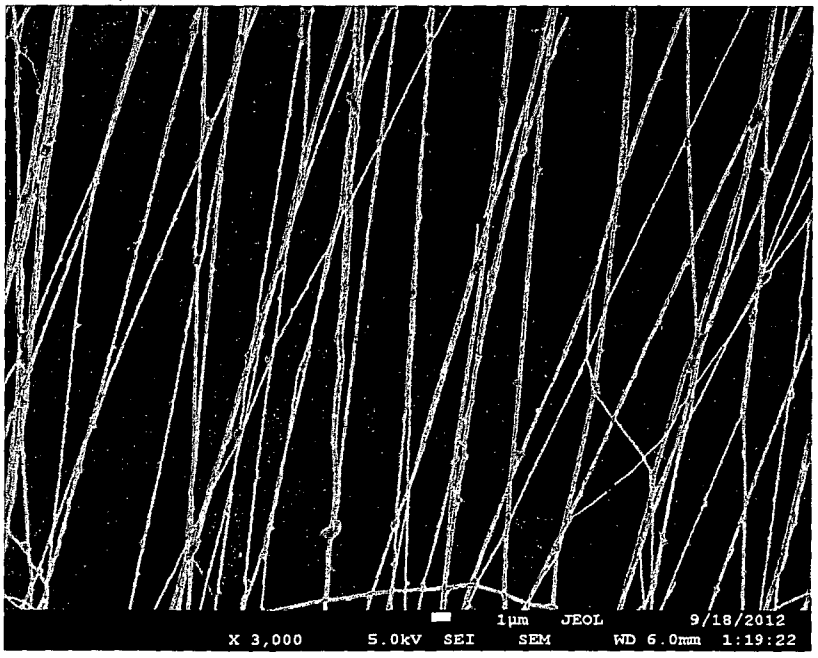
1μm JEOL 9/18/2012
X 3,000 5.0kV SEI SEM WD 6.0mm 1:19:22

FIG. 9

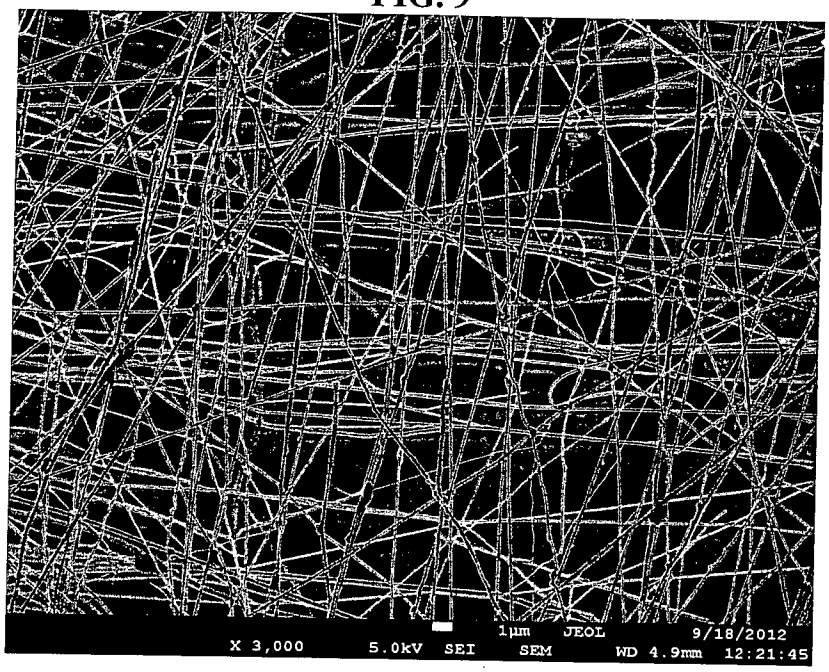

**INTERNATIONAL SEARCH REPORT**

International application No.
**PCT/SG2012/000412**

A. CLASSIFICATION OF SUBJECT MATTER

***C01B 31/04 (2006.01) B82Y 10/00 (2011.01)***

According to International Patent Classification (IPC) or to both national classification and IPC

B. FIELDS SEARCHED

Minimum documentation searched (classification system followed by classification symbols)

Documentation searched other than minimum documentation to the extent that such documents are included in the fields searched

Electronic data base consulted during the international search (name of data base and, where practicable, search terms used)

WPI/EPODOC, INSPEC, STN CAPLUS, Google Scholar. Search terms: graphene, nano metal, thermal, liquid precursor, liquid carbon, pyrolysis, carbonisation, decomposition, breakdown, polyethylene oxide, polyethylene glycol, quenching, rapid cooling, heat sink, heat spreader and like terms.

C. DOCUMENTS CONSIDERED TO BE RELEVANT

| Category* | Citation of document, with indication, where appropriate, of the relevant passages | Relevant to claim No. |
|---|---|---|
| | Documents are listed in the continuation of Box C | |

[X] Further documents are listed in the continuation of Box C

[X] See patent family annex

* Special categories of cited documents:

"A" document defining the general state of the art which is not considered to be of particular relevance

"E" earlier application or patent but published on or after the international filing date

"L" document which may throw doubts on priority claim(s) or which is cited to establish the publication date of another citation or other special reason (as specified)

"O" document referring to an oral disclosure, use, exhibition or other means

"P" document published prior to the international filing date but later than the priority date claimed

"T" later document published after the international filing date or priority date and not in conflict with the application but cited to understand the principle or theory underlying the invention

"X" document of particular relevance; the claimed invention cannot be considered novel or cannot be considered to involve an inventive step when the document is taken alone

"Y" document of particular relevance; the claimed invention cannot be considered to involve an inventive step when the document is combined with one or more other such documents, such combination being obvious to a person skilled in the art

"&" document member of the same patent family

| Date of the actual completion of the international search | Date of mailing of the international search report |
|---|---|
| 8 January 2013 | 08 January 2013 |
| **Name and mailing address of the ISA/AU** | **Authorised officer** |
| AUSTRALIAN PATENT OFFICE<br>PO BOX 200, WODEN ACT 2606, AUSTRALIA<br>Email address: pct@ipaustralia.gov.au<br>Facsimile No.: +61 2 6283 7999 | Andrew Matthews<br>AUSTRALIAN PATENT OFFICE<br>(ISO 9001 Quality Certified Service)<br>Telephone No. 0262832693 |

| INTERNATIONAL SEARCH REPORT<br>C (Continuation). DOCUMENTS CONSIDERED TO BE RELEVANT | | International application No.<br>**PCT/SG2012/000412** |
|---|---|---|
| Category* | Citation of document, with indication, where appropriate, of the relevant passages | Relevant to claim No. |
| X | US 2009/0324897 A1 (CHOI J. et al) 31 December 2009<br>See whole of the document but particuarly the Abstract [0008], [0016], [0048], [0054] and [0056]. | 1-24, 26, 28, 33 |
| X | Takahashi Y. et al 'Synthesis of carbon nanofibers form poly(ethylene glycol) with controlled structure.' Adsorption (2010), Vol 16, pages 57-68. Published online 5 February 2010.<br>See whole of the document but particuarly the Abstract, page 65 column 2, page 57 column 2 and Fig. 14. | 1-26, 33 |
| X | US 2010/0323272 A1 (OZAKI J. et al) 23 December 2010<br>See whole of the document but particularly the Abstract, [0016], [0037], [0063], [0065], [0067] and [0075]. | 1-26, 33-34 |
| X | US 2011/0104442 A1 (YOON S.) 05 May 2011<br>See whole of the document but particularly the Abstract, [0058], [0068], [0069], [0076], [0077], [0078], [0098] and Example 1. | 1-24, 26, 33-34 |
| A | US 2007/0030653 A1 (NORLEY J. et al) 08 February 2007<br>See whole of the document but particularly the Abstract and [0042]. | 31-32, 35 |

| INTERNATIONAL SEARCH REPORT<br>Information on patent family members | International application No.<br>**PCT/SG2012/000412** |
|---|---|

This Annex lists known patent family members relating to the patent documents cited in the above-mentioned international search report. The Australian Patent Office is in no way liable for these particulars which are merely given for the purpose of information.

| Patent Document/s Cited in Search Report | | Patent Family Member/s | |
|---|---|---|---|
| **Publication Number** | **Publication Date** | **Publication Number** | **Publication Date** |
| US 2009/0324897 A1 | 31 Dec 2009 | KR 20090029621 A | 23 Mar 2009 |
| | | US 2009324897 A1 | 31 Dec 2009 |
| | | US 8337949 B2 | 25 Dec 2012 |
| US 2010/0323272 A1 | 23 Dec 2010 | JP 2009208061 A | 17 Sep 2009 |
| | | US 2010323272 A1 | 23 Dec 2010 |
| | | WO 2009098812 A1 | 13 Aug 2009 |
| US 2011/0104442 A1 | 05 May 2011 | EP 2327662 A1 | 01 Jun 2011 |
| | | KR 20110046863 A | 06 May 2011 |
| | | US 2011104442 A1 | 05 May 2011 |
| US 2007/0030653 A1 | 08 Feb 2007 | AU 2002254496 A1 | 21 Oct 2002 |
| | | AU 2002345820 A1 | 08 Jan 2003 |
| | | CA 2621391 A1 | 15 Mar 2007 |
| | | CN 101326406 A | 17 Dec 2008 |
| | | CN 101326406 B | 23 Nov 2011 |
| | | EP 1383644 A2 | 28 Jan 2004 |
| | | EP 1383645 A1 | 28 Jan 2004 |
| | | EP 1401981 A2 | 31 Mar 2004 |
| | | EP 1922514 A2 | 21 May 2008 |
| | | JP 2009508786 A | 05 Mar 2009 |
| | | KR 20070027478 A | 09 Mar 2007 |
| | | KR 101009500 B1 | 18 Jan 2011 |
| | | US 2002157818 A1 | 31 Oct 2002 |
| | | US 2002157819 A1 | 31 Oct 2002 |
| | | US 2002164483 A1 | 07 Nov 2002 |
| | | US 2002166658 A1 | 14 Nov 2002 |
| | | US 2002166660 A1 | 14 Nov 2002 |
| | | US 2002168526 A1 | 14 Nov 2002 |
| | | US 2006272796 A1 | 07 Dec 2006 |
| | | US 2007030653 A1 | 08 Feb 2007 |
| | | WO 02081187 A2 | 17 Oct 2002 |
| | | WO 02081190 A1 | 17 Oct 2002 |
| | | WO 03001133 A2 | 03 Jan 2003 |
| | | WO 2007030309 A2 | 15 Mar 2007 |

Due to data integration issues this family listing may not include 10 digit Australian applications filed since May 2001.

| INTERNATIONAL SEARCH REPORT<br>Information on patent family members | International application No.<br>**PCT/SG2012/000412** |
|---|---|

This Annex lists known patent family members relating to the patent documents cited in the above-mentioned international search report. The Australian Patent Office is in no way liable for these particulars which are merely given for the purpose of information.

| Patent Document/s Cited in Search Report | | Patent Family Member/s | |
|---|---|---|---|
| **Publication Number** | **Publication Date** | **Publication Number** | **Publication Date** |

**End of Annex**

Due to data integration issues this family listing may not include 10 digit Australian applications filed since May 2001.

Biosensors and Bioelectronics 65 (2015) 404–419

Contents lists available at ScienceDirect

Biosensors and Bioelectronics

journal homepage: www.elsevier.com/locate/bios

# 2D and 3D graphene materials: Preparation and bioelectrochemical applications

Hongcai Gao, Hongwei Duan *

*School of Chemical and Biomedical Engineering, Nanyang Technological University, 70 Nanyang Drive, Singapore 637457, Singapore*

ARTICLE INFO

*Article history:*
Received 21 August 2014
Received in revised form
27 October 2014
Accepted 29 October 2014
Available online 31 October 2014

*Keywords:*
Graphene paper
Graphene hydrogel
Graphene foam
Biosensor
Biological fuel cell

ABSTRACT

The attractive properties of graphene materials have stimulated intense research and development in the field of bioelectrochemistry. In particular, the construction of 2D and 3D graphene architectures provides new possibilities for developing flexible and porous carbon scaffolds, which not only inherit some of the key properties of individual graphene sheets, but also develop additional functions that are of considerable interest for bioelectrochemical applications. In this review article, we will first summarize the recently developed approaches to preparing graphene sheets, and then focus on the methods to assemble them into macroscopic 2D and 3D structures. Furthermore, we will highlight the potential applications of these materials in electrochemical biosensors and biological fuel cells.



**Contents**



* Corresponding author.
*E-mail address:* hduan@ntu.edu.sg (H. Duan).

http://dx.doi.org/10.1016/j.bios.2014.10.067
0956-5663/

## 1. Introduction

The successful isolation of high quality graphene with the size of hundreds of microns from graphite in 2004 (Novoselov et al., 2004) aroused tremendous efforts towards investigating the unique properties, controlling the growth, introducing diverse functionalities, and eventually exploring the potential applications of graphene materials (Novoselov et al., 2012; Qian et al., 2011a; Y.W. Zhu et al., 2010a). In particular, graphene derivatives have been actively studied in the field of electrochemistry because of their unique physical and chemical properties in comparison with other carbon materials, such as large specific surface area (2630 $m^2 g^{-1}$) (Stoller et al., 2008), superior electrical conductivity (200 $S m^{-1}$) (Stankovich et al., 2007; Yoo et al., 2011), excellent thermal stability with oxidation resistance temperature up to 601 °C (Wu et al., 2009b), high thermal conductivity between 3080 and 5150 $W m^{-1} K^{-1}$ (Ghosh et al., 2008), remarkable mechanical strength with Young's modulus of around 1.0 TPa (Lee et al., 2008), and outstanding optical transmittance of 97.7% (Nair et al., 2008). Moreover, it also shows fascinating electrochemical properties, including wide electrochemical potential windows, low charge-transfer resistance, and excellent electrochemical activity (Chen et al., 2014; Qian et al., 2011b; Shao et al., 2010b). The aforementioned physical and electrochemical properties enable the widespread use of graphene in the field of bioelectrochemistry, and possibly offer new solutions to address the current energy and healthcare issues that are of great importance for the sustainable development of the society.

Chemically derived graphene, including graphene oxide (GO) and reduced graphene oxide (rGO), are promising building blocks to construct 2D and 3D materials (Bi et al., 2012; Cheng and Li, 2013). In addition to the inherent properties of individual graphene sheets, versatile functionalities can be built in the hierarchical graphene materials for improved performance (Chen et al., 2013; Ren and Cheng, 2013). In comparison with the extensive research on individual graphene sheets, less attention has been focused on 2D and 3D graphene materials. One of the goals of this review is to increase the visibility of the new class of hierarchical materials and call attention for further research from academia and industry. From a practical point of view, the use of these materials into practical applications relies on the development of efficient preparation procedures that allow for tailoring their structures and functions for improved performance. We will first summarize the approaches for preparing chemically derived graphene, with particular focuses on the recently developed environmentally-friendly methods, and then summarize the strategies to assemble individual graphene sheets into 2D and 3D structures. Their bioelectrochemical applications will be discussed afterwards with an emphasis on the specific topics of electrochemical biosensors and biological fuel cells.

## 2. Preparation of graphene sheets

Although the scotch-tape method can directly produce high-quality graphene, it is lack of the feasibility of functionalization and not suitable for large-scale production. A diverse range of approaches, therefore, have been developed to produce graphene, including epitaxial growth (Sutter et al., 2008), chemical vapor deposition (CVD) (Mattevi et al., 2011), liquid-phase exfoliation (Hernandez et al., 2008), chemical exfoliation (Dreyer et al., 2010), and organic synthesis (Wu et al., 2007). Among these methods, chemical exfoliation has attracted widespread interest because it does not rely on special equipments and allows for scaled-up preparation of GO carrying a high density of functional groups, which open the possibility to introduce additional functionalities (Park and Ruoff, 2009). This route is referred as oxidation–exfoliation–reduction process, which generally involves chemical oxidation of graphite into graphite oxide, followed by exfoliation of graphite oxide into single-layered GO, and reduction of GO to rGO with low oxygen to carbon atomic ratio (Fig. 1) (Bai et al., 2011).

### 2.1. Preparation of GO

The precursor of GO is graphite oxide which contains oxygen functionalities and retains stacked structure similar to that of graphite. The history for preparing graphite oxide can be traced back to 1859, when $KClO_3$ and fuming $HNO_3$ were used to oxidize graphite powder, leading to a material with carbon to oxygen ratio around 2:1 (Brodie, 1859). The utilization of $KClO_3$ and $HNO_3$ must be handled with special caution because of the generation of highly toxic $ClO_2$ gas and the possible production of explosion (Compton and Nguyen, 2010). Hummers and Offeman (1958) developed an approach to synthesize graphite oxide with similar level of oxidation but employing different oxidation reagents ($NaNO_3$, $KMnO_4$, and concentrated $H_2SO_4$) in 1958. Through Hummers' method, the reaction can be completed within relatively shorter reaction time while avoiding the generation of hazardous $ClO_2$ gas. A recent study revealed that the amount of basal plane in graphite oxide can be improved by eliminating $NaNO_3$, increasing the amount of $KMnO_4$, and performing the reaction in a 9:1 mixture of $H_2SO_4$ and $H_3PO_4$ (Marcano et al., 2010). The exfoliation of graphite oxide into single-layered GO can be achieved

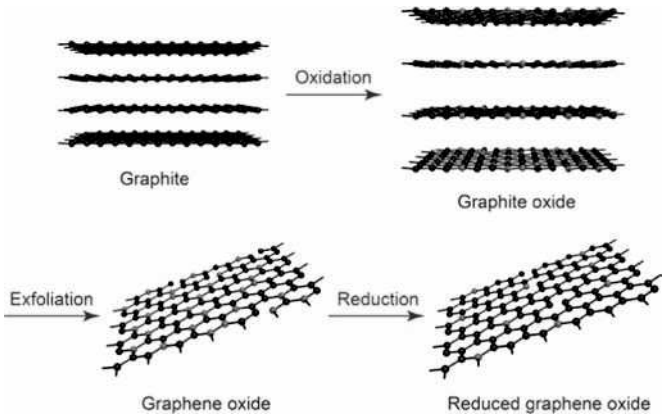


**Fig. 1.** Schematic illustration of the chemical oxidation, exfoliation, and reduction methods to prepare reduced graphene oxide from graphite.

by employing additional energy inputs, e.g., mechanical shaking or ultrasonication (D. Li et al., 2008). Several parameters, including starting materials, oxidation procedures, and the forms of exfoliation energy, play important roles in controlling the size or number of layers of GO. With increasing oxidation time or the amount of oxidants, the average size of GO can be tuned from ~59,000 to ~550 $nm^2$ (Zhang et al., 2009). Ultrasonication is more effective to reduce the size of GO than mechanical shaking (Pan and Aksay, 2011). The number of layers of GO in the final products is strongly dependent on the lateral size and crystallinity of graphite precursors (Wu et al., 2009a).

### 2.2. Reduction of GO

#### 2.2.1. Chemical reduction

The oxidation of graphite by strong oxidants leads to disruption of the $sp^2$ bonding networks, and therefore the oxidation products, both graphite oxide and GO, are electrically insulating materials. A reduction process is necessitated to remove oxygen functionalities (epoxy, carboxyl, and hydroxyl groups), and recover electrical conductivity by restoring the $\pi$-network (D. Chen et al., 2012). The advantage of chemical reduction is that it can be carried out at relatively low temperature or with only moderate heating. Importantly, it also does not rely on sophisticate equipments.

Hydrazine is the most efficient reducing reagent to remove oxygen functionalities from GO, leading to rGO with a carbon to oxygen atomic ratio of around 7 and electrical conductivity of ~7200 S $m^{-1}$ (D. Li et al., 2008). The successful reduction of GO was also achieved by using freshly-prepared solution of $NaBH_4$ (Gao et al., 2009). In comparison with hydrazine, fewer heteroatoms were introduced when $NaBH_4$ as reducing reagent. Nevertheless, alcohol groups on GO cannot be efficiently removed by $NaBH_4$ because of its low activity for reduction of epoxy and carboxyl groups. In order to avoid the utilization of toxic hydrazine and $NaBH_4$, a number of environmentally-benign reagents have been actively explored, including hydrogen iodide (Pei et al., 2010), ascorbic acid (Zhang et al., 2010), alkaline solution (Park et al., 2008), glutathione (Pham et al., 2011), urea (Lei et al., 2012), amino acids (D.Z. Chen et al., 2011), dopamine (L.Q. Xu et al., 2010), metal powders (Fan et al., 2010a, 2010b; Mei et al., 2012), low-valence metal ions (Xue et al., 2011), reducing sugar (C.Z. Zhu et al., 2010), tea water (Y. Wang et al., 2011), and carrot root (Kuila et al., 2012). Among them, ascorbic acid is accepted as an ideal substitute for hydrazine and $NaBH_4$ because of its non-toxicity, remarkable stability in water, and high deoxygenation efficiency. The atomic ratio of carbon to oxygen in rGO reduced by ascorbic acid is comparable to that reduced by hydrazine (Fernandez–Merino et al., 2010).

#### 2.2.2. Electrochemical reduction

Electrochemical reduction is typically achieved by applying a negative potential to GO films coated on conductive substrates. This strategy has several advantages in comparison with chemical reduction (Low et al., 2013; Ramesha and Sampath, 2009; M. Zhou et al., 2009). First, electrons work as intrinsically environmentally-friendly reducing reagent, leading to the formation of rGO without heteroatoms contaminations. Furthermore, highly negative potentials, readily obtainable by adjusting electrochemical parameters, are beneficial for removing more oxygen functionalities in the production of high quality rGO. At last, the resulting rGO is in good contact with electrically conductive substrates, which simplifies the electrode fabrication process and is suitable for further electrochemical applications (Shao et al., 2010a).

Cathodic deposition has been widely employed to prepare metal nanoparticles. Thus, electrochemical reduction also opens the way to prepare nanoparticles modified rGO through one-step manner (C.Z. Zhu et al., 2011). The prepared nanoparticles were directly immobilized on the surface of rGO without any linker molecules, facilitating electron transfers between the two components. In addition, the abundant oxygen functionalities on GO provide more anchoring sites for metal ions than rGO, and consequently, the density of metal nanoparticles from one-step electrochemical reduction procedure are higher than that from two-step method involving chemical reduction of GO followed by electrochemical deposition of metal nanoparticles (Fig. 2) (Gao et al., 2011).

#### 2.2.3. Hydrothermal or solvothermal reduction

It is also possible to remove oxygen functional groups on GO in pure aqueous or organic solvents under hydrothermal or solvothermal conditions. Protons can be generated from water under hydrothermal conditions, and the mechanism for hydrothermal reduction of GO is considered similar to proton catalyzed dehydration of alcohols (Y. Zhou et al., 2009). Because of the reversible properties of proton catalyzed dehydration and hydration reactions, there should always be some residual oxygen functionalities on rGO even at the end of reactions. In solvothermal conditions, the temperature required for reduction of GO decreases as the reducing power of organic solvent increases. The minimum temperatures for GO reduction varied from 120 to 160 °C when the solvents changed from glycol to 1-butanol (Nethravathi and Rajamathi, 2008).

Heteroatoms can be introduced into graphene by adding compounds containing the required heteroatoms into GO dispersion under hydrothermal or solvothermal conditions. For example, nitrogen doped graphene has been prepared when hydrazine was used as doping reagents in both water (Long et al., 2010) and N,N-dimethylformamide (R.H. Wang et al., 2013). Hydrothermal or solvothermal method is also facile to prepare a diverse range of nanomaterials, allowing for one-pot or one-step synthesis of graphene-based nanocomposites if the growth of nanomaterials and reduction of GO occur simultaneously. Various metal oxide and sulfides, including $Co_3O_4$ (Liang et al., 2011), $Mn_3O_4$ (H.L. Wang et al., 2010), $TiO_2$ (Shah et al., 2012), $MoS_2$ (Y.G. Li et al., 2011), CdS and ZnS (P. Wang et al., 2010), have been loaded on graphene by heating reaction mixtures containing GO and desired metal ion precursors under hydrothermal or solvothermal conditions. However, the one-step strategy lacks the ability to precisely control the size and distribution of nanoparticles on graphene.

#### 2.2.4. Thermal reduction

The successful exfoliation of single-layer graphene relies on sufficient oxidation of graphite and adequate pressure during direct thermal treatment process (Schniepp et al., 2006). Therefore, special equipments are generally necessitated to obtain rapid heating rates (typically 2000 °C $min^{-1}$), high temperatures (800–1000 °C), and inert atmospheres (high vacuum, argon or hydrogen gas) (Wang et al., 2012). A number of products can be generated as a result of rapid temperature increase, including $CO_2$, CO, water, and other small hydrocarbon molecules (Jimenez, 1987; Matuyama, 1954). The generated gases at high temperatures create a huge pressure increase between the stacked layers, and eventually result in exfoliation of stacked platelets (McAllister et al., 2007).

Microwave and photo irradiation represent two kinds of innovative heating sources that can be applied for GO reduction. Compared with traditional thermal methods, uniform and rapid heating can be generated by microwave irradiation within a short time at ambient conditions (Y.W. Zhu et al., 2010b). The microwave heating can also promote chemical reactions by lowering activation energies and shortening reaction time. Metal nanoparticles decorated graphene have been prepared in one-step manner upon microwave heating the mixture of GO and metal ion precursors. In contrast to the composites prepared by mixing metal

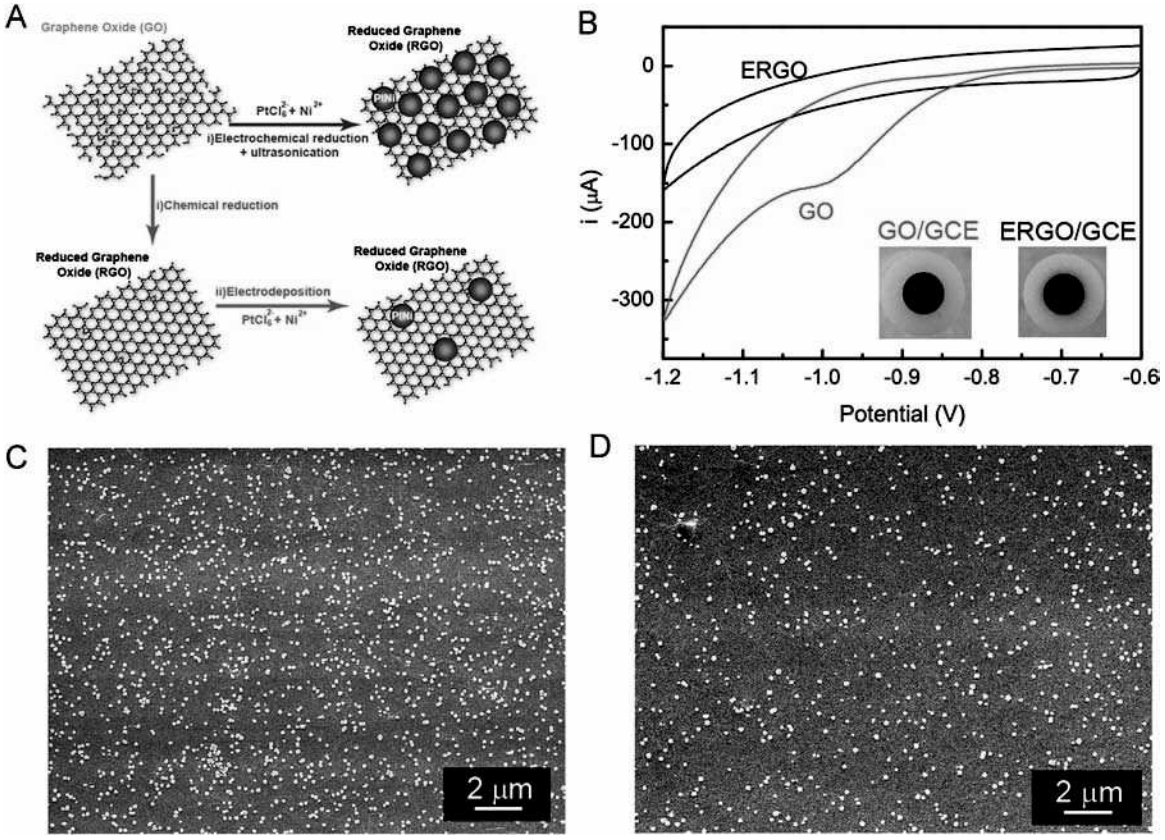


**Fig. 2.** (A) Schematic illustration of the one-step and two-step methods to prepare PtNi nanoparticles modified rGO film. (B) cyclic voltammetry (CV) curves and photographs of GO on glass carbon electrodes (GCE) before and after electrochemical reduction. SEM images of PtNi nanoparticles on rGO films prepared through (C) one-step and (D) two-step methods. Reprinted with permission from ref (Gao et al., 2011). Copyright 2011 American Chemical Society.

nanoparticles and graphene, the one-step procedure produces metal nanoparticles with smaller size and higher density on graphene (Hassan et al., 2009). It is still challenging to reduce GO incorporated into materials with poor thermal conductivity, such as polymers, which may prevent reducing reagents from completely reducing GO. Photothermal reduction can overcome these shortcomings. A camera flash can provide 9 times of thermal energy needed for heating GO above 100 °C, which is more than sufficient to initiate the thermal deoxygenation of GO (Cote et al., 2009a; F. Kim et al., 2010). In addition, photothermal method also enables patterning of GO or GO/polymer films by flashing through photomask, and precisely controls the size, position and shape of the films (Krishnan et al., 2012).

*2.2.5. Photo-catalyzed reduction*

Inorganic photocatalysts, including semiconductors (ZnO and $TiO_2$) (Williams and Kamat, 2009; Williams et al., 2008) (Fig. 3) and plasmonic metal nanoparticles (Ag nanoparticles) (Wu et al., 2011), have been successfully applied in light-assisted reduction of GO, when photoexited electrons were injected from semiconductors or metal nanoparticles into conduction band of GO. However, the inorganic nanomaterials cannot be easily removed from the dispersions containing rGO, potentially affecting the properties and limiting the applications of the resulting materials. The development of organic photocatalysts is a promising way to tackle these problems. Clean rGO sheets were prepared with organic photocatalyst, i.e., Hantzsch 1,4-dihydropyridine (HEH), under UV irradiations. HEH and its aromatic pyridine products were easily removed by extraction with ethyl acetate. The resulting rGO exhibits comparable electrical conductivity to that by hydrazine reduction (Zhang et al., 2012).

*2.2.6. Microbial reduction*

Microbial technology was first achieved for reduction of GO in strictly anaerobic environments (Salas et al., 2010). However, a follow-up work revealed that anaerobic condition is not necessary for the microbial reduction to proceed (G.M. Wang et al., 2011). In these two works, GO was reduced by a dissimilatory metal-reducing bacteria, i.e., *Shewanella*, which generate electrons in metabolic process. The generated electrons are transferrable by anaerobic respiration of cells from the cell interior to electron acceptors in environments (e.g., solid metal oxide particles). The cell membrane of c-type cytochromes promotes the direct electron transfer to GO, and the redox active species produced by the cells function as electron transfer mediators. Both of the direct and indirect pathways are likely involved in the process of extracellular electron transfer (G.M. Wang et al., 2011). Recently, reduction of GO by *Escherichia coli* was also reported in anaerobic conditions containing glucose, and glycolysis process from metabolic activity of the cells was possibly involved in reduction of GO (Akhavan and Ghaderi, 2012).

## 3. Preparation of 2D and 3D graphene materials

The flexible 2D structure of graphene materials make them versatile building blocks to construct 2D and 3D macroscopic materials, in which individual nanosheets are connected by virtue of hydrogen bonding, ionic interaction, hydrophobic effects, and/or $\pi$–$\pi$ interactions. The resulting 2D and 3D graphene materials not only retain some key properties of individual graphene sheets, but also develop collective properties resulting from their unique structures (Wu et al., 2012; Xu and Shi, 2011). Of equal importance

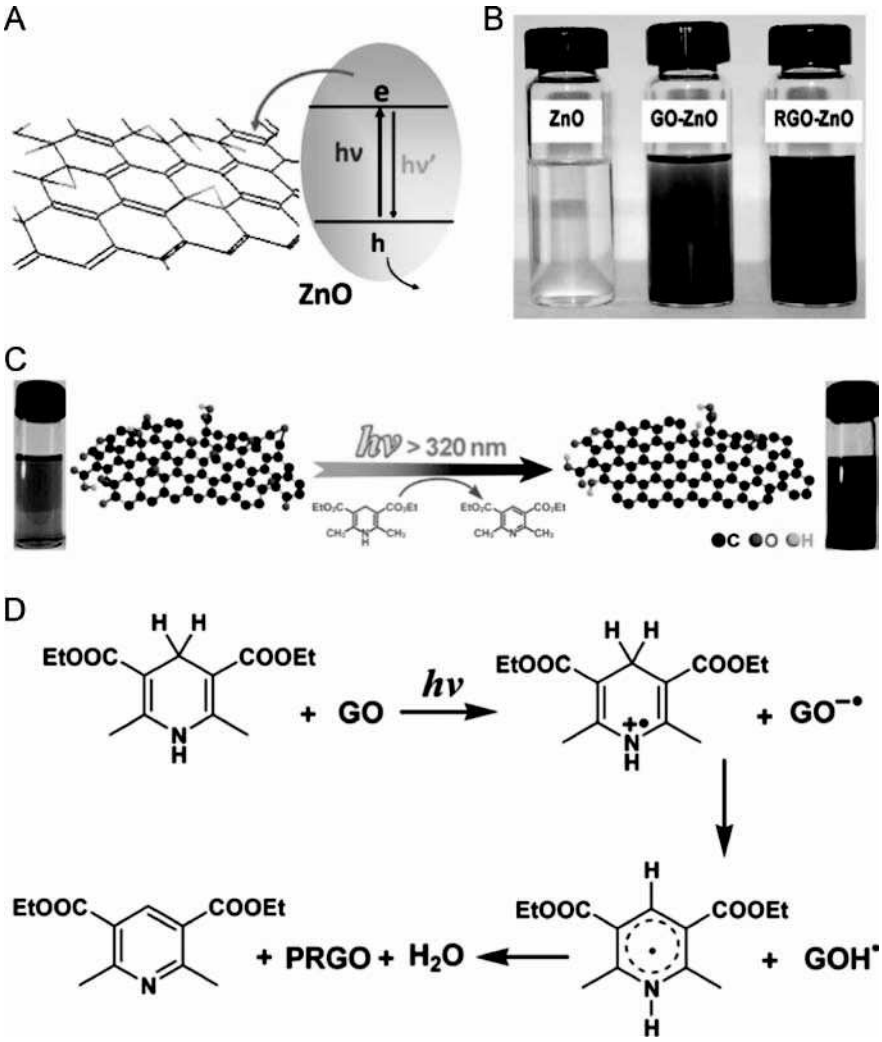


**Fig. 3.** (A) Reduction mechanism of GO by ZnO under UV excitation. (B) Suspensions of ZnO, GO-ZnO, and RGO-ZnO. Reprinted with permission from ref (Williams and Kamat, 2009). Copyright 2009 American Chemical Society. (C) Schematic illustration of photocatalytic reduction of GO by HEH. (D) Proposed chemical reaction mechanism of photochemical reduction of GO by HEH. Reprinted with permission from ref (Zhang et al., 2012). Copyright 2012 American Chemical Society.

is that a great number of functional materials can be incorporated into 2D and 3D graphene materials, improving the performance of pristine graphene materials and extending their applications to new fields.

### 3.1. Methods to prepare 2D graphene materials

#### 3.1.1. Langmuir–Blodgett method

Langmuir–Blodgett technique, an approach commonly used for depositing nanoparticles and macromolecules on substrates as thin films with controlled thickness (Park and Advincula, 2011; Tao et al., 2008), was also applied to prepare transparent graphene films suitable for optoelectronic applications. Unlike traditional transparent electrodes of ITO and FTO, graphene films were prepared in large scale at low cost, and hold great promise in the development of flexible electronic devices. The electrostatic repulsion between negatively charged GO prevents their overlapping, giving rise to stable GO monolayer film at the interfaces of air and the mixture of water/methanol. The formed GO film can be readily transferred to flat substrates through Langmuir–Blodgett technique (Cote et al., 2009b). Morphologies of GO film evolve from individual sheets to close-packed and wrinkled structures by controlling its density during deposition (Zheng et al., 2011). It is much more challenging to prepare rGO films with higher conductivity, because of the limited colloidal stability of rGO in organic solvents. After modification of rGO with surfactant, stable dispersion of rGO in 1,2-dichloroethane was obtained. Transparent and conducting film was then prepared through Langmuir–Blodgett technique from the solution of rGO in water and 1,2-dichloroethane (X.L. Li et al., 2008).

#### 3.1.2. Layer-by-layer assembly

Layer-by-layer technique has been widely adopted for fabricating multilayer films with tunable composition and architectures. The driving forces involved in layer-by-layer assembly generally include electrostatic interactions, hydrogen bonding, and covalent bonding. Based on electrostatic interactions between different charged species, multilayer films of CNTs and rGO have been fabricated from rGO with negatively charged surfaces and amine-functionalized CNTs with positively charged surfaces (Byon et al., 2011). Similarly, rGO carrying positive charge imparted by poly(ethyleneimine) coating can also be assembled with acid treated CNTs with negatively charged surface into hybrid films (Fig. 4) (Yu and Dai, 2010). CNTs incorporated into the hybrid films function as spacers to avoid aggregation of rGO caused by the strong $\pi$–$\pi$ interactions between their basal planes. The layer-by-layer technique was also extended to prepare multilayer films of negatively charged rGO and inorganic nanoparticles (Li et al.,

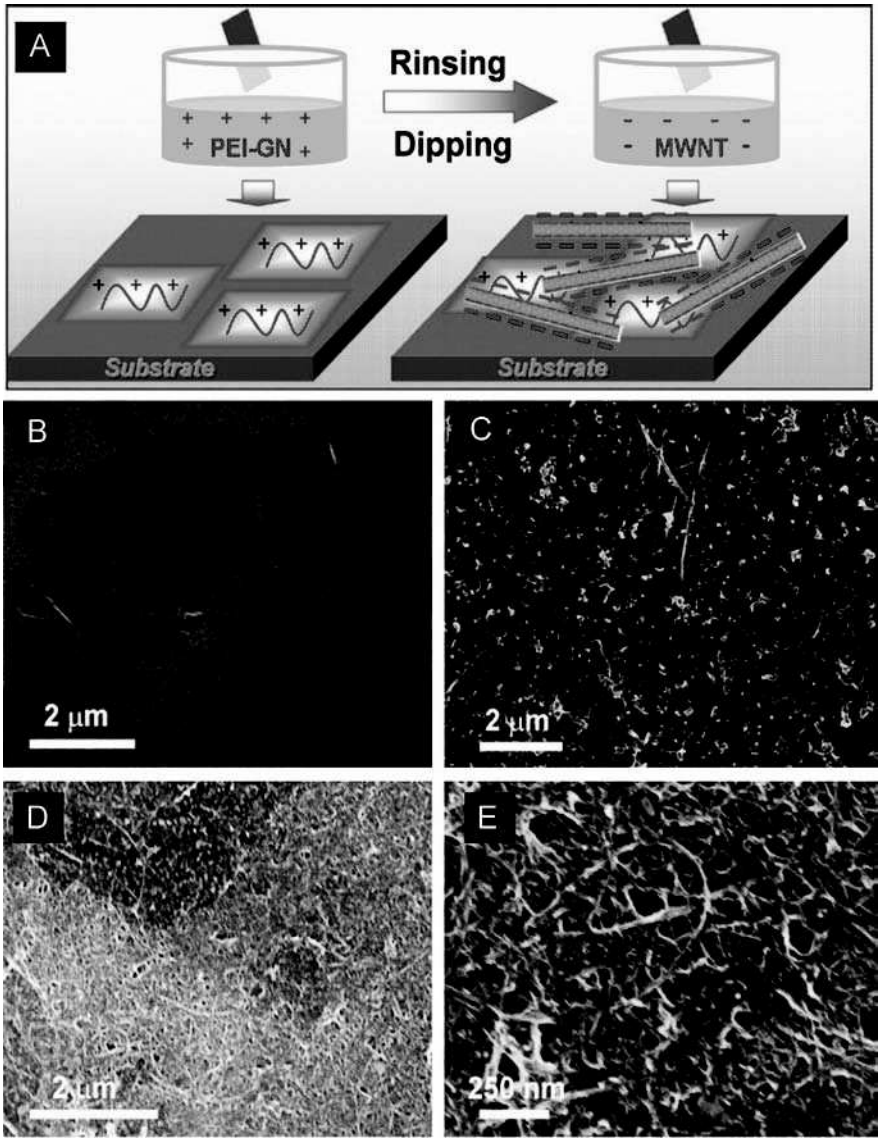


**Fig. 4.** (A) Schematic illustration of the fabrication process for multi-layer films of positively charged PEI modified graphene and negatively charged CNTs on substrates. SEM images of (B) the first layer PEI modified graphene, and (C) the first bilayer graphene and CNTs films deposited on a substrate. (D) and (E) SEM images of the graphene and CNTs films after ninth deposition cycle under low and high magnifications. Reprinted with permission from ref (Yu and Dai, 2010). Copyright 2010 American Chemical Society.

2011a). A example of multilayer films relying on hydrogen bonding was built upon from rGO and poly(vinyl alcohol) (Zhao et al., 2010).

### 3.1.3. *Electrochemical deposition*

Electrophoretic deposition is a technique to deposit thin films through electrical field driven movement of charged colloidal particles towards the electrodes with opposite charges (Van der Biest and Vandeperre, 1999). This method is easy to scale-up and suitable to a wide range of inorganic, polymer, and composite colloidal particles (Chavez-Valdez et al., 2013), leading to precisely controlled film thickness and excellent uniformity at high deposition rates. The charged surfaces of GO and rGO enables the direct electrophoretic deposition of their films. By applying a positive potential of 10 V, the negatively charged GO moves towards the positive electrode and form a uniform film within 10 min. Oxygen functionalities were eliminated in the process possibly because of reactions including oxidation of carboxylate, oxidative decarboxylation, and dimerization of radicals. And consequently, the electrophoretic deposited GO film exhibits two fold increase of electrical conductivity compared with that prepared by filtration method (An et al., 2010). The composition and properties of solution affects the structure of deposited graphene films, as evidenced by porous graphene film obtained by introducing charging and dispersing additive to the solutions (Ata et al., 2012).

Electrophoretic deposition is not restricted to two-dimensional substrates, as manifested by the successful deposition of rGO on three-dimensional nickel foam (Chen et al., 2010), and can be extended to prepare graphene composite films. Hybrid films with different contents of rGO and CNTs were obtained from solutions with different ratios of the two components (G. Zhu et al., 2011). Multilayer films of rGO and quantum dots were prepared by repeated deposition of rGO and quantum dots on flat substrates (Guo et al., 2010). An example of direct deposition of chemically modified graphene with controlled functionalities was transparent films of $MoS_2$-rGO (Lin et al., 2013).

One important finding is that electrodeposition and electrochemical reduction of GO can be achieved simultaneously on conducting substrates through employing negative potentials around $-1.0$ or $-1.2$ V, or repeated cyclic voltammetry (CV) with

the lower potential of about −1.2 V in solutions with pH from 1.5 to 12.5 (L.Y. Chen et al., 2011). The conductivity of GO dispersion, adjustable by adding different amounts of electrolytes, is a crucial factor affecting the deposition process. The suitable conductivity was in the range of 4–25 mS $cm^{-1}$. No detectable deposition occurred, if conductivity of the solution was too low. When the conductivity was higher than 25 mS $cm^{-1}$, GO dispersion became unstable (Hilder et al., 2011). As an extension of the one-step technique, composite films of rGO and metal nanoparticles with a sandwiched structure was successfully prepared from mixtures of GO and metal ion salts under cathodic conditions (Liu et al., 2011). By changing higher and lower potentials in CV scans, electrochemical reduction of GO and polymerization of monomers occurs independently at different potential ranges, leading to the formation of hybrid films of rGO and conducting polymers with multilayer structures. The top layer can be adjusted as conducting polymers or rGO by varying the directions of CV scans (Fig. 5) (Tang et al., 2012).

### 3.1.4. *Vacuum filtration*

Vacuum filtration, traditionally used to prepare paper-like films from inorganic nanomaterials with platelet morphology, such as

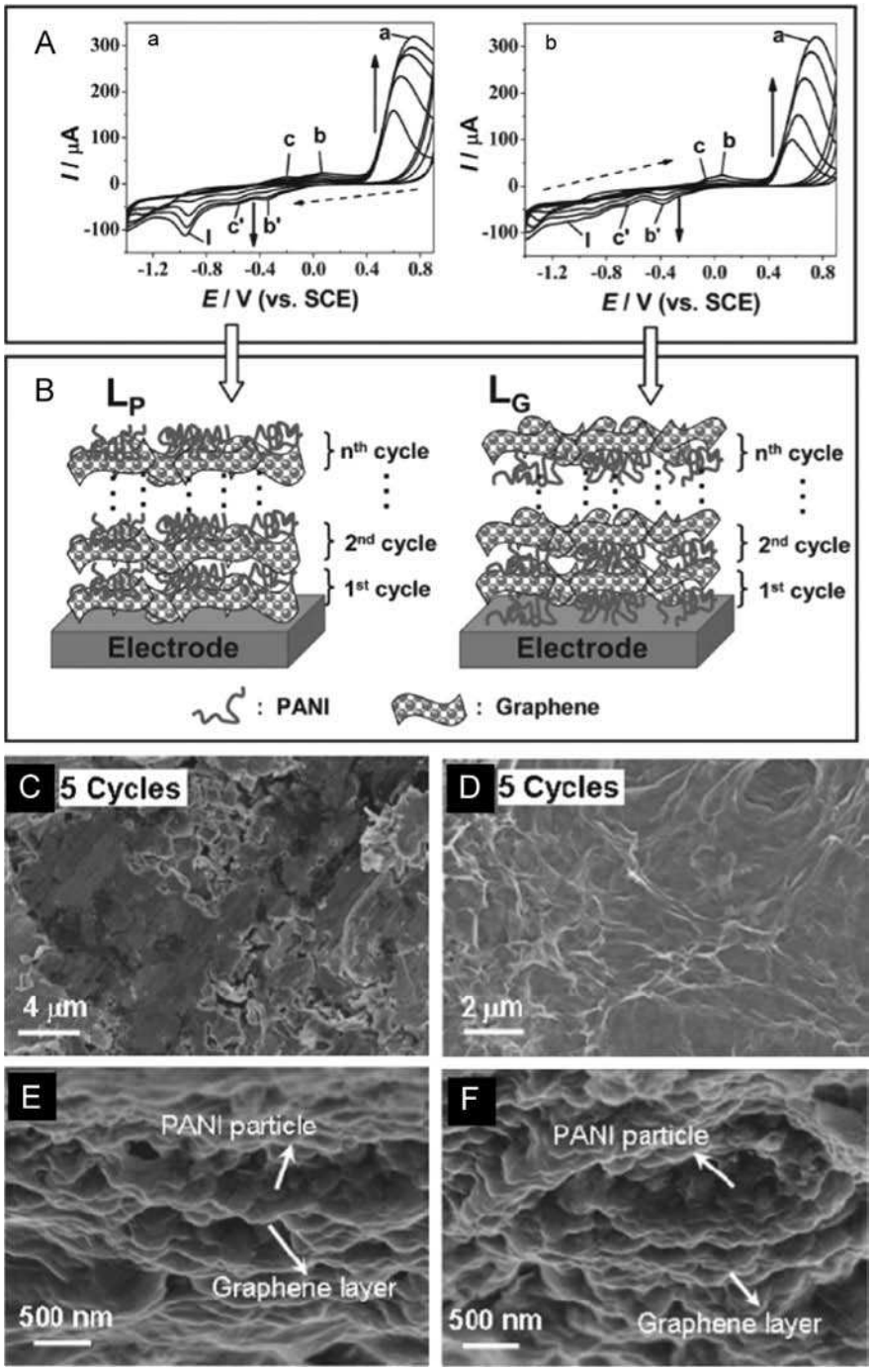


**Fig. 5.** (A) CV curves of co-electrodeposition of GO and aniline with different initial scan directions as indicated by the dash arrows. (B) Schematic illustration of two structures with PANI ($L_P$) and graphene ($L_G$) as the topmost layer. (C and D) Top-view SEM images of the two structures. (E and F) Cross-section SEM images of the two structures. Reprinted with permission from ref (Tang et al., 2012). Copyright 2012 Wiley-VCH Verlag GmbH.

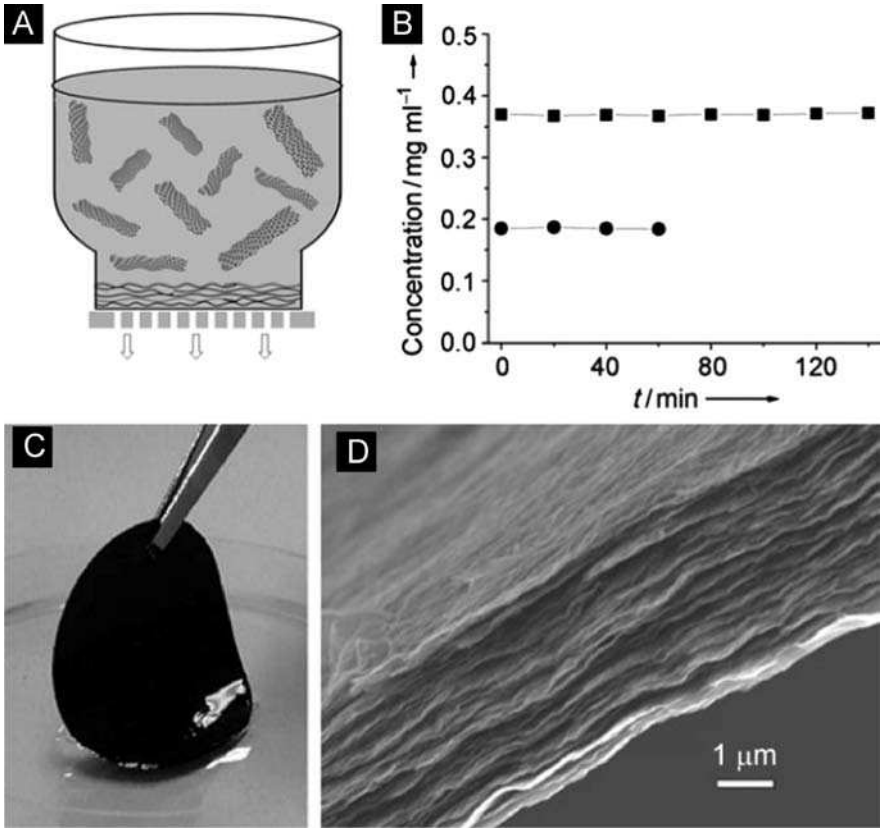


**Fig. 6.** (A) Schematic illustration of the formation process of graphene paper by filtration method. (B) The concentration of graphene versus filtration time for two samples: (■) 24 mL of 0.37 mg mL$^{-1}$ and (●) 24 mL of 0.18 mg mL$^{-1}$. (C) Photograph of the as-formed graphene film peeled from the filter membrane. (D) SEM images of the cross-section view of a free-dried graphene paper. Reprinted with permission from ref (Yang et al., 2011). Copyright 2011 Wiley-VCH Verlag GmbH.

vermiculite and mica (Ballard and Rideal, 1983), was first applied to prepare free-standing graphene paper by filtrating aqueous dispersion of GO through a porous membrane filter in 2007 (Dikin et al., 2007). The thickness of GO paper can be adjusted by changing the volume or concentration of the dispersion. This kind of paper is usually characterized by multilayer structures, because graphene sheets tend to be spontaneously arranged in a sheet-by-sheet manner at the liquid–solid interface (Fig. 6) (Yang et al., 2011). After annealing at 220 °C, Young's modulus of graphene paper increased from ~20 GPa to 41.8 GPa, as tensile strength increased from ~150 MPa to 293.3 MPa. The mechanical performance of graphene paper outperforms other inorganic paper-like materials such as graphite foils, and the conductivity of graphene paper treated at 500 °C reaches 351 S m$^{-1}$ (Chen et al., 2008).

Taking advantages of the colloid nature of graphene and the well-established methods for synthesizing various metal, metal oxide or polymer colloidal nanostructures, vacuum filtration opens the possibility for screening composite materials with desired functionalities introduced into graphene paper. In order to improve biocompatibility, Tween 20 was introduced to prepare graphene paper with no cytotoxicity to mammalian cells, leading the way for biocompatible graphene paper (Park et al., 2010). Aiming at improving electrochemical performances, polyaniline (PANI) nanofibers were uniformly sandwiched between rGO sheets to produce composite graphene paper (Wu et al., 2010). Composite graphene paper of rGO functionalized with metal oxide nanoparticles (e.g., $SnO_2$, NiO, $MnO_2$, and $SiO_2$) can be prepared in a similar way (Li et al., 2011b; D.H. Wang et al., 2010).

#### 3.1.5. Solvent evaporation

It was initially found that GO can be assembled into film at air-liquid interface by simply heating its solution at 80 °C for about 40 min. The size and thickness of the film is determined respectively by surface area of the interface and heating time (Chen et al., 2009). Another work revealed that chemical reduction and self-assembly of GO at the interface can be achieved simultaneously if GO solution containing hydrazine was heated (Zhu et al., 2009). The air–liquid interface provides an ideal platform for hybridizing graphene with other components, leading to composite films with an identical composition to that in solutions (Shao et al., 2012). However, the films at air–liquid interface must be transferred to substrates, and handled carefully to retain structural integrity of the films. We found that if water was completely removed, GO membrane deposited on PTFE substrates can be easily peeled off (Xiao et al., 2013). This strategy was also adopted to prepare rGO paper by adding reducing reagent of hydrogen iodine to GO solution (Cong et al., 2013). However, the mechanical properties of graphene paper prepared by solvent-evaporation are usually poorer relative to that obtained from vacuum filtration.

### 3.2. Methods to prepare 3D graphene materials

#### 3.2.1. Hydrothermal reduction

The first example of 3D graphene materials, i.e., graphene hydrogel, was prepared by hydrothermal treatments of GO dispersions at a concentration not lower than 2 mg mL$^{-1}$ at 180 °C for 12 h (Y.X. Xu et al., 2010). After freeze-dried, electrical conductivity of the prepared graphene hydrogel can reach $5 \times 10^{-3}$ S cm$^{-1}$, and the modulus is as high as 450–490 kPa. The mechanism of forming graphene hydrogel was proposed as follows: Before hydrothermal reduction, the hydrophilic GO sheets are well dispersed in water; with increasing the reduction time, the oxygen functionalities on GO are eliminated gradually, and the conjugated structures are restored; the growing hydrophobic and $\pi$–$\pi$ interactions

between rGO lead to random self-assembly of the flexible sheets in 3D, which eventually form hydrogel with pore size distribution from sub-micrometer to a few micrometers (Zhang and Shi, 2011). If the concentration of GO is lower than 2 mg $mL^{-1}$, the partial overlapping and crosslinking is more difficult to take place between rGO sheets, and only dispersions or aggregated powders can be obtained. In addition, hydrothermal method requires high temperature and long reaction time to form stable graphene hydrogel.

### 3.2.2. Chemical reduction

The presence of reducing reagents, including sodium ascorbate, ascorbic acid, hydroiodic acid, sulfur-containing chemicals, and hydroquinone (Chen and Yan, 2011; Sheng et al., 2011), can promote the reduction and self-assembly of GO into graphene hydrogel under mild condition (~95 °C) in a shorter reaction time (within 1.5 h). A combination of functionalization, lyophilization, and microwave treatment was employed to prepare ultralight graphene hydrogel in which GO was first functionalized and assembled into graphene hydrogel in aqueous solutions containing a weak reducing reagent, i.e., ethylenediamine, and microwave irradiation was then applied to eliminate oxygen functional groups (Hu et al., 2013).

The properties of graphene hydrogel can be easily tuned by introducing different functionalities in chemical reduction and self-assembly process, for example, polymers, CNTs, and metal nanoparticles (Hu et al., 2012; Qiu et al., 2010; Sui et al., 2012). Taking the advantages of the fascinating properties of dopamine, e.g., reducing activity, self-polymerization, and strong adhesion of polydopamine to solid substrates, simultaneous reduction of GO and coating of polydopamine was achieved to produce graphene hydrogel functionalized with polydopamine (Gao et al., 2013). Iron oxide nanoparticles were immobilized on graphene hydrogel through one-step reduction using Fe(II). The composition and morphology of iron oxide nanoparticles can be controlled by adjusting pH of the solutions (Fig. 7) (Cong et al., 2012).

### 3.2.3. Template-directed method

Template-directed method provides an approach to fabricating 3D graphene materials with well-controlled pore size distributions. The commonly used sacrificial templates, i.e., polystyrene (PS) and silica colloidal particles, have been applied to prepare 3D graphene materials. A mixture of PS and GO was filtrated through a membrane. Dissolution of PS particles by toluene resulted in graphene foam with uniform pore structures (Fig. 8) (Choi et al., 2012). Capillary modeling, a more general approach to wrap GO sheets on template particles, was achieved in a device for aerosol spray pyrolysis, leading to uniform hollow rGO capsules (Sohn et al., 2012). The template method was also extended to prepare nitrogen and sulfur doped porous graphene by impregnating solutions containing GO, poly(vinyl pyrrolidone) and sulfonated PS particles onto nickel foam, followed by freeze-drying and calcination in nitrogen atmosphere to remove the template and PVP surfactants (Z.L. Wang et al., 2013).

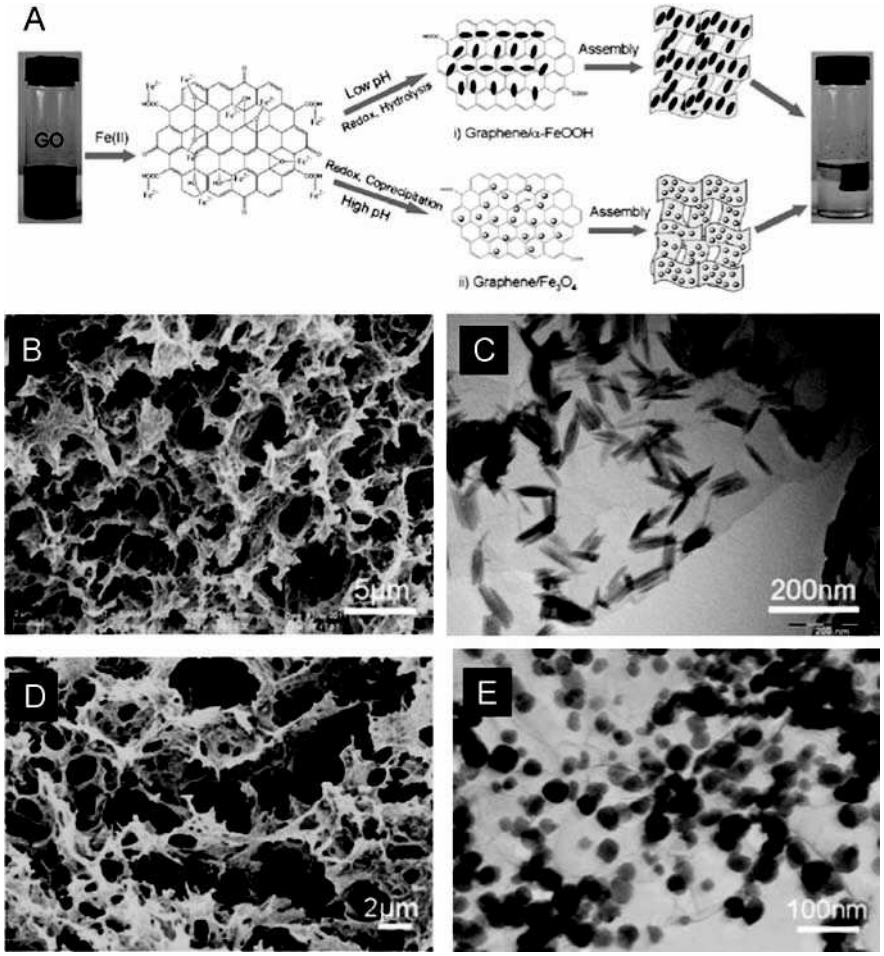


**Fig. 7.** (A) Schematic illustration of the formation mechanism of rGO and iron oxide nanoparticles with different morphologies. (B) SEM and (C) TEM images of rGO and FeOOH. (D) SEM and (E) TEM images of rGO and $Fe_3O_4$. Reprinted with permission from ref (Cong et al., 2012). Copyright 2012 American Chemical Society.

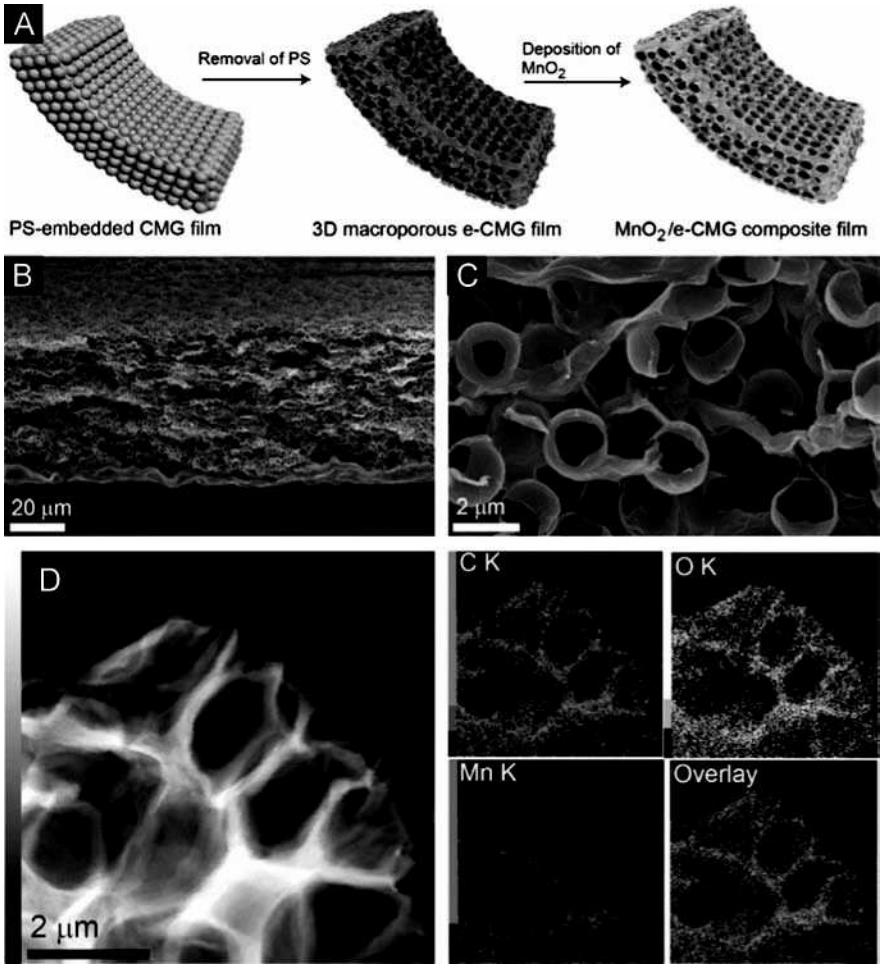


**Fig. 8.** (A) Schematic illustration of the fabrication process of 3D macroporous graphene films through an embossing process with PS as the templates for embossed chemically modified graphene (e-CMG) film and subsequent deposition of $MnO_2$ for $MnO_2$/e-CMG film. (B) Low and (D) high magnified cross-section SEM images of e-CMG films. (D) STEM images and EDS mapping of C, O, Mn, and overlay elements on $MnO_2$/e-CMG film. Reprinted with permission from ref (Choi et al., 2012). Copyright 2012 American Chemical Society.

However, the pore size of graphene foam templated by PS is limited to micrometers due to the relatively larger size of template particles (20 μm). Methyl functionalized silica nanoparticles (30–120 nm) were developed as templates to prepare nanoporous graphene foam (Huang et al., 2012). Core–shell structure of GO wrapped onto silica nanoparticles was prepared by virtue of hydrophobic interaction between amphiphilic GO and methyl groups on silica templates (J. Kim et al., 2010). Centrifugation was then applied to condense the nanoparticles, followed by HF etching of silica templates.

*3.2.4. Chemical vapor deposition*

Chemical vapor deposition (CVD) can produce graphene materials with higher electrical conductivity and fewer defects than that prepared from wet-chemical approaches. Methane was first employed as the carbon precursor to synthesize 3D graphene materials by CVD, using porous nickel foam with 3D interconnected channels as substrate. The resulting graphene foam is monolithic with 3D interconnected graphene sheets, and its density is as low as 5 mg $cm^{-3}$, which is comparable to the lightest aerogel (2–3 mg $cm^{-3}$) (Z.P. Chen et al., 2011). Afterwards, a study revealed that graphene foam exhibiting almost the same morphology can be produced using safer and cheaper carbon precursors such as ethanol (Cao et al., 2011). With ethanol as the precursor, graphene foam coated with a dense layer of CNTs mesh was prepared via a two-step CVD method (Dong et al., 2012a). The monolithic graphene foam with high surface areas and excellent electrical conductivity is a promising candidate for a wide spectrum of applications (Dong et al., 2012b; Maiyalagan et al., 2012; Yong et al., 2012).

## 4. Bioelectrochemical applications of 2D and 3D graphene materials

The self-assembled 2D and 3D graphene materials, functionalized with metal nanoparticles, polymers and biomolecules, are promising candidates for bioelectrochemical applications, especially in the fields of electrochemical biosensors and biological fuel cells. Electrochemical biosensors with high sensitivity have found widespread uses in clinic diagnosis, environment monitoring, and quality controls in industrial, food, and agricultural products (Ronkainen et al., 2010). Biological fuel cells represent an important kind of electrochemical energy conversion devices that can directly transform chemical energy from biomass into electrical energy with high efficiency and low or zero emission of pollutants. The biological fuel cells also have the ability to integrate environmental bioremediation with power production (Logan, 2009).

### 4.1. Electrochemical biosensors

#### 4.1.1. 2D graphene materials for electrochemical biosensors

Real-time and point-of-care detection necessitates the development of portable and wearable medical devices, in which flexible electrodes are the crucial components (Windmiller and Wang, 2013). Graphene paper is a promising scaffold to construct flexible electrodes because of its unique properties, such as high mechanical strength, structural uniformity, and excellent electrical conductivity. A hybrid film was prepared by filtration of Nafion functionalized rGO, and then modified by organophosphorous hydrolase (OPH). The remarkable electrical conductivity of rGO and low interfacial resistance of Nafion empowered OPH-modified graphene film with excellent electrochemical performance towards detection of organophosphate with a sensitivity of 10.7 nA $\mu M^{-1}$ and detection limit of 0.137 $\mu$M. Importantly, after 100 binding cycles, the sensitivity of the flexible biosensor was still as high as 9.7 nA $\mu M^{-1}$ (Choi et al., 2010). In order to achieve real-time detection of biomolecules released from living cells, RGD-peptide, which can facilitate the attachment and growth of cells, was covalently modified onto graphene paper. This flexible electrode was further employed for monitoring of nitric oxide released from endothelial cells, while keeping its original performance after 45 times of bending and relaxing cycles (Guo et al., 2012).

Because of the lack of surface functionalities, it is challenging to modify graphene paper with high density nanoparticles. A combined approach of 2D assembly of gold nanoparticles at oil–water interface coupled with dip-coating method was employed to prepare freestanding graphene paper electrodes covered by closely packed gold nanoparticles. The electrode exhibited excellent electrochemical performance for electro-oxidation of glucose, and superior biocompatibility, and allowed for direct detection of low concentration $H_2O_2$ secreted by living cells (Fig. 9) (F. Xiao et al., 2012b). Another advantage of this modular approach is the feasibility to tune the size, composition and morphology of the active nanoparticles. In a follow-up work, core–shell Au@Pt nanoparticles were successfully coated on graphene paper, and applied for the detection of nitric oxide released by living cells under oxidative stress (Zan et al., 2013). In order to increase surface areas of graphene paper, it was first modified by electrodeposition of $MnO_2$ nanowires, which provide more growing sites for metallic nanoparticles. The constructed electrode was successfully applied for detection of $H_2O_2$ from living cell with a variation of amperometric response less than 5% after 100 repeated bending (F. Xiao et al., 2012a).

#### 4.1.2. 3D graphene materials for electrochemical biosensors

In comparison with 2D graphene paper, it is possible to introduce more enzymes and catalysts into 3D graphene materials because of increased surface areas. Prussian blue modified graphene hydrogel was prepared by adding $FeCl_3$ solution containing ascorbic acid into the mixture of GO and ferricyanide. The detection limit of the prepared electrode for $H_2O_2$ was as low as 5 nM (L. Chen et al., 2012). $Co_3O_4$ nanowires were uniformly deposited

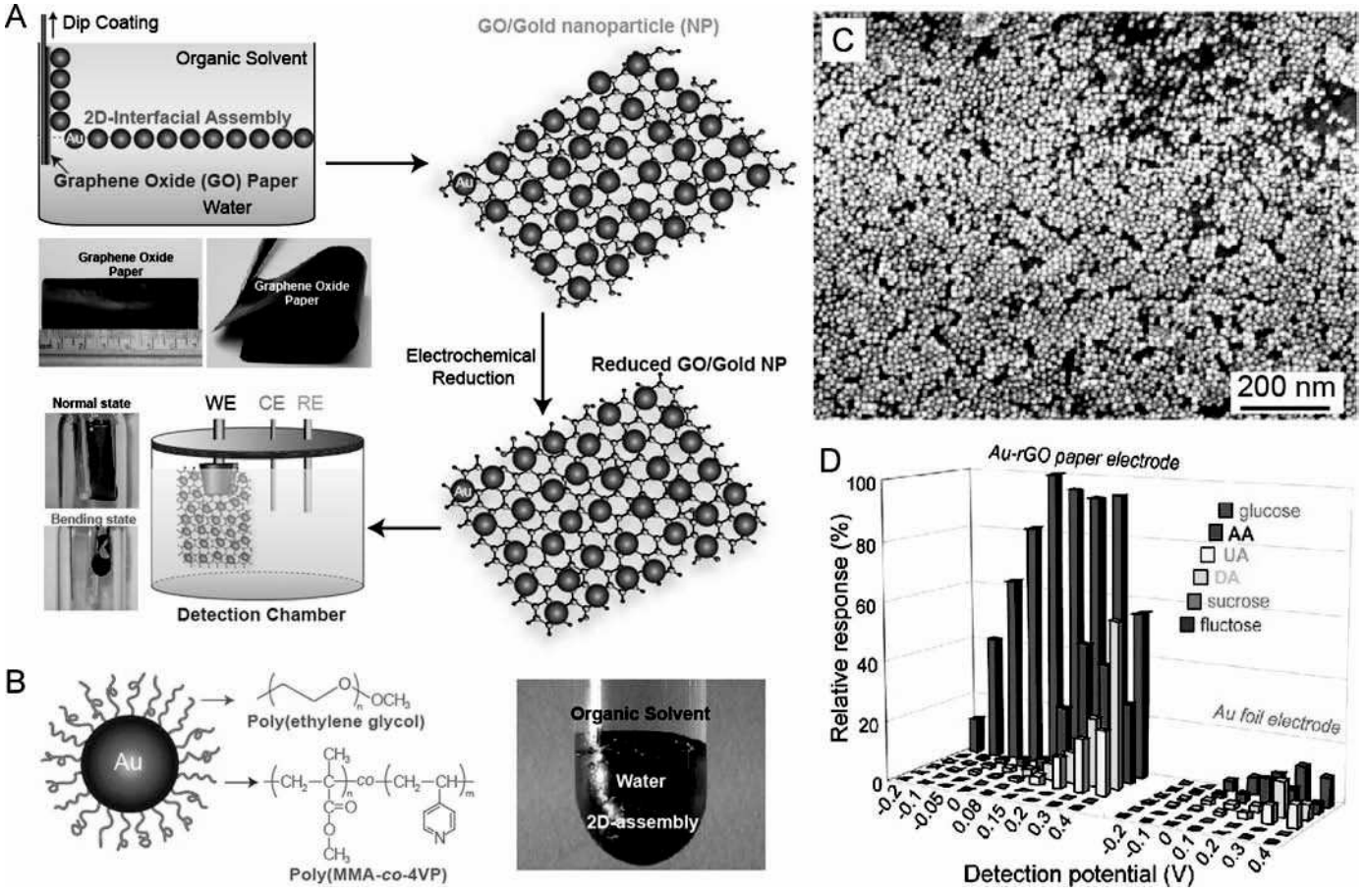


**Fig. 9.** (A) Schematic illustration of the fabrication process from the 2D assembly Au nanoparticles and graphene paper. (B) Structure of the amphiphilic Au nanoparticles and their assembly at the interface of water and organic solvent. (C) SEM images of 2D assembly of Au nanoparticles on graphene paper. (D) Comparison of the prepared Au nanoparticles-rGO paper electrodes and gold foil towards the detection of different molecules. Reprinted with permission from ref (F. Xiao et al., 2012b). Copyright 2012 American Chemical Society.

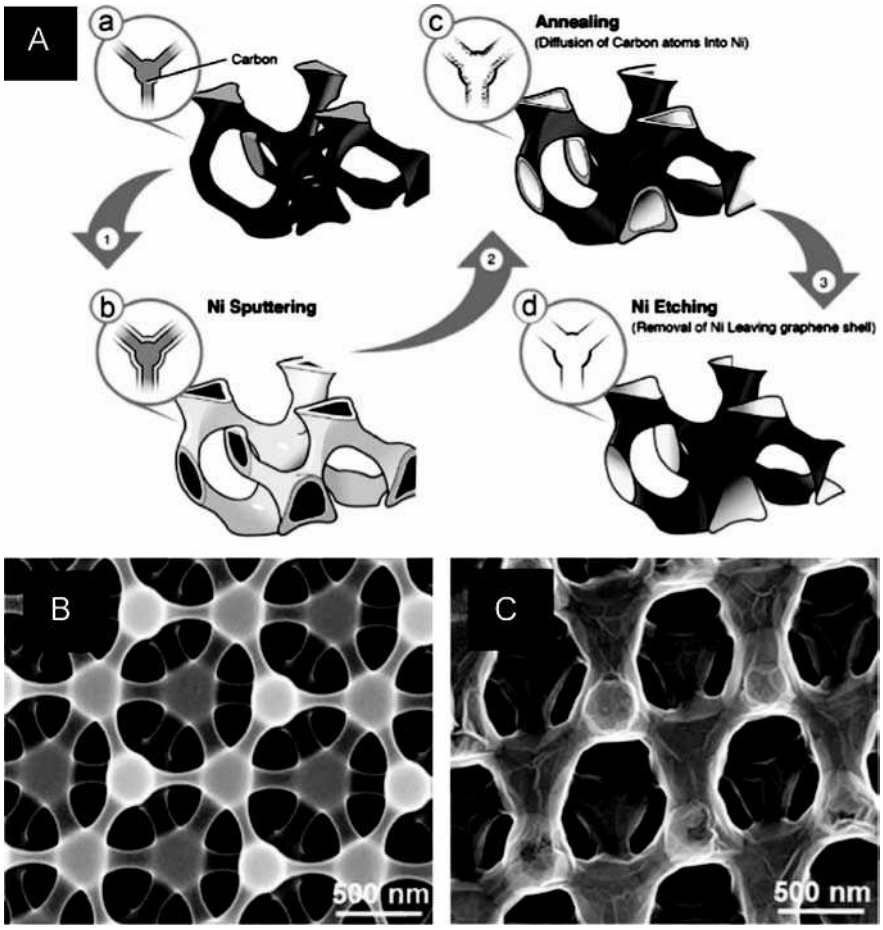


**Fig. 10.** (A) Schematic illustration of the preparation process and mechanism for chemical conversion of amorphous porous carbon to 3D graphene. (B) SEM images of the prepared 3D graphene. (C) SEM images of the 3D graphene after the modification of Pt nanoparticles. Reprinted from ref (X.Y. Xiao et al., 2012a). Copyright 2012 American Chemical Society.

onto CVD-grown 3D graphene foam through hydrothermal method, and used as free-standing electrodes towards the analysis of glucose, affording a detection limit of 25 nM (Dong et al., 2012b). Graphene foam functionalized with nickel was prepared by annealing lithographically defined 3D porous carbon coated nickel at 750 °C for 20 min under the flow of forming gas containing 5% $H_2$ and 95% $N_2$ (Fig. 10) (X.Y. Xiao et al., 2012a). The electrode exhibits a good linear range for glucose concentration from 1 to 10 mM (X.Y. Xiao et al., 2012b). A variety of noble metal nanoparticles, including Pt, Au and Pd were further electrodeposited onto the 3D graphene foam prepared by the lithographic method. The onset potential for $H_2O_2$ reduction appeared at 0.1 V while the reduction peak was observed at −0.1 V on Pd nanoparticles modified graphene foam (Sattayasamitsathit et al., 2013).

### 4.2. Biological fuel cells

#### 4.2.1. 2D graphene materials for biological fuel cells

Among the different types of fuel cells, biological fuel cells are distinguished from the others by utilizing biocatalysts, i.e., complete living cells, organelles, and enzymes, as the anode or cathode to generate electrical power from biomass or biofuels (Cooney et al., 2008). The electron transfer efficiency between biocatalysts and electrodes directly determines bioelectrocatalytic process and performance of biological fuel cells (Logan et al., 2007). A collection of intriguing properties such as high surface areas, excellent biocompatibility and high electrical conductivity enabled the use of graphene-based materials in *E. coli* catalyzed microbial fuel cells. The attachment of bacteria onto the stainless steel mesh anode was enhanced by graphene, and the power density was improved by 17–18 times compared with bare stainless steel mesh electrode or the one modified with polytetrafluoroethylene (Zhang et al., 2011). To further enhance the interaction of negatively charged bacteria with graphene film coated on carbon paper, a positively charged layer of poly(3,4-ethylenedioxythiophene) (PEDOT) was deposited on the graphene film by electropolymerization. The short-circuit current achieved by the microbial fuel cell based on graphene/PEDOT anode was 3.59 A $m^{-2}$, which is almost 7 times higher than that achieved by carbon paper electrode. The maximum power output reached 873 mW $m^{-2}$ on the graphene/PEDOT electrode, representing a 15-fold increase relative to the result from carbon paper bioanodes (Y. Wang et al., 2013).

The application of 2D graphene film in enzymatic biofuel cells was also demonstrated in multilayer electrodes. When graphene was used as spacer, the multilayer films of multiwalled carbon nanotubes or methylene green were readily assembled onto electrodes through layer-by-layer strategy based on electrostatic and/or $\pi$–$\pi$ interactions (X. Wang et al., 2011). The biocatalyst of glucose dehydrogenase was then dip-coated on the multilayer film to prepare bioanodes. The layer-by-layer strategy enables the formation of structurally uniform multilayer film, and the coverage of graphene was increased upon repeating assembly processes. In couple with laccase-based biocathode, the assembled glucose/oxygen biofuel cell exhibits an open-circuit voltage of 0.69 V and a

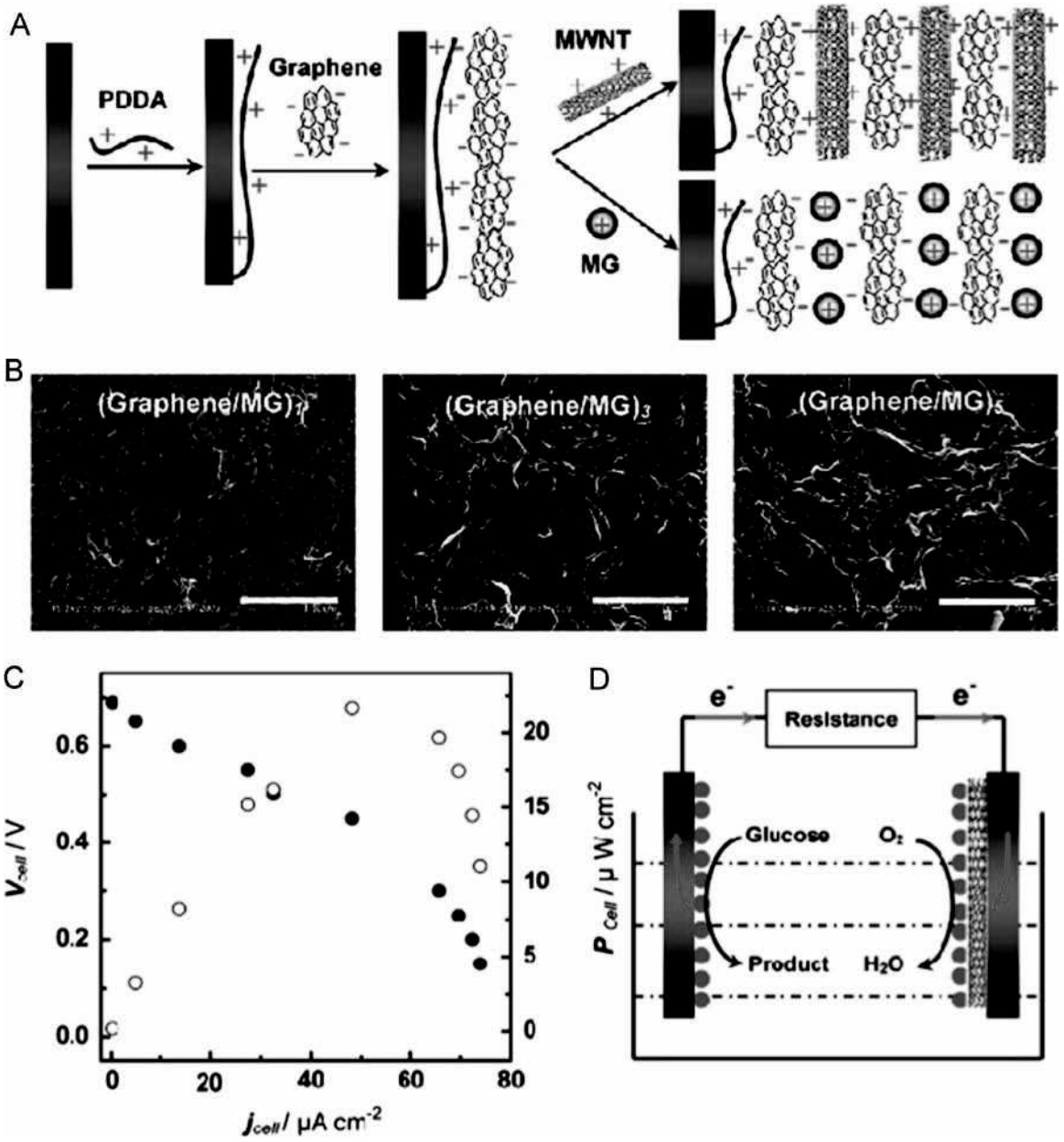


**Fig. 11.** (A) Schematic illustration of the fabrication process of multi-layered film with graphene as spacer. (B) SEM images of the graphene/methylene green film with different number of layers. (C) Polarization curve of the assembled glucose/oxygen biofuel cell and the dependence of the power output on the current density in the quiescent phosphate buffer containing $NAD^+$ and glucose under ambient condition. (D) Schematic illustration of the glucose/oxygen biofuels cell. Reprinted with permission from ref (X. Wang et al., 2011). Copyright 2012 American Chemical Society.

maximum power density of 22.50 μW cm$^{-2}$ at 0.48 V in phosphate buffer solution containing 10 mM $NAD^+$ and 30 mM glucose (Fig. 11).

*4.2.2. 3D graphene materials for biological fuel cells*

3D graphene materials with increased surface areas for bacterial colonization or biocatalysts immobilization are emerging as new electrode substrates for biological fuel cells. In order to increase electrical conductivity of graphene sponge, stainless-steel current collectors were incorporated into 3D graphene material. The maximum power density produced by the composite anode was 14 times of that produced by graphene-sponge anode. And importantly, the cost was estimated to be at least one order of magnitude less than commercial graphite electrode (Xie et al., 2012). A feasible deposition method was developed to prepare 3D rGO-nickel foam anode for microbial fuel cells, in which the loading amount of rGO and electrode surface areas were controlled by the number of rGO loading cycles. The uniform macroporous scaffold enables effective mass diffusion of the culture medium, and provides large accessible surface area for microbial colonization. Furthermore, the controlled deposition method was suitable for fabricating large-scale electrodes. At steady state of power generation, the microbial fuel cells with rGO-nickel foam produced a substantially higher power density than that of nickel foam and other conventional carbon based electrode. The optimal volumetric power density reached 661 W m$^{-3}$ based on the volume of the anode material, or 27 W m$^3$ based on the volume of the anode chamber (H.Y. Wang et al., 2013).

Free-standing 3D graphene electrode made it possible to develop light-weight devices with high performance. Ice segregation induced self-assembly, a freeze casting technique towards the preparation of macroporous materials with aligned structures

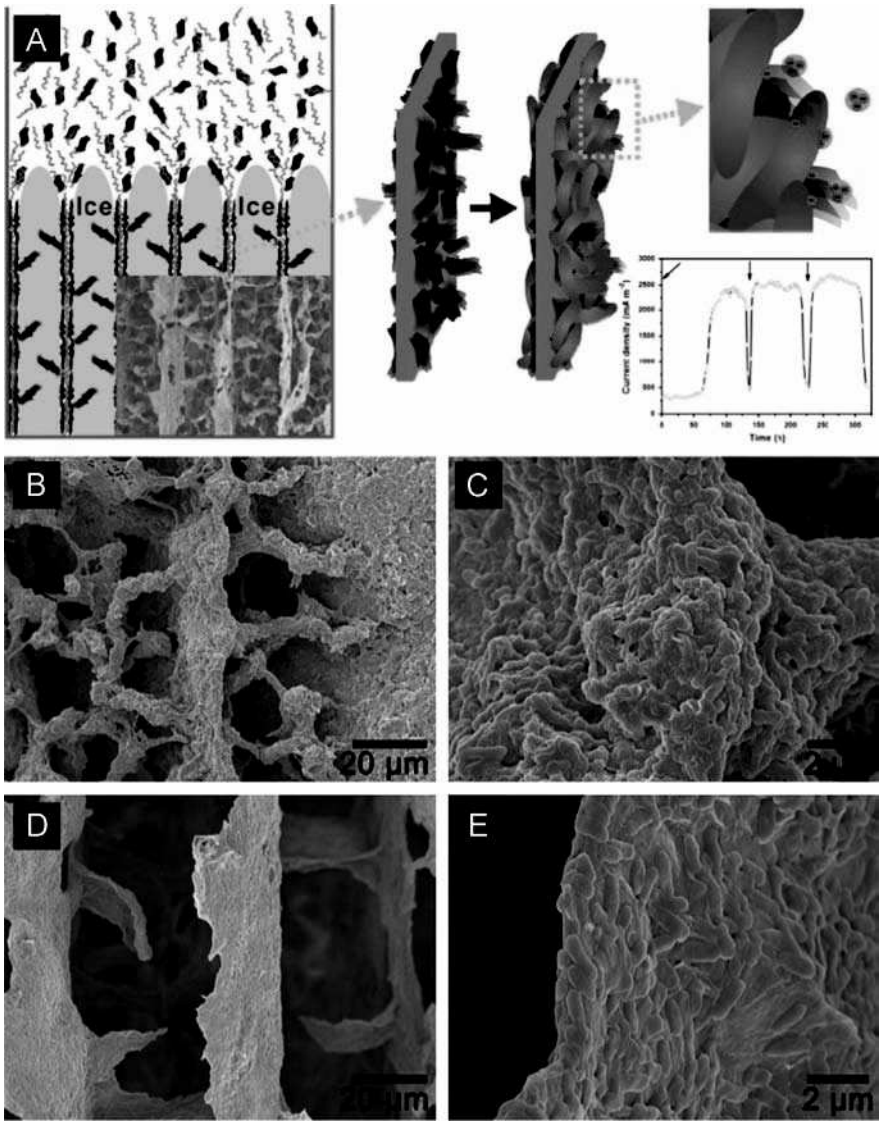


**Fig. 12.** (A) Schematic illustration of the fabrication process of 3D chitosan/vacuum-stripped graphene from the ice segregation induced self-assembly. SEM images of (B and C) chitosan/vacuum-stripped graphene, and (D and E) the scaffolds after incubation with bacteria. Reprinted with permission from ref (He et al., 2012). Copyright 2012 American Chemical Society.

(Vickery et al., 2009), was applied to prepare 3D chitosan/vacuum-stripped graphene (CHI/VSG) scaffold with hierarchically porous structures. The prepared macroporous material can facilitate colonization of bacteria in the scaffold interior and enhance the contact of biocompatible VSG and bacteria, and the meso-micropores increase the available surface area of graphene for electron transfer (Fig. 12). The synergistic effect of hierarchical pores in the anode significantly improved the performance of microbial fuel cells, leading to a maximum power density of 1530 mW $m^{-2}$, which is 78 times higher than that based on carbon cloth anode (19.5 mW $m^{-2}$) (He et al., 2012). In order to overcome the unfavorable adhesion of bacteria on hydrophobic graphene sheets, hydrophilic PANI was electrodeposited on monolithic graphene foam, resulting in a confluent biofilm of *Shewanella oneidensis* on graphene surface. The bacteria also densely adhered on graphene surface deep inside the 3D electrode, whereas only some of outmost surface was coated by biofilm on 3D graphene without PANI functionalization. The maximum power density obtained from the microbial fuel cell based on 3D graphene/PANI is ~768 mW $m^{-2}$, which is about 4 times higher than that from carbon cloth (~158 mW $m^{-2}$) (Yong et al., 2012).

## 5. Conclusions and perspectives

The flexible structures and tunable functionalities make graphene sheets an attractive type of building blocks for 2D and 3D materials. A number of approaches have been developed to fabricate these materials, which not only preserve the inherent properties of individual graphene sheets, but also develop additional functions arising from their hierarchical structures. Despite the considerable achievements in this area during the last a few years, their successful implementation into practical applications will require further research efforts from different areas combining multiple disciplines including chemistry, physics, engineering, material and biological science.

The research on hierarchical structures based on graphene sheets is still in its infancy, with key issues to be addressed in future studies. First, increasing evidence has demonstrated that the structures and properties of 2D and 3D graphene architectures are highly dependent on those of the building blocks. However, it is still challenging to synthesize monodisperse graphene sheets with controlled sizes, shapes and functionalities. Second, the electrical conductivity is a crucial factor that determines the

performances of graphene materials. Nonetheless, there is still a lack of approaches to efficiently restore the aromatic framework to produce graphene sheets with low oxygen to carbon ratios. Third, the relationships between the structures and properties of the hierarchical graphene materials have still not been fully understood, and consequently it is desired to explore guidelines for rational design and synthesis of these materials. Finally, the application of 2D and 3D graphene materials is not limited to the above-mentioned research areas, and it is possible to introduce novel functional building blocks into 2D and 3D graphene materials with enhanced performance in other fields through the existing and newly-developed methods.

## Acknowledgments

H.D. thanks the Program of Nanyang Assistant Professorship and the Arkray-NTU joint research project for financial support. H.G. is a recipient of graduate research scholarship supported by Nanyang Technological University, Singapore.

## References

Akhavan, O., Ghaderi, E., 2012. Carbon 50 (5), 1853–1860.
An, S.J., Zhu, Y.W., Lee, S.H., Stoller, M.D., Emilsson, T., Park, S., Velamakanni, A., An, J. H., Ruoff, R.S., 2010. J. Phys. Chem. Lett. 1 (8), 1259–1263.
Ata, M.S., Sun, Y., Li, X., Zhitomirsky, I., 2012. Colloid Surf. A: Physicochem. Eng. Asp. 398, 9–16.
Bai, H., Li, C., Shi, G.Q., 2011. Adv. Mater. 23 (9), 1089–1115.
Ballard, D.G.H., Rideal, G.R., 1983. J. Mater. Sci. 18 (2), 545–561.
Bi, H.C., Xie, X., Yin, K.B., Zhou, Y.L., Wan, S., He, L.B., Xu, F., Banhart, F., Sun, L.T., Ruoff, R.S., 2012. Adv. Funct. Mater. 22 (21), 4421–4425.
Brodie, B.C., 1859. Phil. Trans. R. Soc. Lond. 149, 249–259.
Byon, H.R., Lee, S.W., Chen, S., Hammond, P.T., Shao-Horn, Y., 2011. Carbon 49 (2), 457–467.
Cao, X.H., Shi, Y.M., Shi, W.H., Lu, G., Huang, X., Yan, Q.Y., Zhang, Q.C., Zhang, H., 2011. Small 7 (22), 3163–3168.
Chavez-Valdez, A., Shaffer, M.S.P., Boccaccini, A.R., 2013. J. Phys. Chem. B 117 (6), 1502–1515.
Chen, C.M., Yang, Q.H., Yang, Y.G., Lv, W., Wen, Y.F., Hou, P.X., Wang, M.Z., Cheng, H. M., 2009. Adv. Mater. 21 (29), 3007–3011.
Chen, D., Feng, H.B., Li, J.H., 2012. Chem. Rev. 112 (11), 6027–6053.
Chen, D.Z., Li, L.D., Guo, L., 2011. Nanotechnology 22 (32), 325601.
Chen, H., Muller, M.B., Gilmore, K.J., Wallace, G.G., Li, D., 2008. Adv. Mater. 20 (18), 3557–3561.
Chen, J., Li, C., Shi, G.Q., 2013. J. Phys. Chem. Lett. 4 (8), 1244–1253.
Chen, L., Wang, X.J., Zhang, X.T., Zhang, H.M., 2012. J. Mater. Chem. 22 (41), 22090–22096.
Chen, L.Y., Tang, Y.H., Wang, K., Liu, C.B., Luo, S.L., 2011. Electrochem. Commun. 13 (2), 133–137.
Chen, W.F., Yan, L.F., 2011. Nanoscale 3 (8), 3132–3137.
Chen, Y., Zhang, X., Yu, P., Ma, Y.W., 2010. J. Power Sources 195 (9), 3031–3035.
Chen, Z., Yu, D.S., Xiong, W., Liu, P.P., Liu, Y., Dai, L.M., 2014. Langmuir 30 (12), 3567–3571.
Chen, Z.P., Ren, W.C., Gao, L.B., Liu, B.L., Pei, S.F., Cheng, H.M., 2011. Nat. Mater. 10 (6), 424–428.
Cheng, C., Li, D., 2013. Adv. Mater. 25 (1), 13–30.
Choi, B.G., Park, H., Park, T.J., Yang, M.H., Kim, J.S., Jang, S.Y., Heo, N.S., Lee, S.Y., Kong, J., Hong, W.H., 2010. ACS Nano 4 (5), 2910–2918.
Choi, B.G., Yang, M., Hong, W.H., Choi, J.W., Huh, Y.S., 2012. ACS Nano 6 (5), 4020–4028.
Compton, O.C., Nguyen, S.T., 2010. Small 6 (6), 711–723.
Cong, H.P., Ren, X.C., Wang, P., Yu, S.H., 2012. ACS Nano 6 (3), 2693–2703.
Cong, H.P., Ren, X.C., Wang, P., Yu, S.H., 2013. Energy Environ. Sci. 6 (4), 1185–1191.
Cooney, M.J., Svoboda, V., Lau, C., Martin, G., Minteer, S.D., 2008. Energy Environ. Sci. 1 (3), 320–337.
Cote, L.J., Cruz-Silva, R., Huang, J.X., 2009a. J. Am. Chem. Soc. 131 (31), 11027–11032.
Cote, L.J., Kim, F., Huang, J.X., 2009b. J. Am. Chem. Soc. 131 (3), 1043–1049.
Dikin, D.A., Stankovich, S., Zimney, E.J., Piner, R.D., Dommett, G.H.B., Evmenenko, G., Nguyen, S.T., Ruoff, R.S., 2007. Nature 448 (7152), 457–460.
Dong, X.C., Ma, Y.W., Zhu, G.Y., Huang, Y.X., Wang, J., Chan-Park, M.B., Wang, L.H., Huang, W., Chen, P., 2012a. J. Mater. Chem. 22 (33), 17044–17048.
Dong, X.C., Xu, H., Wang, X.W., Huang, Y.X., Chan-Park, M.B., Zhang, H., Wang, L.H., Huang, W., Chen, P., 2012b. ACS Nano 6 (4), 3206–3213.
Dreyer, D.R., Park, S., Bielawski, C.W., Ruoff, R.S., 2010. Chem. Soc. Rev. 39 (1), 228–240.
Fan, Z.J., Kai, W., Yan, J., Wei, T., Zhi, L.J., Feng, J., Ren, Y.M., Song, L.P., Wei, F., 2010a. ACS Nano 5 (1), 191–198.
Fan, Z.J., Wang, K., Wei, T., Yan, J., Song, L.P., Shao, B., 2010b. Carbon 48 (5), 1686–1689.
Fernandez-Merino, M.J., Guardia, L., Paredes, J.I., Villar-Rodil, S., Solis-Fernandez, P., Martinez-Alonso, A., Tascon, J.M.D., 2010. J. Phys. Chem. C 114 (14), 6426–6432.
Gao, H.C., Sun, Y.M., Zhou, J.J., Xu, R., Duan, H.W., 2013. ACS Appl. Mater. Interfaces 5 (2), 425–432.
Gao, H.C., Xiao, F., Ching, C.B., Duan, H.W., 2011. ACS Appl. Mater. Interfaces 3 (8), 3049–3057.
Gao, W., Alemany, L.B., Ci, L.J., Ajayan, P.M., 2009. Nat. Chem. 1 (5), 403–408.
Ghosh, S., Calizo, I., Teweldebrhan, D., Pokatilov, E.P., Nika, D.L., Balandin, A.A., Bao, W., Miao, F., Lau, C.N., 2008. Appl. Phys. Lett. 92 (15), 151911.
Guo, C.X., Ng, S.R., Khoo, S.Y., Zheng, X.T., Chen, P., Li, C.M., 2012. ACS Nano 6 (8), 6944–6951.
Guo, C.X., Yang, H.B., Sheng, Z.M., Lu, Z.S., Song, Q.L., Li, C.M., 2010. Angew. Chem. Int. Ed. 49 (17), 3014–3017.
Hassan, H.M.A., Abdelsayed, V., Khder, A., AbouZeid, K.M., Terner, J., El-Shall, M.S., Al-Resayes, S.I., El-Azhary, A.A., 2009. J. Mater. Chem. 19 (23), 3832–3837.
He, Z.M., Liu, J., Qiao, Y., Li, C.M., Tan, T.T.Y., 2012. Nano Lett. 12 (9), 4738–4741.
Hernandez, Y., Nicolosi, V., Lotya, M., Blighe, F.M., Sun, Z.Y., De, S., McGovern, I.T., Holland, B., Byrne, M., Gun'ko, Y.K., Boland, J.J., Niraj, P., Duesberg, G., Krishnamurthy, S., Goodhue, R., Hutchison, J., Scardaci, V., Ferrari, A.C., Coleman, J.N., 2008. Nat. Nanotechnol. 3 (9), 563–568.
Hilder, M., Winther-Jensen, B., Li, D., Forsyth, M., MacFarlane, D.R., 2011. Phys. Chem. Chem. Phys. 13 (20), 9187–9193.
Hu, C.G., Cheng, H.H., Zhao, Y., Hu, Y., Liu, Y., Dai, L.M., Qu, L.T., 2012. Adv. Mater. 24 (40), 5493–5498.
Hu, H., Zhao, Z.B., Wan, W.B., Gogotsi, Y., Qiu, J.S., 2013. Adv. Mater. 25 (15), 2219–2223.
Huang, X.D., Qian, K., Yang, J., Zhang, J., Li, L., Yu, C.Z., Zhao, D.Y., 2012. Adv. Mater. 24 (32), 4419–4423.
Hummers, W.S., Offeman, R.E., 1958. J. Am. Chem. Soc. 80 (6) (1339-1339).
Jimenez, P.S.V., 1987. Mater. Res. Bull. 22 (5), 601–608.
Kim, F., Luo, J.Y., Cruz-Silva, R., Cote, L.J., Sohn, K., Huang, J.X., 2010. Adv. Funct. Mater. 20 (17), 2867–2873.
Kim, J., Cote, L.J., Kim, F., Yuan, W., Shull, K.R., Huang, J.X., 2010. J. Am. Chem. Soc. 132 (23), 8180–8186.
Krishnan, D., Kim, F., Luo, J.Y., Cruz-Silva, R., Cote, L.J., Jang, H.D., Huang, J.X., 2012. Nano Today 7 (2), 137–152.
Kuila, T., Bose, S., Khanra, P., Mishra, A.K., Kim, N.H., Lee, J.H., 2012. Carbon 50 (3), 914–921.
Lee, C., Wei, X.D., Kysar, J.W., Hone, J., 2008. Science 321 (5887), 385–388.
Lei, Z.B., Lu, L., Zhao, X.S., 2012. Energy Environ. Sci. 5 (4), 6391–6399.
Li, D., Muller, M.B., Gilje, S., Kaner, R.B., Wallace, G.G., 2008. Nature Nanotechnol. 3 (2), 101–105.
Li, X.L., Zhang, G.Y., Bai, X.D., Sun, X.M., Wang, X.R., Wang, E., Dai, H.J., 2008. Nat. Nanotechnol. 3 (9), 538–542.
Li, Y.G., Wang, H.L., Xie, L.M., Liang, Y.Y., Hong, G.S., Dai, H.J., 2011. J. Am. Chem. Soc. 133 (19), 7296–7299.
Li, Z.P., Mi, Y.J., Liu, X.H., Liu, S., Yang, S.R., Wang, J.Q., 2011a. J. Mater. Chem. 21 (38), 14706–14711.
Li, Z.P., Wang, J.Q., Liu, X.H., Liu, S., Ou, J.F., Yang, S.R., 2011b. J. Mater. Chem. 21 (10), 3397–3403.
Liang, Y.Y., Li, Y.G., Wang, H.L., Zhou, J.G., Wang, J., Regier, T., Dai, H.J., 2011. Nat. Mater 10 (10), 780–786.
Lin, J.Y., Chan, C.Y., Chou, S.W., 2013. Chem. Commun. 49 (14), 1440–1442.
Liu, C.B., Wang, K., Luo, S.L., Tang, Y.H., Chen, L.Y., 2011. Small 7 (9), 1203–1206.
Logan, B., Cheng, S., Watson, V., Estadt, G., 2007. Environ. Sci. Technol. 41 (9), 3341–3346.
Logan, B.E., 2009. Nat. Rev. Microbiol. 7 (5), 375–381.
Long, D.H., Li, W., Ling, L.C., Miyawaki, J., Mochida, I., Yoon, S.H., 2010. Langmuir 26 (20), 16096–16102.
Low, C.T.J., Walsh, F.C., Chakrabarti, M.H., Hashim, M.A., Hussain, M.A., 2013. Carbon 54, 1–21.
Maiyalagan, T., Dong, X.C., Chen, P., Wang, X., 2012. J. Mater. Chem. 22 (12), 5286–5290.
Marcano, D.C., Kosynkin, D.V., Berlin, J.M., Sinitskii, A., Sun, Z.Z., Slesarev, A., Alemany, L.B., Lu, W., Tour, J.M., 2010. ACS Nano 4 (8), 4806–4814.
Mattevi, C., Kim, H., Chhowalla, M., 2011. J. Mater. Chem. 21 (10), 3324–3334.
Matuyama, E., 1954. J. Phys. Chem. 58 (3), 215–219.
McAllister, M.J., Li, J.L., Adamson, D.H., Schniepp, H.C., Abdala, A.A., Liu, J., Herrera-Alonso, M., Milius, D.L., Car, R., Prud'homme, R.K., Aksay, I.A., 2007. Chem. Mater. 19 (18), 4396–4404.
Mei, X.G., Zheng, H.Q., Ouyang, J.Y., 2012. J. Mater. Chem. 22 (18), 9109–9116.
Nair, R.R., Blake, P., Grigorenko, A.N., Novoselov, K.S., Booth, T.J., Stauber, T., Peres, N. M.R., Geim, A.K., 2008. Science 320 (5881) (1308-1308).
Nethravathi, C., Rajamathi, M., 2008. Carbon 46 (14), 1994–1998.
Novoselov, K.S., Fal'ko, V.I., Colombo, L., Gellert, P.R., Schwab, M.G., Kim, K., 2012. Nature 490 (7419), 192–200.
Novoselov, K.S., Geim, A.K., Morozov, S.V., Jiang, D., Zhang, Y., Dubonos, S.V., Grigorieva, I.V., Firsov, A.A., 2004. Science 306 (5696), 666–669.
Pan, S.Y., Aksay, I.A., 2011. ACS Nano 5 (5), 4073–4083.
Park, J.Y., Advincula, R.C., 2011. Soft Matter 7 (21), 9829–9843.
Park, S., An, J.H., Piner, R.D., Jung, I., Yang, D.X., Velamakanni, A., Nguyen, S.T., Ruoff, R.S., 2008. Chem. Mater. 20 (21), 6592–6594.

Park, S., Mohanty, N., Suk, J.W., Nagaraja, A., An, J.H., Piner, R.D., Cai, W.W., Dreyer, D.R., Berry, V., Ruoff, R.S., 2010. Adv. Mater. 22 (15), 1736–1740.
Park, S., Ruoff, R.S., 2009. Nature Nanotechnol. 4 (4), 217–224.
Pei, S.F., Zhao, J.P., Du, J.H., Ren, W.C., Cheng, H.M., 2010. Carbon 48 (15), 4466–4474.
Pham, T.A., Kim, J.S., Kim, J.S., Jeong, Y.T., 2011. Colloid Surf. A: Physicochem. Eng. Asp. 384 (1–3), 543–548.
Qian, Y., Lu, S.B., Gao, F.L., 2011a. J. Mater. Sci. 46 (10), 3517–3522.
Qian, Y., Lu, S.B., Gao, F.L., 2011b. Mater. Lett. 65 (1), 56–58.
Qiu, L., Yang, X.W., Gou, X.L., Yang, W.R., Ma, Z.F., Wallace, G.G., Li, D., 2010. Chem. Eur. J. 16 (35), 10653–10658.
Ramesha, G.K., Sampath, S., 2009. J. Phys. Chem. C 113 (19), 7985–7989.
Ren, W.C., Cheng, H.M., 2013. Nature 497 (7450), 448–449.
Ronkainen, N.J., Halsall, H.B., Heineman, W.R., 2010. Chem. Soc. Rev. 39 (5), 1747–1763.
Salas, E.C., Sun, Z.Z., Luttge, A., Tour, J.M., 2010. ACS Nano 4 (8), 4852–4856.
Sattayasamitsathit, S., Gu, Y.E., Kaufmann, K., Jia, W.Z., Xiao, X.Y., Rodriguez, M., Minteer, S., Cha, J., Burckel, D.B., Wang, C.M., Polsky, R., Wang, J., 2013. J. Mater. Chem. A 1 (5), 1639–1645.
Schniepp, H.C., Li, J.L., McAllister, M.J., Sai, H., Herrera-Alonso, M., Adamson, D.H., Prud'homme, R.K., Car, R., Saville, D.A., Aksay, I.A., 2006. J. Phys. Chem. B 110 (17), 8535–8539.
Shah, M., Park, A.R., Zhang, K., Park, J.H., Yoo, P.J., 2012. ACS Appl. Mater. Interfaces 4 (8), 3893–3901.
Shao, J.J., Lv, W., Guo, Q.G., Zhang, C., Xu, Q., Yang, Q.H., Kang, F.Y., 2012. Chem. Commun. 48 (31), 3706–3708.
Shao, Y.Y., Wang, J., Engelhard, M., Wang, C.M., Lin, Y.H., 2010a. J. Mater. Chem. 20 (4), 743–748.
Shao, Y.Y., Wang, J., Wu, H., Liu, J., Aksay, I.A., Lin, Y.H., 2010b. Electroanalysis 22 (10), 1027–1036.
Sheng, K.X., Xu, Y.X., Li, C., Shi, G.Q., 2011. New Carbon Mater. 26 (1), 9–15.
Sohn, K., Na, Y.J., Chang, H., Roh, K.M., Jang, H.D., Huang, J.X., 2012. Chem. Commun. 48 (48), 5968–5970.
Stankovich, S., Dikin, D.A., Piner, R.D., Kohlhaas, K.A., Kleinhammes, A., Jia, Y., Wu, Y., Nguyen, S.T., Ruoff, R.S., 2007. Carbon 45 (7), 1558–1565.
Stoller, M.D., Park, S.J., Zhu, Y.W., An, J.H., Ruoff, R.S., 2008. Nano Lett. 8 (10), 3498–3502.
Sui, Z.Y., Meng, Q.H., Zhang, X.T., Ma, R., Cao, B., 2012. J. Mater. Chem. 22 (18), 8767–8771.
Sutter, P.W., Flege, J.I., Sutter, E.A., 2008. Nat. Mater. 7 (5), 406–411.
Tang, Y.H., Wu, N., Luo, S.L., Liu, C.B., Wang, K., Chen, L.Y., 2012. Macromol. Rapid Commun. 33 (20), 1780–1786.
Tao, A.R., Huang, J.X., Yang, P.D., 2008. Acc. Chem. Res 41 (12), 1662–1673.
Van der Biest, O.O., Vandeperre, L.J., 1999. Annu. Rev. Mater. Sci. 29, 327–352.
Vickery, J.L., Patil, A.J., Mann, S., 2009. Adv. Mater. 21 (21), 2180–2184.
Wang, D.H., Kou, R., Choi, D., Yang, Z.G., Nie, Z.M., Li, J., Saraf, L.V., Hu, D.H., Zhang, J. G., Graff, G.L., Liu, J., Pope, M.A., Aksay, I.A., 2010. ACS Nano 4 (3), 1587–1595.
Wang, G.M., Qian, F., Saltikov, C., Jiao, Y.Q., Li, Y., 2011. Nano Res. 4 (6), 563–570.
Wang, H.L., Cui, L.F., Yang, Y.A., Casalongue, H.S., Robinson, J.T., Liang, Y.Y., Cui, Y., Dai, H.J., 2010. J. Am. Chem. Soc. 132 (40), 13978–13980.
Wang, H.Y., Wang, G.M., Ling, Y.C., Qian, F., Song, Y., Lu, X.H., Chen, S.W., Tong, Y.X., Li, Y., 2013. Nanoscale 5 (21), 10283–10290.
Wang, P., Jiang, T.F., Zhu, C.Z., Zhai, Y.M., Wang, D.J., Dong, S.J., 2010. Nano Res 3 (11), 794–799.
Wang, R.H., Wang, Y., Xu, C.H., Sun, J., Gao, L., 2013. RSC Adv 3 (4), 1194–1200.
Wang, X., Wang, J.F., Cheng, H.J., Yu, P., Ye, J.S., Mao, L.Q., 2011. Langmuir 27 (17), 11180–11186.
Wang, Y., Shi, Z.X., Yin, J., 2011. ACS Appl. Mater. Interfaces 3 (4), 1127–1133.
Wang, Y., Zhao, C.E., Sun, D., Zhang, J.R., Zhu, J.J., 2013. ChemPlusChem 78 (8), 823–829.
Wang, Z.L., Xu, D., Huang, Y., Wu, Z., Wang, L.M., Zhang, X.B., 2012. Chem. Commun. 48 (7), 976–978.
Wang, Z.L., Xu, D., Wang, H.G., Wu, Z., Zhang, X.B., 2013. ACS Nano 7 (3), 2422–2430.
Williams, G., Kamat, P.V., 2009. Langmuir 25 (24), 13869–13873.
Williams, G., Seger, B., Kamat, P.V., 2008. ACS Nano 2 (7), 1487–1491.
Windmiller, J.R., Wang, J., 2013. Electroanalysis 25 (1), 29–46.
Wu, D.Q., Zhang, F., Liang, H.W., Feng, X.L., 2012. Chem. Soc. Rev. 41 (18), 6160–6177.
Wu, J.S., Pisula, W., Mullen, K., 2007. Chem. Rev. 107 (3), 718–747.
Wu, Q., Xu, Y.X., Yao, Z.Y., Liu, A.R., Shi, G.Q., 2010. ACS Nano 4 (4), 1963–1970.
Wu, T.S., Liu, S., Luo, Y.L., Lu, W.B., Wang, L., Sun, X.P., 2011. Nanoscale 3 (5), 2142–2144.
Wu, Z.S., Ren, W.C., Gao, L.B., Liu, B.L., Jiang, C.B., Cheng, H.M., 2009a. Carbon 47 (2), 493–499.
Wu, Z.S., Ren, W.C., Gao, L.B., Zhao, J.P., Chen, Z.P., Liu, B.L., Tang, D.M., Yu, B., Jiang, C. B., Cheng, H.M., 2009b. ACS Nano 3 (2), 411–417.
Xiao, F., Li, Y.Q., Gao, H.C., Ge, S.B., Duan, H.W., 2013. Biosens. Bioelectron 41, 417–423.
Xiao, F., Li, Y.Q., Zan, X.L., Liao, K., Xu, R., Duan, H.W., 2012a. Adv. Funct. Mater. 22 (12), 2487–2494.
Xiao, F., Song, J.B., Gao, H.C., Zan, X.L., Xu, R., Duan, H.W., 2012b. ACS Nano 6 (1), 100–110.
Xiao, X.Y., Beechem, T.E., Brumbach, M.T., Lambert, T.N., Davis, D.J., Michael, J.R., Washburn, C.M., Wang, J., Brozik, S.M., Wheeler, D.R., Burckel, D.B., Polsky, R., 2012a. ACS Nano 6 (4), 3573–3579.
Xiao, X.Y., Michael, J.R., Beechem, T., McDonald, A., Rodriguez, M., Brtunbach, M.T., Lambert, T.N., Washburn, C.M., Wang, J., Brozik, S.M., Wheeler, D.R., Burckel, D. B., Polsky, R., 2012b. J. Mater. Chem. 22 (45), 23749–23754.
Xie, X., Yu, G.H., Liu, N., Bao, Z.N., Criddle, C.S., Cui, Y., 2012. Energy Environ. Sci. 5 (5), 6862–6866.
Xu, L.Q., Yang, W.J., Neoh, K.G., Kang, E.T., Fu, G.D., 2010. Macromolecules 43 (20), 8336–8339.
Xu, Y.X., Sheng, K.X., Li, C., Shi, G.Q., 2010. ACS Nano 4 (7), 4324–4330.
Xu, Y.X., Shi, G.Q., 2011. J. Mater. Chem. 21 (10), 3311–3323.
Xue, Y.H., Chen, H., Yu, D.S., Wang, S.Y., Yardeni, M., Dai, Q.B., Guo, M.M., Liu, Y., Lu, F., Qu, J., Dai, L.M., 2011. Chem. Commun. 47 (42), 11689–11691.
Yang, X.W., Qiu, L., Cheng, C., Wu, Y.Z., Ma, Z.F., Li, D., 2011. Angew. Chem. Int. Ed. 50 (32), 7325–7328.
Yong, Y.C., Dong, X.C., Chan-Park, M.B., Song, H., Chen, P., 2012. ACS Nano 6 (3), 2394–2400.
Yoo, J.J., Balakrishnan, K., Huang, J.S., Meunier, V., Sumpter, B.G., Srivastava, A., Conway, M., Reddy, A.L.M., Yu, J., Vajtai, R., Ajayan, P.M., 2011. Nano Lett. 11 (4), 1423–1427.
Yu, D.S., Dai, L.M., 2010. J. Phys. Chem. Lett. 1 (2), 467–470.
Zan, X.L., Fang, Z., Wu, J., Xiao, F., Huo, F.W., Duan, H.W., 2013. Biosens. Bioelectron 49, 71–78.
Zhang, H.H., Liu, Q., Feng, K., Chen, B., Tung, C.H., Wu, L.Z., 2012. Langmuir 28 (21), 8224–8229.
Zhang, J.L., Yang, H.J., Shen, G.X., Cheng, P., Zhang, J.Y., Guo, S.W., 2010. Chem. Commun. 46 (7), 1112–1114.
Zhang, L., Liang, J.J., Huang, Y., Ma, Y.F., Wang, Y., Chen, Y.S., 2009. Carbon 47 (14), 3365–3368.
Zhang, L., Shi, G.Q., 2011. J. Phys. Chem. C 115 (34), 17206–17212.
Zhang, Y.Z., Mo, G.Q., Li, X.W., Zhang, W.D., Zhang, J.Q., Ye, J.S., Huang, X.D., Yu, C.Z., 2011. J. Power Sources 196 (13), 5402–5407.
Zhao, X., Zhang, Q.H., Hao, Y.P., Li, Y.Z., Fang, Y., Chen, D.J., 2010. Macromolecules 43 (22), 9411–9416.
Zheng, Q.B., Ip, W.H., Lin, X.Y., Yousefi, N., Yeung, K.K., Li, Z.G., Kim, J.K., 2011. ACS Nano 5 (7), 6039–6051.
Zhou, M., Wang, Y.L., Zhai, Y.M., Zhai, J.F., Ren, W., Wang, F.A., Dong, S.J., 2009. Chem. Eur. J. 15 (25), 6116–6120.
Zhou, Y., Bao, Q.L., Tang, L.A.L., Zhong, Y.L., Loh, K.P., 2009. Chem. Mater. 21 (13), 2950–2956.
Zhu, C.Z., Guo, S.J., Fang, Y.X., Dong, S.J., 2010. ACS Nano 4 (4), 2429–2437.
Zhu, C.Z., Guo, S.J., Fang, Y.X., Han, L., Wang, E.K., Dong, S.J., 2011a. Nano Res 4 (7), 648–657.
Zhu, G., Pan, L.K., Lu, T., Xu, T., Sun, Z., 2011b. J. Mater. Chem. 21 (38), 14869–14875.
Zhu, Y.W., Cai, W.W., Piner, R.D., Velamakanni, A., Ruoff, R.S., 2009. Appl. Phys. Lett. 95 (10), 103104.
Zhu, Y.W., Murali, S., Cai, W.W., Li, X.S., Suk, J.W., Potts, J.R., Ruoff, R.S., 2010a. Adv. Mater. 22 (35), 3906–3924.
Zhu, Y.W., Murali, S., Stoller, M.D., Velamakanni, A., Piner, R.D., Ruoff, R.S., 2010b. Carbon 48 (7), 2118–2122.